Universitat Politecnica de Catalunya

Departament d'Enginyeria Electrica

PhD Thesis

Probabilistic analysis to assess the impact of the charge of electric vehicles on distribution grids under normal operation

Autor: **Eduard Valsera-Naranjo**

Directors: **Andreas Sumper**
Roberto Villafafila-Robles

Barcelona, March 2014

Universitat Politecnica de Catalunya
Departament d'Enginyeria Electrica
Centre d'Innovació Tecnològica en Convertidors Estàtics i Accionaments
Av. Diagonal, 647. Pl. 2
08028 Barcelona

Primera impressió, March 2014

UNIVERSITAT POLITÈCNICA DE CATALUNYA
BARCELONATECH
Escola de Doctorat

Acta de qualificació de tesi doctoral

Curs acadèmic:

Nom i cognoms

Programa de doctorat

Unitat estructural responsable del programa

Resolució del Tribunal

Reunit el Tribunal designat a l'efecte, el doctorand / la doctoranda exposa el tema de la seva tesi doctoral titulada _____

_____.

Acabada la lectura i després de donar resposta a les qüestions formulades pels membres titulars del tribunal, aquest atorga la qualificació:

☐ NO APTE ☐ APROVAT ☐ NOTABLE ☐ EXCEL·LENT

(Nom, cognoms i signatura) President/a	(Nom, cognoms i signatura) Secretari/ària

(Nom, cognoms i signatura) Vocal	(Nom, cognoms i signatura) Vocal	(Nom, cognoms i signatura) Vocal

_____, _____ d'/de _____ de _____

El resultat de l'escrutini dels vots emesos pels membres titulars del tribunal, efectuat per l'Escola de Doctorat, a instància de la Comissió de Doctorat de la UPC, atorga la MENCIÓ CUM LAUDE:

☐ SÍ ☐ NO

(Nom, cognoms i signatura) Presidenta de la Comissió de Doctorat	(Nom, cognoms i signatura) Secretària de la Comissió de Doctorat

Barcelona, _____ d'/de _____ de _____

To my family.

La ciencia se compone de errores,
que a su vez son los pasos hacia la verdad.

Julio Verne

La inteligencia consiste no sólo en el conocimiento,
sino también en la destreza de aplicar
los conocimientos en la práctica.

Aristóteles

Acknowledgements

Firstly, I would like to thank to my family the support they have always given me in every step I have made during my life and for their wise advice in the difficult moments. I would like to thank to Sònia her support and patience.

I am indebted to several of my colleagues whose help made possible to complete my thesis. My advisor, Dr. Andreas Sumper, who has been motivating me since I got to CITCEA-UPC in 2007 as 3rd year student. I also would like to thank him the dedication and effort he has put in assessing and guiding me during the process to achieve this thesis. I would like to thank Dr. Roberto Villafila for his advice. Finally, I would like to thank the CITCEA-UPC team. Thanks to them I could discovered my true vocation and during the time I spent there I could grew not only professionally but also personally.

I would like to mention the priceless help and support I got from Adrià (whom I first met in CITCEA-UPC) especially during the hard times. Finally, I would like to thank to Paola, Marcela and David for kindly helping me when I needed it.

Abstract

The incorporation of high levels of small-scale non-dispatchable distributed generation is leading to the transition from the traditional 'vertical' power system structure to a 'horizontally-operated' power system, where the distribution networks contain both stochastic generation and load (such as electric vehicles recharging). This fact increases the number of stochastic inputs and dependence structures between them need to be considered. The deterministic analysis is not enough to cope with these issues and a new approach is needed. Probabilistic analysis provides a better approach.

This PhD thesis describes the grid impact analysis of charging electric vehicles (EV) using charging curves with detailed battery modelling. A probabilistic method using Monte Carlo was applied to a typical Spanish distribution grid, also using mobility patterns of Barcelona. To carry out this analysis, firstly, an IEEE test system was adapted to a typical distribution grid configuration; secondly, the EV and its battery types were modeled taking into account the current vehicle market and the battery characteristics; and, finally, the recharge control strategies were taken in account.

Once these main features were established, a statistical probabilistic model for the household electrical demand and for the EV charging parameters was determined. With these probabilistic models, the Monte Carlo analysis was performed within the established scenario in order to study the lines' and the transformers' loading levels. The results show that an accurate model for the battery gives a more precise estimation about the impact on the grid. Additionally, mobility patterns have been proved to be some of the most important key aspects for these type of studies.

Resumen

La incorporación de altos niveles a generación distribuida no despachable a pequeña escala está causando la transición de los tradicionales sistemas eléctricos de potencia 'verticales' a los sistemas de potencia 'operados horizontalmente', en donde dichas redes de distribución pueden contener tanto generación como consumos de carácter estocástico (p. ej. La recarga de vehículos eléctricos). Este hecho incrementa el número de variables estocásticas y las dependencias entre estas de forma considerable. Los análisis determinísticos no son suficientes para lidiar con estos nuevos factores y se necesita enfocar el problema de otro modo. Los análisis probabilísticos proporcionan una mejor manera de abordar la situación.

Esta tesis describe el impacto de la recarga de vehículos eléctricos (para los cuales se ha usado un modelo detallado para las curvas de carga y descarga de sus baterías) en la red eléctrica. El método probabilístico Monte Carlo se ha aplicado a una red de equiparable a una red distribución española donde también se han considerado patrones de movilidad de vehículos (en este caso de la ciudad de Barcelona). Para llevar a cabo los análisis, en primer lugar se ha adaptado una red de estudio de IEEE con los parámetros de la red de distribución española. A continuación se ha modelado el comportamiento de las baterías de los vehículos eléctricos a partir de las características de baterías de modelos reales de vehículos eléctricos que ya están en el mercado. Finalmente, se han considerado diferentes estrategias de control en el momento de realizar la recarga de vehículos eléctricos.

A partir de los datos obtenidos se han generado modelos estadísticos tanto para los consumos domésticos de la red como para la recarga de los vehículos eléctricos. Con dichos modelos se ha llevado a cabo un análisis Monte Carlo para estudiar los niveles de carga tanto de líneas como de transformadores. Los resultados obtenidos demuestran la importancia del correcto modelado de las baterías ya que se aumenta la precisión de los análisis. Adicionalmente, los patrones de movilidad de la zona a estudiar han demostrado ser clave en este tipo de estudio.

Dissertation outline

The present PhD thesis is divided in four parts plus an introductory chapter.

Part I introduces the necessity of probabilistic assessment of electric power systems and battery modelling. Chapter 2 describes the basis of probabilistic analysis and yields the basis for further analysis. Chapter 3 describes the process of EV's battery modelling.

Part II presents the probabilistic models used in the study. Chapter 4 describes the main steps to be followed to perform the analysis. Chapter 5 describes the process to generate the probabilistic model for the grid's electrical demand. Finally, chapter 6 presents the process to generate the probabilistic model for EV's demand.

In part III the study case is presented. In chapter 7 the scenario for the simulations is presented. Chapter 8 and chapter 9 present the impact of the EV's recharge without considering the household consumption and considering it respectively.

Finally, part IV summarizes the conclusions of this work and present future work-lines.

Contents

List of Figures

List of Tables

Chapter 1

State of the art

The growing interest in the introduction of fossil fuel alternatives into the transportation and the large number of projects regarding this issue show that in the future the presence of the electric vehicle (EV) in the electric system will be significant. Important cities in the world, such as New York, have been the scenario of reference studies about the potential impact of Plug-in Hybrid EV technology on grid operations and electricity system planning [4]. This study illustrates how the proper management of charging patterns can lead to the utilisation of the current grid without investing in infrastructure. Other studies, like [5], conclude that in cases where Plug-in Hybrid EVs obtain the energy from electricity for 40% of their miles, penetrations up to 50% by the vehicle fleet would not require the increase of electric generation capacity under optimal dispatch rules.

Therefore, it is possible to assume a future with a strong presence of EVs [6]. Under these conditions, the use of wind, solar and renewable energies is generally a potential alternative [7, 8] energy source. This situation will represent an opportunity for EVs to be part of an integrated electric system, with the ability to adapt to varying conditions by performing ancillary services like power-frequency, power factor or voltage regulation. However, an EV implementation introduces complexities of this integrated system into the grid. Depending on power level, timing, and duration of the EV connection to the grid, there could be a wide variety of impacts on grid constraints, capacity requirements, fuel types used and emissions generated [9], which must be managed in order to reach an optimal dispatch rule. A control system able to optimally manage all constraints and variables of electrical transportation will lead to moderate investments into the grid and therefore to its implementation.

1.1 Types of vehicles

Vehicles can be classified mainly into three groups: Internal Combustion Engine vehicles (ICE vehicles), Hybrid Electrical Vehicles (HEV) and Battery Electrical Vehicles (BEV). The ICE vehicles are the vehicles which its only propulsion system is an internal combustion engine and its only energy source is its fuel tank. The HEV vehicles usually combine at least two types of different propulsions. I.e. a HEV can have a hydrogen engine and an electrical motor. Finally, the BEV get all the propulsion energy from a battery which feeds an electrical motor. It is important to highlight that both HEV and BEV can get plugged to an electrical outlet to recharge their batteries.

Two ways of combining ICE and electrical motors are currently used in HEV: sharing the same shaft to the vehicle's differential transmission and through different shafts. The Hybridization Factor (HF) is defined by [10, 11] in order to calculate the ratio of propulsion power which comes from the electrical motor (P_{EP}) and from the ICE (P_{ICE}) in a HEV (equation 1.1).

$$HF = \frac{P_{EP}}{P_{EP} + P_{ICE}} \tag{1.1}$$

1.1.1 Internal Combustion Engine Vehicle definition

An ICE vehicles is a vehicle which gets its propulsion energy from an ICE which transforms chemical energy from the fuel into kinetic energy. The combustion of the fuel (usually a fossil fuel) takes place in a combustion chamber where the fuels gets mixed with an oxidizer (normally air) and propels a piston. Nowadays, ICE vehicles are equipped with an auxiliary electrical motor which enhances the fuel economy by 5-15% (in city/urban environments) through turning off the ICE during coasting, braking or stopping [1, 12].

1.1.2 Hybrid Electrical Vehicle definition

An HEV combines a traditional ICE propulsion system with an electrical propulsion system in order to achieve a better fuel economy. Currently, six drive train architectures types of HEV can be distinguished [1, 12] (figure 1.1.2).

- **Mild-HEV**. This type of HEV (figure 1.1(a)) is propelled solely by an electrical generator. In this type of vehicle the ICE shares the shaft with the electrical motor. As a consequence of sharing the shaft, this

HEV can run without the electrical motor but it cannot run without the ICE. This type of architecture reaches up to a 30% of fuel efficiency and allows to reduce the size of the ICE [13].

- **Series full-HEV**. In this type of HEV architecture (figure 1.1(b)) the electrical motor is the only propulsion system. This kind of vehicles are also known as Extended Range Electric Vehicles (EREV) due to the fact that the ICE is used to recharge the vehicle's battery through a high efficiency ICE. Despite of having the advantage of the battery reduction, its efficiency drops in a 25.7%. This fact makes this type of HEV the less efficient among the rest of types of HEV. It includes regenerative breaking as the main system to recover and store energy [1, 12, 14, 15].

- **Parallel full-HEV**. This HEV (figure 1.1(c)) are able to propel the vehicle in three possible ways: through the electrical motor, through the ICE and combining both the electrical motor and the ICE. The parallel full-HEV count with a higher efficiency due to size of its battery and its electrical motor compared to the previous types of HEV [1, 12].

- **Series-parallel full-HEV**. This configuration (figure 1.1(d)) combines the series and parallel configuration. Nevertheless, adding both functionalities adds more complexity to the vehicle.

- **Complex full-HEV**. These HEV (figure 1.1(e)) are similar to the series-parallel full-HEV regarding its propulsion system. The major difference is that the ICE does not injects power directly to the electrical motor but it recharges the battery through a power converter which allows a better performance of the vehicle when its running as in a EREV mode.

- **Series-parallel PHEV**. The final combination (figure 1.1(f)) shares the same properties as the previous one but it allows the possibility of recharging its batteries from a power outlet. This feature allows a cost saving in the fuel due to the price of electricity compared to the price of fuel and it is a most environmental friendly alternative if the electric energy comes from renewable energy sources.

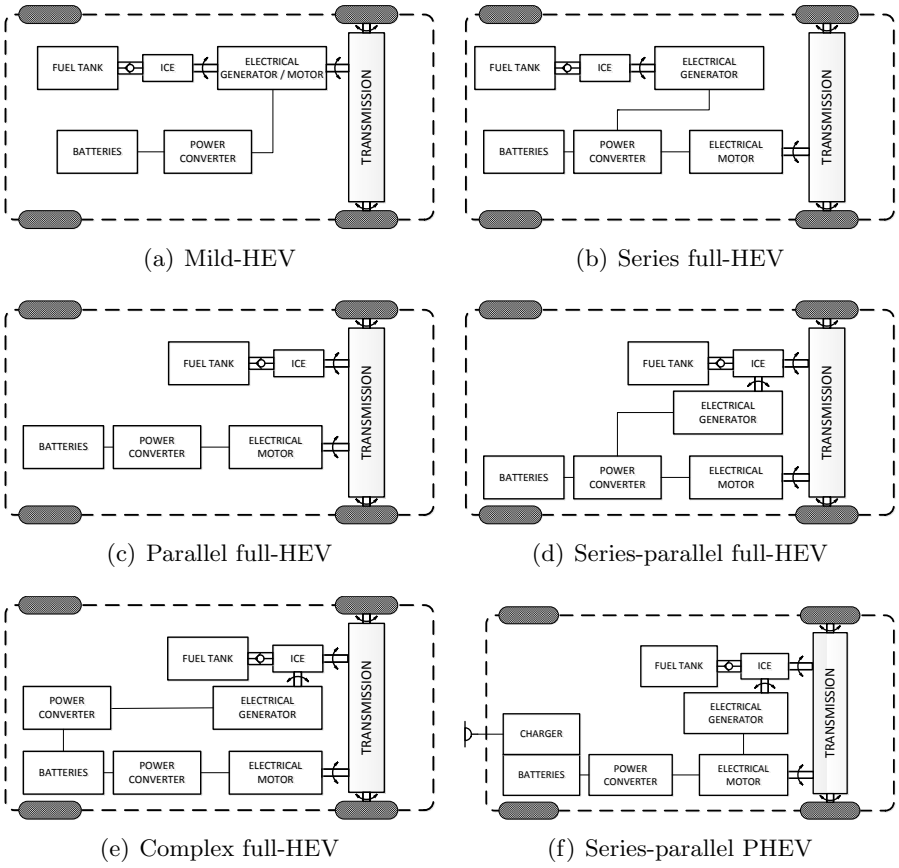

(a) Mild-HEV (b) Series full-HEV

(c) Parallel full-HEV (d) Series-parallel full-HEV

(e) Complex full-HEV (f) Series-parallel PHEV

Figure 1.1: HEV drive train architectures [1]

1.1.3 Electrical Vehicle definition

Pure electrical vehicle, also known as Battery Electrical Vehicle (BEV) or All-Electric Vehicle (AEV), are vehicles which its only power source is electrical energy stored in a battery (or energy storage system in the case of a fuel cell vehicle.). Currently, six drive train architectures types of BEV can be distinguished [1, 12] (figure 1.1.3).

- **Conventional configuration with a clutch**. This type of drive train architecture (figure 1.2(a)) is the direct conversion from an ICE to a BEV: the ICE is replaced by the battery, the power converter and the electrical motor and the rest of the drive train is kept. This type is the less efficient due to the size and the weigh of the clutch and the gearbox.
- **Conventional configuration without a clutch**. This type of configuration (figure 1.2(b)) is similar to the previous one described but the clutch is removed to reduce the weight. In some cases the gearbox is replaced by a fixed gearing to loose extra weight and reach a better efficiency.
- **Conventional configuration with integrated gearbox-differential**. This type of BEV (figure 1.2(c)) presents an integrated gearbox-differential system into the electrical motor. In this situation the only shaft kept is drive train which joins the wheels. This configuration gains compactness compared to the previous conventional architectures presented.
- **Independent electrical motors per drive wheel**. This configuration (figure 1.2(d)) is an evolution of the previous one and its main enhancement respect the previous is that the drive shaft is split into two system (one for each drive wheel) with its own power converter. This system allows better control of the vehicle particularly when cornering.
- **Independent electrical motors per drive wheel with integrated gearing**. This type of architecture (figure 1.2(e)) is like the previous (figure 1.2(d)) but it has no shafts due to the fact that a fixed gearing is integrated in the wheel and the electrical motor is just located in its side.
- **In-wheel drive**. The electrical motors are directly integrated in each drive wheel and its controlled is performed by its respective converters (figure 1.2(f)).

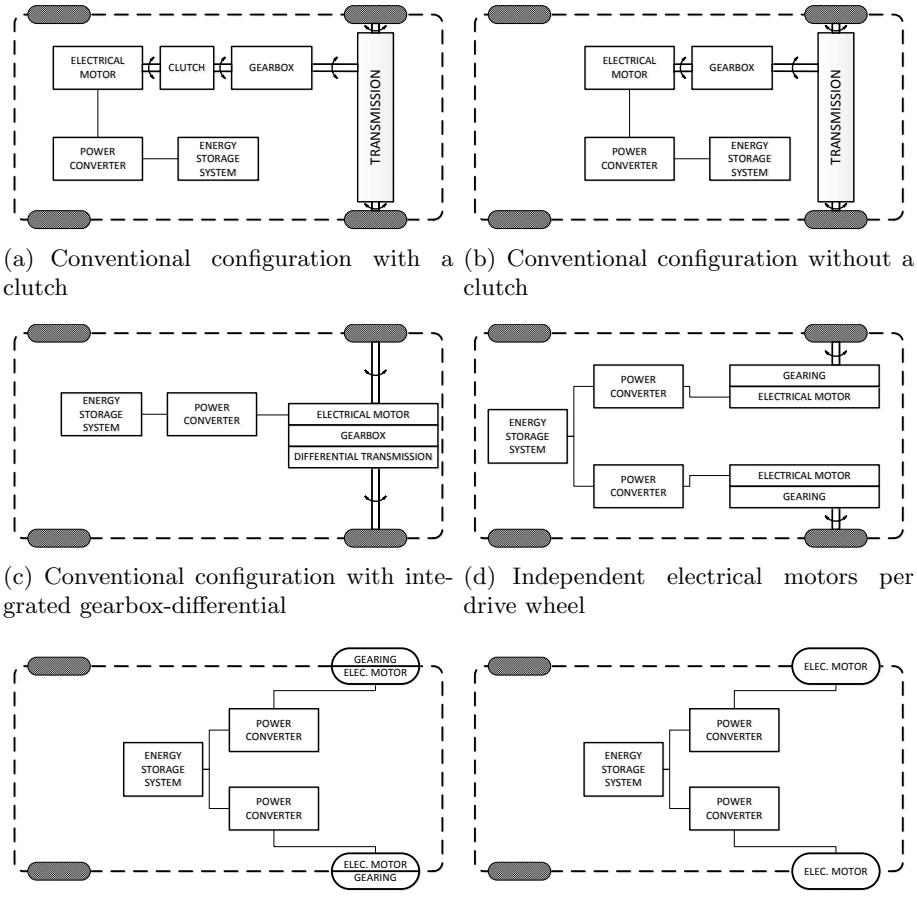

(a) Conventional configuration with a clutch

(b) Conventional configuration without a clutch

(c) Conventional configuration with integrated gearbox-differential

(d) Independent electrical motors per drive wheel

(e) Independent electrical motors per drive wheel with integrated gearing

(f) In-wheel drive

Figure 1.2: HEV drive train architectures [1]

1.1.4 Modes of operation

The HEV and PHEV combine both an ICE and usually an electric motor to propel. In order to increase the driving range of the vehicle, some modes of operation can be performed taking into account the SOC (*State Of Charge*) of the vehicle. Two modes of operation can be performed in a HEV or a PHEV [16]:

Charge sustaining mode (CS) The vehicle operates with the objective of keeping constant its current SOC. In this mode of operation both the ICE and the electrical motor operate jointly.

Charge depleting mode (CD) The vehicle operates with the objective of getting a net decrease in its battery SOC. Therefore, only the electrical motor will be used until the limit SOC (SOC_L) is reached [17, 18].

1.2 Types of energy storage systems in the EV

In contrast to the ICE vehicles or the HEV, the EV do not posses any system to get energy from a fuel tank. Instead of this system, the EV come generally with a combination of these three energy storage systems: batteries, ultracapacitors and flywheel systems.

1.2.1 Battery

Batteries are electrochemical devices consisting of several electrochemical cells which convert chemical energy into electric energy. Two types of batteries exists: primary batteries (also known as disposable batteries) and secondary batteries (rechargeable batteries). The primary batteries are designed to be used once and then discarded. The secondary batteries are designed to be used recharged and used as many time as its life cycle allows it. Therefore, the battery types used on EV are the secondary battery type.

There are five battery types currently suitable for transportation in the market [1, 19, 20, 21]:

- Lead-acid
- Nickel
- Zebra
- Lithium
- Metal-air

The Lead-acid battery is the cheapest type of battery presented. These batteries are typically used in ICE vehicles and are the least environmental friendly and heavy battery types presented. Its characteristics are [1]:

- **Specific Energy** $[Wh/kg]$**.** From 30 Wh/kg in the *metal foil lead acid* batteries to 50 Wh/kg in the *Valve regulated lead acid* batteries. The regular lead-acid battery are around 35 Wh/kg.
- **Energy density** $[Wh/l]$**.** Typically, this type of battery has energy density closer to the 100 Wh/l.
- **Specific power** $[W/kg]$**.** The range of values are from 150 W/kg to 900 W/kg but the typical models have values of 180 W/kg.

- **Life cycles.** Regular lead-acid batteries have approximately 1000 life cycles. However, advance lead-acid batteries can reach the 1500 life cycles.
- **Efficiency [%].** The efficiencies are generally over the 80%.
- **Production cost [€/kWh].** The production costs of these batteries are estimated to be in the range of 45-150 €/kWh.

The Nickel battery types are more environmentally friendly than the Lead-acid batteries. Its characteristics are [19, 20]:

- **Specific Energy** $[Wh/kg]$**.** The values of the specific energy of these batteries are 50-95 Wh/kg. However, the most commonly used Nickel battery, the Nickel-Cadmium battery, have specific energies in the range of 50-60 Wh/Kg.
- **Energy density** $[Wh/l]$**.** The energy densities for this batteries vary from 60 Wh/l to 300 Wh/l which corresponds to the Ni-Cd type.
- **Specific power** $[W/kg]$**.** Ni-Cd batteries have a specific power of 200 W/kg but the other Ni batteries have values from 100 W/kg to 300 W/kg.
- **Life cycles.** The life cycles of these batteries are estimated to be around 2000. However, the Ni-Zn type only reaches the 300 cycles.
- **Efficiency [%].** For most of these battery types, the efficiencies reach values up to 75%.
- **Production cost [€/kWh].** The average production cost for these batteries is approximately 155 €/kWh. Nevertheless, the Ni-Cd batteries have costs in the range of 200-250 €/kWh.

The ZEBRA batteries, built by sodium nickel chloride (NaNiCl), are batteries that need to keep temperatures in the range of 300-350 ^{o}C to remain efficient. These type of batteries present less life-cycle-cost than the lead-acid batteries [22] but have the drawback of losing 90 Wh when the battery is not used [23]. Its characteristics are [19, 20]:

- **Specific Energy** $[Wh/kg]$**.** Its specific energy is rated from 90-120 Wh/kg.
- **Energy density** $[Wh/l]$**.** The energy density values are around 160 Wh/l.

- **Specific power** $[W/kg]$**.** The values are from 155 W/kg an in some models the specific power can reach up to 230 W/kg.
- **Life cycles.** The life cycles are rated in approximately 1200.
- **Efficiency [%].** For all the documented ZEBRA battery models its efficiencies are around the 80%.
- **Production cost [€/kWh].** The production costs of these batteries are estimated to be in the range of 230-345 €/kWh. However, some models can reach the 450 €/kWh.

Lithium batteries have the main advantage of not having the memory effect and no poisonous metals (i.e. mercury, cadmium or lead) but it is most expensive type [1]. Its characteristics are [1, 19]:

- **Specific Energy** $[Wh/kg]$**.** Several types of Lithium batteries can be found in the market with values of specific energy in the range of 80-250 Wh/kg. The battery with the lowest specific energy is the Lithium-titanate (LiTiO/NiMnO2) battery with values from 80-100 Wh/kg. The highest specific energy is reached by the Lithium-ion battery with values in the range of 118-250 Wh/kg.
- **Energy density** $[Wh/l]$**.** The lowest value of energy density for the lithium batteries is rated in 220 Wh/l. However, the Lithium-ion type can reach values up to 400 Wh/l.
- **Specific power** $[W/kg]$**.** For most Lithium batteries, the values of specific power are in the range of 200-450 W/kg. However, the Lithium-iron phosphate type ($LIFePO_4$) reaches values form 2000 W/kg up to 4500 W/kg and the Lithium-titanate (LiTiO/NiMnO2) reaches values around 4000 W/kg.
- **Life cycles.** The vast majority of Lithium batteries have approximately 2000 life cycles except the Lithium-titanate (LiTiO/NiMnO2) which can get up to 18000.
- **Efficiency [%].** Efficiencies in this type of batteries are in the range of 80-95%.
- **Production cost [€/kWh].** The Lithium-titanate (LiTiO/NiMnO2) has a production cost of 2000 €/kWh. However, in the rest of batteries the costs are in the range of 110-350 €/kWh.

Metal-air batteries have the main advantage of higher specific energy and density respect the Lithium batteries. Its main disadvantage are its limited life cycle and its reduced specific power [24]. Its characteristics are [1]:

- **Specific Energy** $[Wh/kg]$**.** Most of metal-air batteries possess a specific energy in the range of 220-460 Wh/kg. However, the Lithium-air type reaches values up to 1800 Wh/kg.
- **Energy density** $[Wh/l]$**.** The documented energy densities for metal-air batteries are values around the 1400 Wh/l.
- **Specific power** $[W/kg]$**.** The values are in the range of 60-140 W/kg [20].
- **Life cycles.** Life cycles of these batteries are rated in 200.
- **Efficiency [%].** Efficiencies in this type of batteries are up to 60% [20].
- **Production cost [€/kWh].** Production costs are in the range of 90-120 €/kWh.

1.2.2 Ultracapacitor

Ultracapacitors are in essence similar to regular capacitors but have capacitances 20 times higher than regular capacitors, no maintenance are immune to ambient temperature variations and have a longer life cycle . Its characteristics are [1]:

- **Specific Energy** $[Wh/kg]$**.** Ultracapacitors' specific energies are in the range of 5-15 Wh/kg.
- **Specific power** $[W/kg]$**.** The values are in the range of 1-2 MW/kg.
- **Life cycles.** Ultracapacitors can last up to 40 years.
- **Efficiency** [%]**.** Efficiencies in ultracapacitors over the 95%.

1.2.3 Flywheel

Flywheel energy storage systems work under the principle of storing kinetic energy accelerating a rotor to a very high speed and keeping it as rotational energy. The output of this device could be mechanical energy or electrical energy. Its characteristics are [1]:

- **Specific Energy** $[Wh/kg]$**.** Specific energies are in the range of 10-150 Wh/kg.
- **Specific power** $[W/kg]$**.** The values are in the range of 2-10 kW/kg.
- **Life cycles.** Its life cycle is rated up to 15 years.
- **Efficiency** [%]**.** Efficiencies in flywheels are around 80%.

1.3 Types of energy generation systems in the EV

The objective of implementing an energy generation system in an EV is to extend the range of it. The most used energy generation systems in commercial EVs are [1]: fuel cells, photovoltaic cells, automotive thermoelectric generators (ATEG) and regenerative braking.

1.3.1 Fuel cells

A fuel cell is an energy conversion system which converts chemical energy into electrical energy. Fuel cells perform this process through electrolysis (giving heat and water as byproduct) proving to be a valuable option regarding against oil dependencies and hazardous CO_2 emissions [22, 23]. Therefore, fuel cells in transportation suppose a great advantage due to its low emissions, system simplicity, silence and its high efficiency operation [25].The most used fuel cells are [1]:

- Direct methanol fuel cells (DMFC)
- Proton exchange membrane fuel cells (PEMFC)
- Alkaline electrolyte fuel cells (AFC)
- Phosphoric acid fuel cells (PAFC)
- Molten carbonate fuel cells (MCFC)
- Solid oxide fuel cells (SOFC)

The U.S Department of Energy, studied the effect of temperature in the output power in fuel cells [25]. This study, shows that the SOFC can work at the highest temperatures being these in the range of 700-1000^{o}C with power outputs from 1 kW to 2000 kW. The MCFC operate between the 600^{o}C and the 700^{o}C being able to provide from 300 kW to 10000 kW which make these type of fuel cells the most potent type. The PAFC operate in temperatures around the 200^{o}C providing power in the range of 100-400 kW. The AFC, PEMFC and DMFC operate below the 100^{o}C with power outputs up to 100 kW.

1.3.2 Photovoltaic cells

Photovoltaic (PV) energy its been transportation sector since 20 years ago [26, 27, 28]. Even at the beginning of the introduction of photovoltaics in transportation PV panels were not conceived as an option for ICE vehicles [29], nowadays vehicles such as 2010 Prius, Aptera 2, Audi A8 and Mazda 929 include the option of a solar sunroof for air conditioning purposes [1]. Table 1.1 shows the seven types of photovoltaic technologies and their respective efficiencies [30, 31, 32, 33, 34, 35, 36, 37, 38].

Table 1.1: PV technologies efficiencies

PV Technology	**Efficiency** [%]
Mono-crystalline silicon	20,3-23,4
Polycrystalline	15-18,2
Thin film	8-19,9
Very high performance PV cells	21-41,1
Concentrator PV technology	25-42,2
Third generation	2,0-18,7
Innovative panel designs	1,7-10

Even a fully solar powered vehicle still remains a challenge due to the space limitation and the low generated energy, some car manufacturers have started to include PV on the rooftop. Through maximizing the surface of the PV on the vehicle [39] and through control algorithms [40] the overall efficiency can be increased [41].

1.3.3 Automotive thermoelectric generators

Thermoelectric generators (TEG) are devices which convert heat directly into electricity using the *Seebeck effect* phenomenon. Thus, ATEG convert waste heat from an ICE into electrical energy. ATEG systems can last up to 20 years without any maintenance with a low €/Watt with efficiencies in the range of 40-70% [42].

The first *Seebeck effect* devices where made of bimetallic junctions, but nowadays *Seebeck effect* devices use semiconductor p-n junctions due to its high electrical conductivity and its low thermal conductivity. The most used materials used in these devices are Bi_2Te_3, PbTe, and SiGe. Other materials like BiSb or $FeSi_2$ are less used due to high sublimation rates or bad mechanical strength even its good thermoelectric properties [1, 43, 44].

1.3.4 Regenerative braking

Conventional ICE vehicles use less than a 20% of energy to propel [45, 46]. It has been estimated that approximately a 50% percent of the energy used to brake the vehicle can be recovered using regenerative braking systems and can enhance the driving range in a 10-25% [47, 48].

Regenerative braking is a type of braking mechanism that instead wasting excess kinetic energy to heat due to friction in the brake linings, it converts this excess of energy in other form of energy. The regenerative brake operates jointly with the friction brake due to the fact that it can not absorb enough energy to stop the vehicle by itself. Therefore, due to safety issues, both the regenerative brake and the friction brake operates togethe in an specific ration (depending on the control implemented).There are currently four mechanism to capture the energy in a regenerative brake [1]:

- The electrical energy is directly stored in an *Energy Storage System* (ESS).
- The mechanical energy from the shaft rotation is stored in *Flywheel Energy System* (FES) as rotating energy.
- Energy is stored in canisters through a compressed gas.
- Energy stored in a spring as potential energy.

In the first typology of regenerative brake, the energy is stored as electricity in an *ESS* through an electric motor/generator. The energy recovered from braking is around the 50% an it is currently being used in HEV and EV [49, 50]. In the second type of regenerative brake, the rotational energy is stored in a Flywheel. In this system, over than the 70% of the braking energy can be recovered and it is mostly used in F1 (where is also known as KERS). The third system uses a hydraulic motor to compress gas to use it as energy storage [51]. It can reach values of more than the 70% of brake energy recovering and it is used mainly in heavy-duty delivery vehicles [49, 50]. The final system stores gravitational energy through a spring as potential energy. It has been used in some train applications but the data about its energy braking recovery ratio are not conclusive.

1.4 Charger topologies

Chargers play a crucial role in the EV's implementation. Due to the fact that the battery life and the charging time is linked to the charger, in order to be competitive in the market the chargers must be [2]: efficient, high power density capable, reliable, low cost, low volume and low weight. The most important drawback that chargers can produce is the one related to the harmonic effects on electric utility distribution grids [52, 53]. However, these effects can be reduced with an active rectifier front end [2]. The following standards address the issue of harmonic injection in the grid: IEEE-1547, SAE-J2894, IEC1000-3-2 and U.S National Electric Code (NEC) 690.

Electric vehicle's chargers can be classified according to: their power levels, unidirectional or bidirectional power flow, on-board or off-board location and conductive or inductive charging. This section describes these possible classifications.

1.4.1 Power Levels

The proper deployment of charging infrastructure and electric power supply equipment (EVSE) is a vital issue due to the fact that their availability in the market is the key to reduce on-board requirements and costs. Even the high number of available charger technologies and standards, this is a complex tasks because a correct deployment has to deal with [2]: charging time, demand policies, distribution, extent, regulatory procedures, etc. Table 1.4.1 show the charging power levels (based on [2, 3]).

Level 1

Level 1 charging level is the slowest method (table 1.4.1). This level is designed to work in AC (1 phase) with voltage levels of 120 V (US) and 230 V (EU). Even it could use the J1772 connector, it could also use the regular house outlet connector [2]. Charging infrastructure has been reported to cost $500-$800 [54, 55].

Level 2

Level 2 charging level (table 1.4.1) is the main method to be used in private or public facilities [2]. This charging level is designed to work in AC (1 phase or 3 phase) with voltage levels of 240 V (US) and 400 V (EU). It might need dedicated ESVE and the charger must be on-board the vehicle.

The installation costs of Level 2 infrastructure are in the range of $1.000-$3.000 [56] (unit cost per residential unit of $3000 [2, 55]). However, some cases such as the Tesla Roadster have an additional cost of $3.000 [57].

Level 3

Level 3 charing method is designed to be used as a commercial fast-charge level, able of recharging the vehicle's battery in less than 1 hour. This method uses an off-board 3 phase circuit charger (mainly to perform ac-dc controlled conversion) (table 1.4.1). The installation costs of Level 3 charging infrastructure are in the range of $30.000-$160.000 [58, 59]. The maintenance of this type of installation has been reported to another major cost [2, 60].

Table 1.2: Charging power levels (based on [2, 3])

Power Level	Voltage Levels	Use	Supply Equipment	Number of phases	Location	Power Ouput	Expected charging time	Vehicle Technology
Level 1	120 Vac (US) 230 Vac (EU)	Household or office charging	Household outlet	1 phase	On-board charger	1,4 kW (12 A) 1,9 kW (20 A)	4-11 hours 11-36 hours	PHEVs (5-15 kWh) EVs (16-50 kWh)
Level 2	240 Vac (US) 400 Vac (EU)	Private or public outlets	Dedicated ESVE	1 phase or 3 phase	On-board charger	4 kW (17 A) 8 kW (32 A) 19,2 kW (80 A)	1-4 hours 2-6 hours 2-3 hours	PHEVs (5-15 kWh) EVs (16-50 kWh) EVs (3-50 kWh)
Level 3	208 - 600 Vac or Vdc	Dedicated charging facility	Dedicated ESVE	3 phase	Off-board charger	50 kW 100 kW	0,4-1 hours 0,2-0,5 hours	EVs (20-50 kWh)

1.4.2 Unidirectional and bidirectional chargers

Regarding the power flow's direction, two possibilities exist when referring to chargers:

Unidirectional The electricity flows from the grid to the vehicle in order to recharge the vehicle's battery (*grid-to-vehicle*) [2].

Bidirectional The electricity can flow from the grid to the vehicle and from the vehicle to the grid. In the second option the electrical vehicle injects power into the grid (*vehicle-to-grid*).

Unidirectional chargers usually consist on a two AC/DC stage converter with an active filter in the grid's side. However, nowadays tendency is to implement the whole converter in a single stage type due to the benefits that it entails regarding the weight, volume and losses reduction [61]. Due to their simplicity in the control, their low cost (compared to the bidirectional type) and their performance, in a high EV penetration grid this type of chargers can fulfill most utilities requirements avoiding the safety hazards of bidirectional chargers [2, 62, 63].

Bidirectional chargers usually consist on a two AC/DC stage converter and support battery recharge (G2V) and battery power injection into the grid (V2G). The first converter AC/DC stage is connected on the grid's side and is responsible for the correct power factor during the process [64]. The second converter DC/DC stage has the function of regulating the battery's charge/discharge current [65]. When operating in the charging mode, the AC/DC stage has to guarantee a determined current angle in order to control the reactive power and when injecting back the power to the grid, it must return current in a similar sinusoidal form trying inject in power stabilization way [62, 66, 67, 68, 69]. Bidirectional chargers are only expected to work in the Level 2 power level (section 1.4.1) because the power limitations in Level 1 (less than 1,9 kW) and the connection time in Level 3 (which is conceived to be less than 1 hour) [2].

1.4.3 On-board and off-board chargers

The vehicle's charger location has been under discussion since the beginning of EV's deployment. Basically, two possible locations exist for the chargers: on-board and off-board.

On-board location allows to recharge the vehicle anywhere (when an appropriate power source is available) due to the fact that are power electronics of the vehicle the responsible for the batteries' charging. This location gives more flexibility to the driver because only has to look for a power outlet regardless the standard [2]. However, due to cost, weight and space limitations [70, 71, 72], this location only allows *Level 1* charging level.

In the other hand, off-board chargers reduce the weight and the space of the battery charger enhancing the vehicles electric range. Additionally, due to the fact that the charger is off-board the vehicle, the limitations of weight and space are reduced and this configuration allows *Level 2* and *Level 3*. Nevertheless, the off-board charging location option is less flexible in the sense that the vehicle's owner needs to know the exact spots where the battery can be recharged due to the typology and standards of the vehicle. It is important to highlight that in this type of charger location, the risk of vandalism needs to be taken into account [73].

1.4.4 Conductive and Inductive charging

When recharging the vehicle two main possibilities exist: conductive and inductive charging. In conductive charging, the cable is needed to connect the EV with the power outlet [3]. It is the most frequent used option and it allows the three charging levels (*Level 1*, *Level 2* and *Level 3*). The main drawback of this option is that a cable is needed and there is no feasible possibility to recharge the vehicle while moving.

The inductive charging mode uses the electro-magnetic induction principle to transfer the power from the charger to the vehicle. This charging mode does not need any cable to perform the charge and therefore the EV's recharge can be performed while the EV is parked or stopped at a traffic light (*stationary*) or when the vehicle is moving (*contactless roadbed EV charging*). This alternative reduces the necessity of fast-charge infrastructure due to the fact that the recharge can be performed while traveling, and thus the recommended charging levels for this mode are *Level 1* and *Level 2*. However, the major drawback of this alternative are the low power density and efficiencies reached through this mode and specially the manufacturing complexity of the needed infrastructure to perform the recharge [74, 75, 76, 77, 77].

1.5 Impact of the charging into the grid

When studying the impact of an EV fleet recharge in a grid, several aspects have to be considered prior to starting the process. Firstly, the electric grid used in the study, taking into account the type of grid, its topology, its voltage level and daily load profile is important. Secondly, the EV type, its battery features and the EV fleet modelling should be defined, and finally, the recharging control strategy has to be considered.

When studying the impact of EV recharge on electric grids, most of the authors [78, 79, 80, 81]chose the distribution grid type to perform their simulations. The IEEE has standardised distribution models and available data from real grids corresponding to distribution grids.

Regarding the load profile modelling, [78] used the hourly average household load curve (available from the RELOAD data base used by the Electricity Module of the National Energy Modelling System (NEMS)). A one year period with three different day types (typical weekday, weekend and peak day) and nine load types (space cooling, space heating, water heating, cooking, cloth clothes drying, refrigeration, freezing, lighting and others) were taken into consideration. In [79], a household load profile was extracted from the measurements from [82]. These measurements were taken during over the course of 24 hours in 15-minute intervals with a resolution of 15 minutes during on an arbitrary winter day. Random load profiles based on probability density functions were used in [83]. Finally, in [81], grid load profiles were extracted from from the Stockholm Office of Research and Statistics, 2009 [84] (most critical case). Regarding EV modelling, most authors used a generic EV model. However, other authors chose a real model, such as the Chevy Volt [78]. The driving ranges of electric vehicles differ amongst the different types of EVs in [78, 81]: the values for the driving range of electric vehicles are between 32.7 km and 64.37 km. However, regarding the state of charge (SOC) for starting the recharge, the values established for the different types are similar , between 20% and 30% [78, 79, 80].

Depending on the chosen EV typology, the capacity of its batteries varies drastically. For Plug-in Hybrid EV batteries, the capacity values reported in literature are: 8 kWh [83], 8.2 kWh (2.7h of recharging time) [81] and 11 kWh (8.8 kWh considering minimum allowable SOC) [79]. In contrast, pure EVs have a capacity of 16 kWh, which almost doubles the capacity of the studied Plug-in Hybrid EVs [78].

For the specific case of the Chevy Volt EV, the main features of its lithium-ion battery are: an energy of 16 kWh, a voltage of 320 V to 350 V, a full recharge time from 6 to 6.5 hours using a 110V outlet and an electric driving

range of 64.37 km (40 miles) [78].

Considering vehicle fleet modelling, several authors have taken into account the average travelled distance, the methodology for the fleet modelling and the penetration of EVs into the grid.

The travelled distance indicates the required capacity for the battery and the energy consumed by the proposed EV. The values proposed for the travelled distance per day are 0.01 km/day to 16.1 km/day [83], 16.1 km/day to 32.2 km/day [83] or 32.7 km/day [81].

Regarding the methodology for fleet modelling, in [78], its authors estimate how many vehicles would be in a transformer based on the established EV penetration and also check the transformer loading capacity. Other authors have modelled the vehicle fleet as a single large battery which comprises the sum of all batteries [80]. And finally, other authors estimated the total energy amount for private car transportation for the entire year and then it was divided by 365 in order to obtain the energy for a single day [81].

Finally, for the EV penetration, most authors use values from 0% to 20%-30% of the EV penetration [78, 79, 80, 83, 85], although one author makes the hypothesis of reaching 100% of the EV penetration [81].

The EV recharging control strategy determines how the EV obtains energy from the grid. These strategies are based on how and when the recharge is performed. According to the reviewed literature, the recharge can be performed on one of three levels: fast, quick or slow charge. The period of the day when the recharge is performed is usually determined by the peak and off-peak times of the daily load profile.

Four strategies are studied in [78]: slow charging when the vehicles arrive at home (6 pm), slow charging of peak charging, quick-charging (240V/30A) when the vehicles arrive at home (6 pm) and quick-charging (240V/30A) of peak charging. In order to deal with possible overloads in the transformer, the author proposes controlling household loads when charging vehicles through an Advanced Metering Infrastructure (AMI) and performing a stagger charge for the EV's recharge.

In [79], two possibilities are suggested: uncoordinated and coordinated charging. Uncoordinated charging is based on the concept in which each individual vehicle starts the recharge at a random time step, while with coordinated charging, the recharge is performed by minimising the grid's power losses through an optimisation problem, using quadratic programming and dynamic programming. In [81], the concept of controlled recharges is also suggested. In the studied paper, unregulated charging establishes that people recharge their cars as soon as they get home if there are no economic incentives; while in the regulated charging through Demand Side

Management, the load is shifted from peak to valley periods.

Two strategies of recharge time distribution are suggested in [80]: continuous recharge and timed recharge (22-6h; 21-9h). It also proposes Vehicle to Grid (V2G) for the support of the grid in peak periods.

Finally, [86] introduces the concept of recharging the EV at the workplace in a recharging infrastructure where the recharge is feasible, independent of the number of available outlets and the line's loading. Four scenarios are suggested: a NO-EV scenario where no charging strategy is required, a Plug and Play scenario where no pricing mechanisms are used and where EV users recharge their cars if available outlets exist, an enhanced workplace access scenario where recharge at work is plausible even when the workplace does not offer any outlets, and an off-peak scenario where the recharge is performed between 6am and 8pm.

Simulating the most realistic scenarios is critical in order to assess the grid impact of recharging EVs. The aim of this PhD thesis is to model, in the most detailed way, the recharge load curve of EVs using detailed battery models. The most commonly used analysis reported in literature [78, 79, 87, 80, 81, 83, 85] uses the constant load model, which, as a conservative approach, presents the worst case, with the disadvantage that the grid impact will be overestimated. In order to proof the grid impact analysis method using detailed battery modelling, a standardised IEEE grid has been adapted to reproduce a typical distribution grid in Barcelona, combined with mobility patterns. The steps to achieve these goals are: modelling the electrical system, establishing the rules for the probabilistic model for household electrical demands and the EV demand (due to its recharge), by implementing the previous conditions in a grid and analysing the results obtained through the Monte Carlo Method.

Part I

Probabilistic analysis basis and modelling

Chapter 2

Probabilistic Analysis

A probabilistic analysis is based on application of statistics for probability assessment of uncertainty. Its core is the idea of representing information through probability densities. The methodology for probabilistic uncertainty analysis follows these general steps:

- Modeling inputs
  It includes the identification of all parameters that may contribute to the uncertainty, the collection of the stochastic data and the processing of such data to describe and represent uncertainty by probability distribution functions.

- Modeling dependence of input data
  Determine correlation of input variables is needed.

- Probabilistic load flow
  Propagation of uncertainty through statistical sampling of the input into the objective function in multiple runs and presentation of outputs as probability distribution functions.

2.1 Modeling inputs

A probabilistic analysis needs to obtain the probability distribution functions that describe and represent the uncertainty of inputs. The modeling of such random variables can be done from their statistical data. Utilities usually collect sample values of the performance of the system variables. In most cases, such data can be used for probabilistic analysis by codified into a probability density functions. The statistical inference can be performed in four ways [88]:

- by developing a non-parametric or numerically defined distribution,
- by fitting one of the standard theoretical distributions,
- by determining the maximum entropy distribution,
- by subjective codification of judgement.

Mean and variance are the basic descriptors of a random variable. A number of methods can be used for estimation of distribution parameters from the samples: the method of moments, the method of maximum likelihood and the Bayesian method [88, 89]. However, the exact values of such parameters are unknown and the statistic computed is an estimator. The method of moments is usually used. It uses as sample moment the estimators of the population moments, namely, sample mean $\overline{x}$ and sample variance s^2.

The probability distribution models that describe the behavior of random variables from statistical information can be generated by either fitting a numerically defined curve into a histogram or fitting one of the theoretical distributions. In order to verify the selected theoretical distribution for representing random variables, statistical tests, known as goodness-of-fit test, should be performed to validate the appropriateness of the selection. Among the number of continuous probability densities, *Normal* or *Gaussian* and *Weibull* distributions are commonly used in power systems studies [88].

Loads at power systems have been traditionally modeled according to a normal distribution [90, 91, 92]. The load modeling and forecasting is affected by several factors as type of customer, time, weather and economic trends. Load forecasting normally have to consider variations in human behavior, environmental and economic conditions, and electrical appliances and installations. Load forecasting has become very important for utilities and a lot of methods are being developed as regression analysis, neural networks and decision tree [93, 94]. Load present a high dependence of cyclic

human behavior for seasons, day of week and time of day [95]. Such dependence can be removed dividing the load in different groups with similar statistical characteristics, that is, considering time-frames [96, 97, 98]. The load can be modeled as a normal distribution at each time-frame. For example, in [99] the daily load is classified into four different groups: from Tuesday to Friday, Monday, Saturday and Sunday.

Probabilistic analysis of traditional power systems have mostly included only the uncertainty of demand. In modern power systems, a significant part of power production is expected to be provided by renewable based generation units. Thus, the generation of traditional power plants should be operated and controlled according to the generation of renewable based units, taking into account the system restrictions [100]. Therefore, forecasting of such renewable based generation has an important role and a lot of prediction models are proposed, above all for wind power [101, 102, 103].

Load following generation might be modeled as load, that is, as normal distribution for different time-frames. However, generation units based on renewable sources poses new challenges, since the variability of the prime movers is important and these neither follow a Gaussian *pdf* nor may present a time dependence. For example, wind speed is sometimes modeled as a Weibull distribution. The energy conversion system, that is, the wind turbine, presents a curve that provides the output power from each wind speed. As Figure 2.1 depicts, the distribution of the power generated by a wind turbine presents a concentration at the zero and the nominal output power, and then the power of wind turbines can not be modeled as a Weibull distribution.

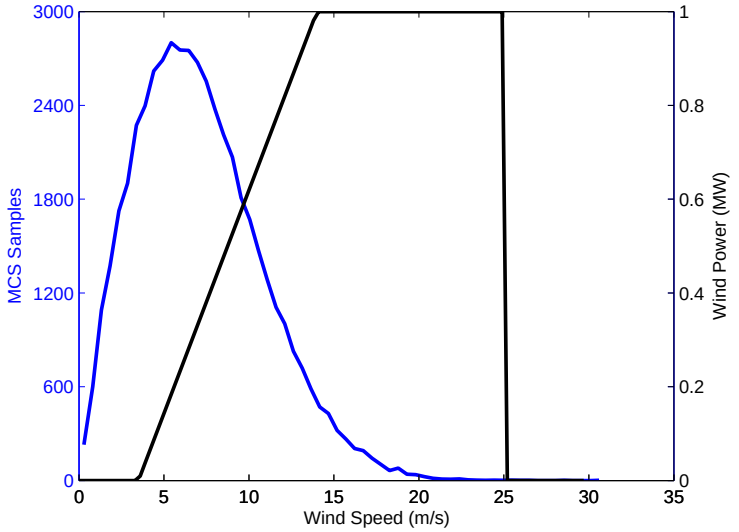

(a) Weibull distribution of wind speed with mean 8 m/s and shape parameter of 2. Power curve of wind turbine with $v_{cut-in} = 3.5$ m/s, $v_{rated} = 14$ m/s, $v_{cut-off} = 25$ m/s

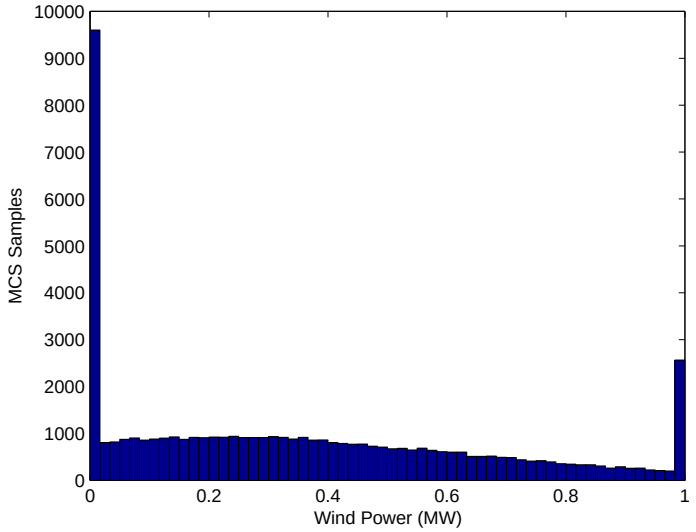

(b) Output power of 1 MW wind turbine

Figure 2.1: Speed/power curve and output power of a wind turbine.

2.2 Modeling the stochastic dependencies

After deriving the probability distribution function model of each system input (called marginal distribution), two methodologies can be used for modeling the stochastic dependencies:

- The Stochastic Bounds Methodology (SBM)
  It is applied in order to tackle model stochastic dependencies through the definition of stochastic bounds, i.e. extreme dependence structures that can bound all real cases [104].

- The Joint Normal Transform (JNT)
  It is used when it is required to model the exact dependence structure between clusters, based on the mutual correlations obtained by data analysis [105].

In general, stochastic generators and system loads situated in relatively small geographic areas are highly correlated, that is, they follow similar fluctuations. Thus, these can be clustered in groups that has a strong positive correlation in order to reduce the number of variables.

On one hand, the SBM method provides the worst-case scenarios: independence (lower bound) and comonotonicity (upper bound). This methodology permits a better understanding of the impact of DG based on renewable sources, providing important information for assessing the risk of the system. This method can be very realistic in the cases of geographically small systems, due to the existence of strong positive dependencies between the system inputs, while it can lead to conservative results in large power systems due to the great differences between the lower stochastic bound and maximum stochastic bound that can appear.

On the other hand, JNT is a technique that proposes a more realistic dependence modeling of systems involving a large number of stochastic inputs. Thus, clusters of strongly positively correlated inputs are used and the exact dependence structure between the clusters is modeled based on some correlation matrix. This method is less time-simulation consuming than the SBM and surely more accurate, as it deals with the precise relationship among clusters. However, the data to feed it is definitely harder to obtain, because such correlations are not readily available.

It should be pointed out when measuring the dependence if the functions are linear or not. The Pearson correlation (normalized covariance) is useful for measuring linear dependence, that is, for probability functions that are linear as the normal distribution. However, it may lead to counter-intuitive

results for non-linear functions. Therefore, other measures of correlation should be used if non-linear functions are considered. There are different methods to cope with this issue, as the Spearman correlation coefficient for ranked data, the Kendall τ coefficient, and the point-biserial and phi correlation coefficients [106].

This approach for measuring and modeling the dependence of non-linear functions is described in [107] and the case study is reproduced in [108]. Further work regarding dependence structures can be found in [109].

2.3 Probabilistic Load Flow

Load flow equations are a set of non-linear equations with multi-variable inputs. The probabilistic analysis when both generation and load have a stochastic behavior can be performed through a probabilistic load flow (PLF). There are two main approaches for PLF: analytical or numerical. The evolution of such methods can be found in [110] and more recently in [111].

The analytical method is usually referred to as PLF in a narrow sense [88]. It were firstly proposed in the seventies [112] and have included DG units lately [113, 114]. However, such method originally assumes a linearization of the load flow equations and independence of input variables that can lead to not exact results. Different methods have been proposed to diminish such errors and improve the PLF [115, 116, 117, 118, 113, 119, 114, 120, 121, 122].

The numerical method is normally based on the Monte Carlo (MC) simulation method. MC simulation has been widely applied to any aspects of power systems involving random variables [88]. The two main features of MC simulation are random number generation and random sampling. MC based load flow consists on applying such samples, generated according to the probability distribution functions of generation and loads and their correlations, into deterministic load flow equations and computing statistically the results, that is, the voltages, angles and power flows. Examples of MC method applied to PLF for systems with DG units can be found at [123, 124, 125].

The Monte Carlo simulation, although more time consuming, is the most suitable method for PLF in order to overcome the limits of the analytical methods and deal with multivariate uncertainty considering different timeframes and when there are complex relations between systems inputs or such inputs are not linear [98].

Chapter 3

Battery model

In order to perform further simulations, this chapter describes the mathematical model of the EV's batteries. Mainly, three types of battery model exist: the empirical model, the electro-chemical model and the electrical model. The chosen model is the electrical due to its easy implementation and due to the fact that it considers the charge level of the battery. Additionally, this model is able to represent the charge/discharge cycles of the battery. With this model the four main battery types can be studied: Lead-acid, Lithium, Nickel-Cadmium and Nickel metal hydride.

3.1 Battery basic concepts

As an introduction to this chapter, the following concepts regarding the batteries performance are defined below:

C rate The C rate is a variable that stands for the current that a battery can sustain during an hour. For example, a 1C rate indicates that a battery of 1,8 Ah would be discharged in 1 hour at a current of 1,8 A. A 2C rate means that the same battery would be discharged at a current of 3,6 A in half-hour.

Peukert's Law The Peukert's law relates the capacity of a battery with its current; the capacity of a battery decreases at higher currents. It establishes that the voltage drop is a direct consequence of the internal resistance of the battery. Additionally, it determines that for high current rates in a battery only the most superficial layers of a battery intervene and therefore less energy is delivered.

3.2 Battery model of the discharging process

The model is based on Trembay's model [126] and it is represented by a controlled voltage source with an internal resistance (figure 3.1).

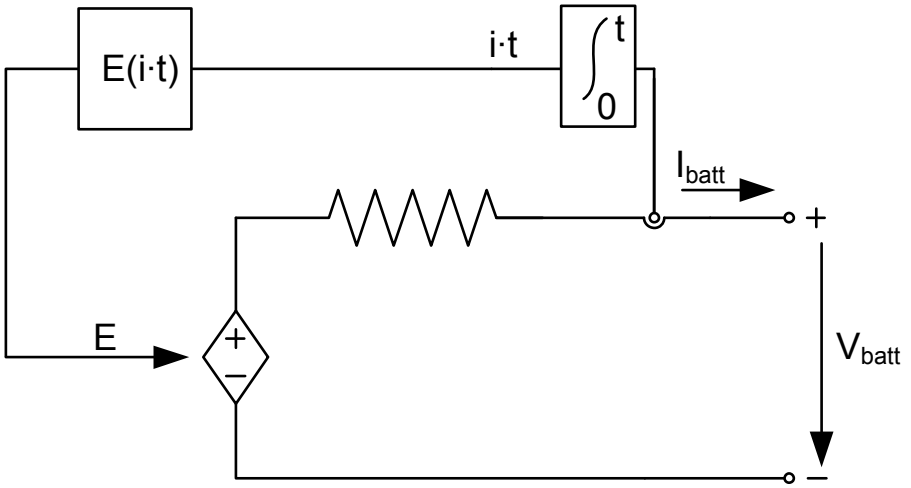

Figure 3.1: Trembay's battery electrical model

The battery voltage during its discharge yields in equations 3.1, 3.2 and 3.3.

$$E = E_0 - K \cdot \frac{Q}{Q - it} + A \cdot exp(-B \cdot it) \tag{3.1}$$

$$A = E_{full} - E_{exp} \tag{3.2}$$

$$V_{batt} = E - R \cdot i \tag{3.3}$$

Where:

- E= voltage without a load [V]
- E_0= constant voltage of the battery [V]
- K= polarization voltage [V]
- Q= battery capacity [Ah]

- it= actual battery capacity [Ah]
- B= time constant $[Ah^{-1}]$
- V_{batt}= battery voltage [V]
- A= voltage drop of the exponential region [V]
- R= internal resistance [Ω]
- i= current of the battery [A]

Equations 3.1 and 3.3 model a non-linear voltage which is affected by the current's value and with the state of charge of the battery. This model shows the fact that when the battery is completely depleted and no current is flowing, the voltage drops. Additionally, this model also considers that the maximum voltage is reached when the battery is fully charged.

The model can be divided in three zones according its behaviour (figure 3.2). The nominal section which is represented by $(K \cdot \frac{Q}{Q-it})$ comes from Shepherd's original model [127], whereas the exponential term $(A \cdot exp(-B \cdot it))$ was added in order to cope with the initial exponential behaviour of the discharge process. The constant term E_0 is responsible for shifting the curve through the vertical axis in order to adjust the values to the battery features.

However, the presented model has the following limitations or previous hypothesis:

- Constant internal resistance during charge/discharge cycles.
- Battery's capacity remains constant.
- Temperature has no effect on charge/discharge cycles.
- Auto-discharge effect is disregarded.
- Memory effect is not considered.
- Current is considered negative during the charge process and positive for the discharge process.

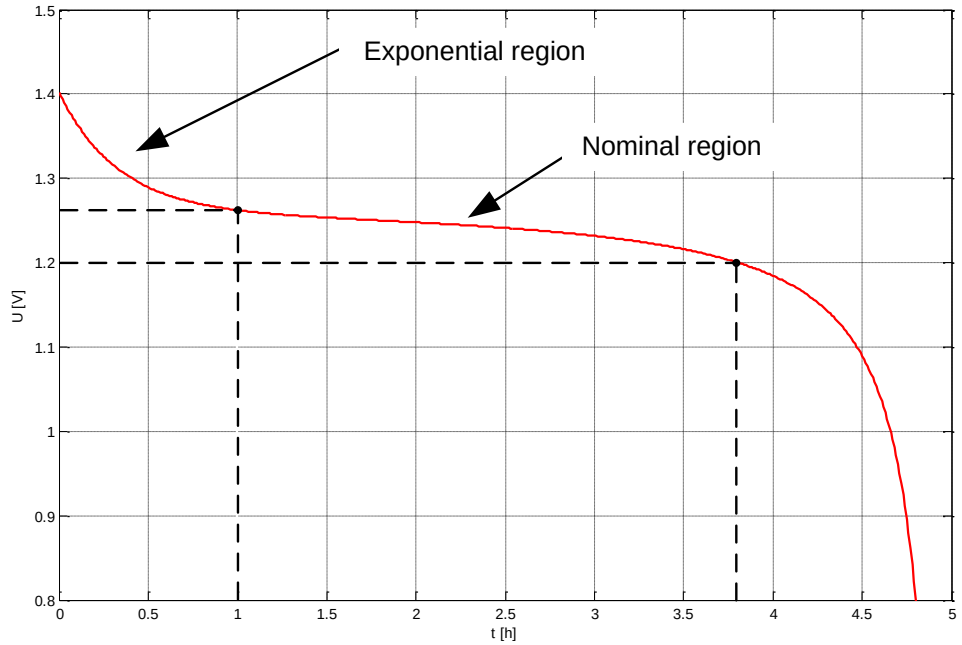

Figure 3.2: Nickel metal hydride battery, 1,2 V and 6,5 Ah

3.2.1 Obtention of battery's characteristics parameters

Whereas most of the parameters of the model can be obtained directly from the battery datasheet, others have to be calculated from the discharge curve.

Below there is an example of a battery model obtention through its discharge curve (figure 3.3) and with the following initial parameters:

- R=0,0046 Ω
- Q=6,5 Ah
- V=1,2 V

The three points from the figure 3.3 with known values used in order to get the model are:

- E_{full}: voltage when the battery is fully charged.
- E_{exp}: voltage when the exponential region ends and the nominal region starts.

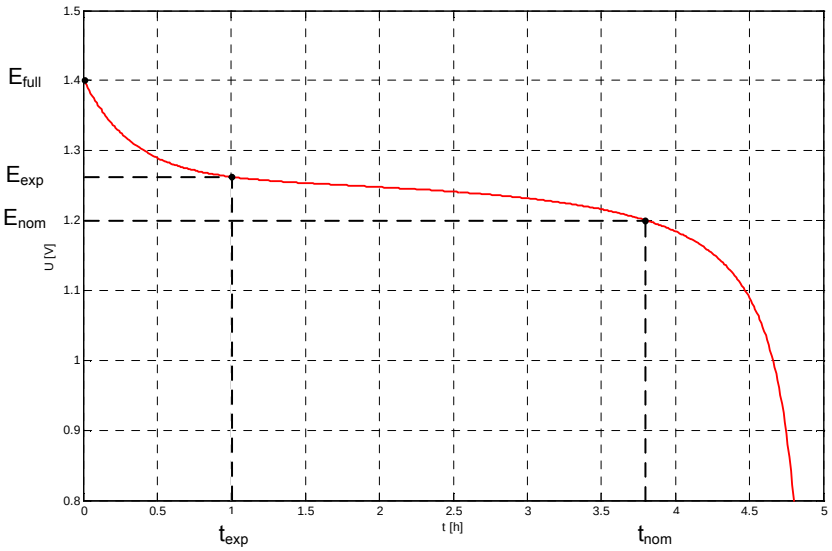

Figure 3.3: Discharge curve at 0,2 C.

- E_{nom}: voltage when the nominal region ends.
- Q_{nom}: battery's capacity when the nominal region ends.

With the previous given values, the first step in the process is getting the parameters of the exponential region $A \cdot exp(-B \cdot it)$.

- A: exponential region voltage drop

$$A = E_{full} - E_{exp} = 1,4V - 1,26V = 0,14V$$

- B: exponential region discharge constant

$$A \cdot exp(-B \cdot it) = A \cdot exp(\frac{-t}{\tau}) \Rightarrow \tau = \frac{1}{B \cdot i}$$

$$3\tau = t_{fexp} = \frac{3}{B \cdot i}$$

$$B = \frac{3}{t_{fexp} \cdot i} = 2,308Ah^{-1}$$

The parameters of the term $K \cdot \frac{Q}{Q-it}$ are calculated using equation 3.1:

- K= polarization voltage

$$\triangle E = (A - K) - (-K \cdot \frac{Q}{Q - Q_{nom}}) = K \cdot \frac{Q_{nom}}{Q - Q_{nom}} + A$$

$$\triangle E = E_{full} - E_{nom} + A \cdot exp(-B \cdot Q_{nom})$$

$$K = \frac{(E_{full} - E_{nom} + A \cdot exp(-B \cdot Q_{nom}) - A) \cdot (Q - Q_{nom})}{Q_{nom}}$$

$$K = \frac{1,4 - 1,2 + 0,14 \cdot exp(-2,308 \cdot 4,9) - 0,14) \cdot (6,5 - 4,9)}{4,9}$$

$$K = 0,01633V$$

Once all the parameters are known, the value for E_0 can be found:

- E_0: constant voltage of the battery

$$E_0 = E_{full} + K + R \cdot i - A$$

$$E_0 = 1.4 + 0.0125 + 0.0046 \cdot 1.3 - 0.15 = 1.272$$

3.3 Battery model of the charging process

The previous model (equations 3.1 and 3.3) can be adapted to the charging process (equation 3.4). Figure 3.4 shows the charging process of the same battery of the section 3.2.1.

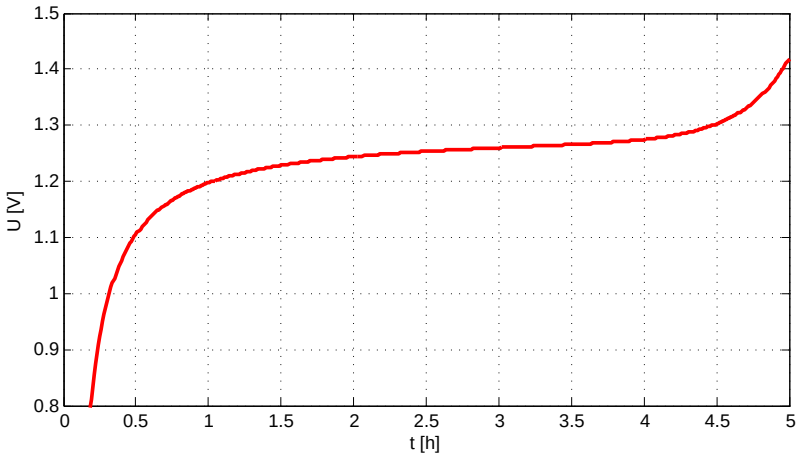

Figure 3.4: Voltage during the charging process.

$$E = E_0 + K \cdot \frac{Q}{it} + A \cdot exp(-B \cdot (it + Q)) \tag{3.4}$$

However, the equation 3.5 does not consider the possibility that the battery could be completely depleted. Additionally, it is a well known fact that the batteries' capacity never reach the 100% and its value is usually set at 80% in order to extend the live of the battery [128]. To cope with this issue, the hypothesis that the battery SoC is always in the range of the 15% and 95% is made.

Therefore, equation 3.5 solves this issue by introducing the term $Q \cdot \frac{Q_0}{100}$ which represents the initial SoC of the battery (where Q_0 is the initial SoC of the battery).

$$E = E_0 + K \cdot \frac{Q}{it - Q \cdot \frac{Q_0}{100}} + A \cdot exp(B \cdot (-it + Q \cdot \frac{Q_0}{100}) - B \cdot Q) \tag{3.5}$$

Nevertheless, analyzing several battery data-sheets, its been observed that the maximum voltage is reached at the 70-75% of the SoC [129, 130] instead

that a the 100% which is the value obtained in the equation 3.5. Equation 3.6 solves this issue (figure 3.5).

$$E = \begin{cases} E_0 + 0.7 \cdot K \cdot \frac{Q}{it - Q \cdot \frac{Q_0}{100}} + \\ +A \cdot exp(B \cdot (-it + Q \cdot \frac{Q_0}{100}) - 0.7 \cdot B \cdot Q) \quad if \quad (-it + Q \cdot \frac{Q_0}{100}) > 0.7 \\ \\ E_0 - K + A \qquad if \qquad (-it + Q \cdot \frac{Q_0}{100}) < 0.7 \end{cases} \tag{3.6}$$

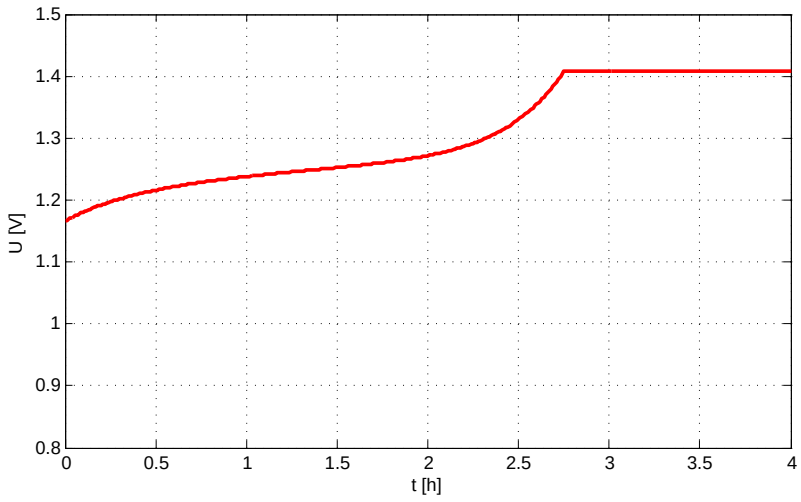

Figure 3.5: Charging voltage with Q_0 at 15% and correcting the maximum voltage at the 70% of the SoC.

3.3.1 Current modelling during the charging process

The charge of the batteries is performed in two stages (section 3.3): constant current in the first stage and constant voltage during the last stage (when SoC reaches the 70%). Once the constant voltage region is reached, the current decreases progressively.

Knowing that the charging current during the last stage can be modelled as

$$I = Q \cdot V_c \cdot exp(\tau \cdot t) \tag{3.7}$$

the time constant τ can be obtained when the reaming energy to charge is the 30% of the SoC. Being Q_W the maximum capacity of the battery and V_C the discharge speed, then:

$$\int_0^\infty E \cdot Q \cdot V_c \cdot exp(\tau \cdot t) = 0.3 \cdot Q_W \tag{3.8}$$

$$\tau = \frac{E \cdot Q \cdot V_c}{0.3 \cdot Q_W} \tag{3.9}$$

Combining equation 3.7 with the obtained τ and considering the two stages of the charging process, the model of the charging current can be calculated with equation 3.10.

$$I_{batt} = \begin{cases} Q \cdot V_c \cdot exp(\frac{(E_0+A-K)\cdot V_c \cdot Q}{0.3 \cdot Q_W} \cdot (-t + \frac{0.7}{V_c} - \frac{Q_0}{V_c \cdot 100})) \\ if \ \ (-it + Q \cdot \frac{Q_0}{100}) > 0.7 \\ \\ Q \cdot V_c \ \ if \ \ (-it + Q \cdot \frac{Q_0}{100}) < 0.7 \end{cases} \tag{3.10}$$

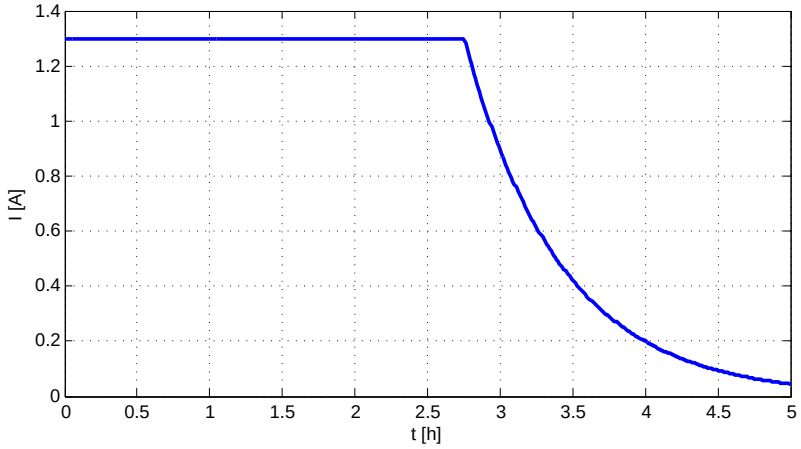

Figure 3.6: Charging current at 0.2 C.

3.4 Application of the battery modelling process to existing EVs

The obtention of the characteristic parameters of the batteries has been obtained through the Kokam data-sheets (in this case from Kokam SLPB 30205130H). The given values are for one individual cell of a battery. It is assumed that the discharge voltage of all battery cells will be equal during the process. The battery global voltage and the global internal resistance will be calculated by multiplying each cell voltage and each cell internal resistance by the number of cells in series and the global capacity multiplying each cell capacity by the number of cells in parallel. Table 3.1 shows the parameters used in the calculations.

Through the table 3.1, the battery parameters of different EVs are calculated (table 3.2).

Figures 3.7 and 3.8 show the difference amongst the Mini, the MIEV and Prius during a charging process.

Table 3.1: Cell parameters

Parameters	
E_{full}	4,2 V
E_{exp}	3,7 V
E_{nom}	3,5 V
t_{exp}	0,6 h
t_{nom}	0,9 h
I	1,0C A
R	5,5 mΩ
Q	5 Ah

Table 3.2: Battery parameters of different brands of EVs

	Mini Mini-E	**Mitsubishi I-MIEV**	**Tesla Tesla**	**Smart Fortwo**	**Toyota Plug-in Prius**
n cells in series	102	88	101	92	55
Q [Ah]	92	50	141	41	25
V [V]	380	330	375	340	201
Q [kWh]	35	16	53	14	5
R [Ohms]	0,3049	0,4840	0,1970	0,6171	0,6050
A	61,2	52,8	60,6	55,2	33,0
B	0,04658	0,08571	0,03040	0,10453	0,17143
K	3,04623	2,62812	3,01636	2,74758	1,64257
E0	398,30	343,63	394,39	359,25	214,77

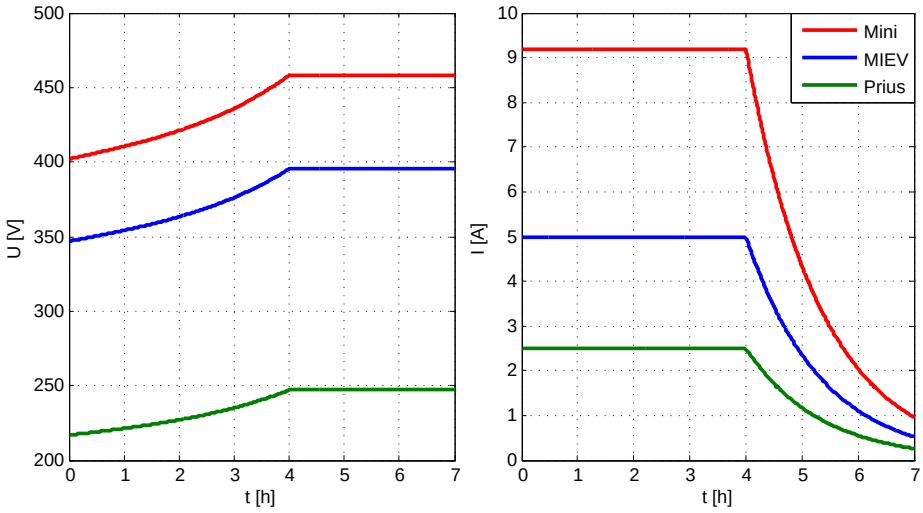

Figure 3.7: Voltage and current curves during the charging process ($Q_0 = 30\%$, $I = C10$).

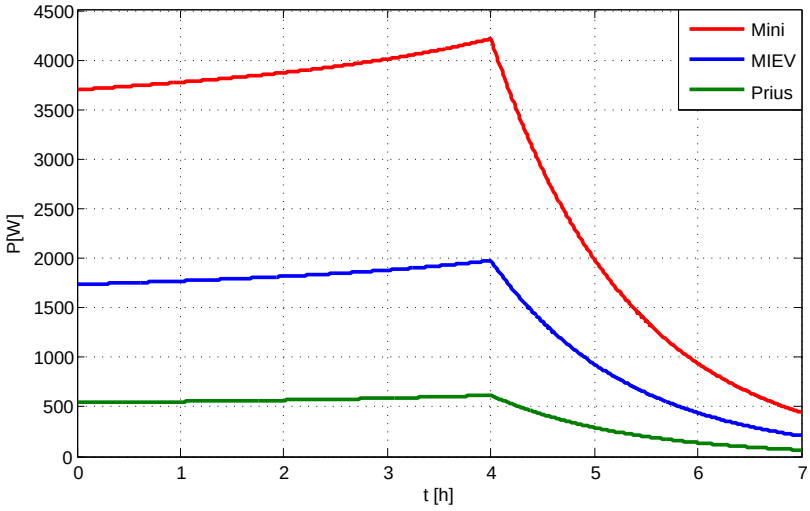

Figure 3.8: Power curve during the charging process ($Q_0 = 30\%$, $I = C10$).

Part II

Probabilistic models

Chapter 4

General model used for the study

Evaluating the impact of EV recharge on a grid through a deterministic analysis will only lead to the analysis of a specific scenario. In situations, where many possibilities are expected, the most common procedure is to analyse the most critical situation. However, the most critical situation is not always the most feasible one. The Monte Carlo method allows one to ensure that, under specific conditions, the results will be within a range of values with a predefined probability. Because the model will be under deterministic and probabilistic conditions, it is important to have a valid model for both situations.

4.1 Time horizon

The chosen time horizon for the simulations is the time lapse of 24 hours. This time horizon will be divided into one hour periods. The assumption of independence amongst different days is made; therefore, no data relationship is expected between day $t-1$ and day t.

4.2 Statistical Variables

When performing Monte Carlo simulations, the first step is to define the statistical variables. In this case the chosen statistical variables are:

- Regular electric demand
- Demand due to EV recharge

Both statistical variables will be modelled as regular loads, each one independent from the other one. In the same way as regular loads, these two variables have been modelled as an active and a reactive power, with the result of two inputs for each statistical variable; there is, however, just one

input, since active and reactive power are related through a fixed power factor which does not vary.

Both regular demand and the demand due to EV recharge are modelled as aggregated load in each node. Equation 7.2 shows the aggregation of EVs in each node b, for each hour h and each iteration i.

$$P_{b\_h\_i} = \sum_{j=1}^{n_{EV}} P_{EVj} \tag{4.1}$$

4.3 Description of the algorithm for the probabilistic load flow implementing the statistical model for the household and EV consumption

Figure 4.1 shows the algorithm for the load dispatching. The algorithm is based on the Monte Carlo method. In this diagram two main parts can be observed:

- Sample generation of the statistical variables
- Execution of probabilistic load flows

In the first part of the algorithm, the values for household and EV consumption are generated. Thus, the first step in the process is to obtain the statistical models for these two consumptions. For each different type of consumption, active and reactive power will be determined for each node, hour and iteration. As a result, the active and reactive power are $P_{DD\_h\_b\_i}$ and $Q_{DD\_h\_b\_i}$ for household demand and $P_{EV\_h\_b\_i}$ $Q_{EV\_h\_b\_i}$ for the EV consumption. The subscripts DD and EV stand for a consumption related to the household demand and for the EV recharge, respectively. The subscripts h, b and i correspond to the obtained value for the hour h, at the node b of the grid at the current iteration i. The statistical model for the household consumption, *"Statistical model of* $P_{DD\_h\_b\_i}$ $Q_{DD\_h\_b\_i}$*"*, is obtained by studying Spanish load profiles over the course of one year (Section 5). The statistical model for the EV consumption *"Statistical model of* $P_{EV\_h\_b\_i}$ $Q_{EV\_h\_b\_i}$*"*, comes from a study where variables, such as urban mobility, technical EV features and the number of EVs in the scenarios, are taken into account [131] (Section 6). The next step in this sample generation is to chose the number of iterations i and define the number of nodes b which comes defined for the study grid. Once these values have been defined, the samples for the household and EV consumption can be generated through their respective statistical models previously obtained.

In the second part of the algorithm, the probabilistic load flow is run. It consists of an iterative process where a deterministic load flow is performed with the previously generated probabilistic values for each node, each iteration and each hour. The results of this process are the voltages of each node per load flow and iteration, and the line and transformer loadings per load flow and iteration. All these values will allow the determination of the confidence intervals and therefore the tools to compare and evaluate the different generated scenarios.

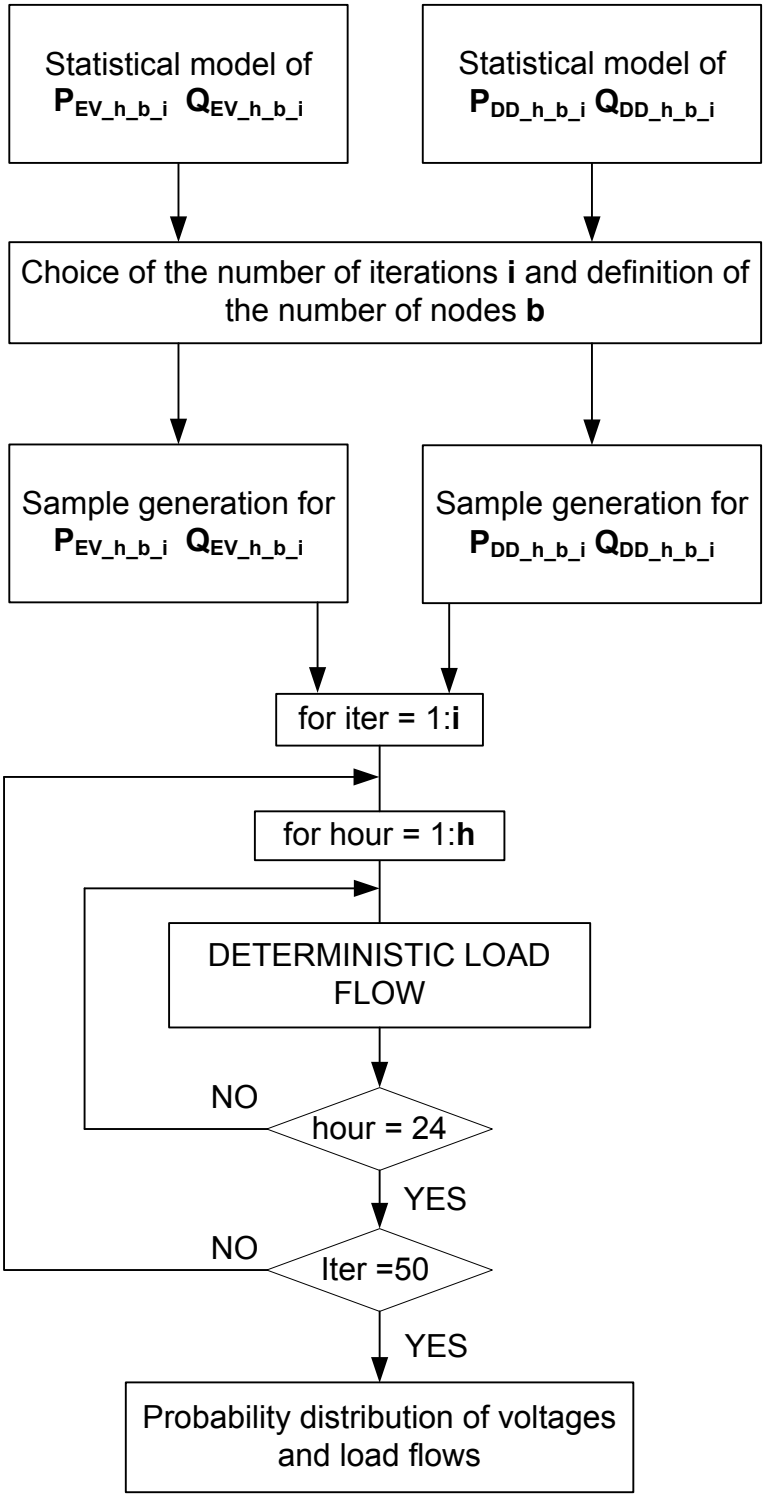

Figure 4.1: Flow diagram for the general procedure

Chapter 5

Generating the probabilistic model for the grid's electrical demand

Electrical consumption cycles can be classified depending on its predictable patterns. These patterns can be established either for seasons, for weekdays or for weekend days. For instance, weekdays and weekend days will have different curve shapes, even for the same week. The main factors that determine these patterns are climate and human behaviour. So therefore, it is expected that northern countries have different load patterns than tropical countries.

A method to obtain the probabilistic model for the electrical demand is presented in this section. This model is obtained through two steps:

1. The creation of a statistical model able to generate random values according to previously defined conditions.

2. The generation of samples for the performed load flows and for each iteration.

5.1 Data processing

In order to generate a probabilistic model for the electrical demand, two authors [132, 133] have concluded that using a normal distribution is a reasonable approach. As a result, this will be the distribution used in this study.

The data used to build the statistical model has been extracted from the Spanish TSO REE (*Red Eléctrica de España*) and corresponds to Spain's electricity demand from January to September of 2009. Figure 5.1 depicts the daily load profiles of Spain from January to September. Each line represents a day load profile and every month has a different line colour. Different

load patterns can be distinguished and since it is necessary to have an accurate model, this data is aggregated according to the similarities of the patterns.

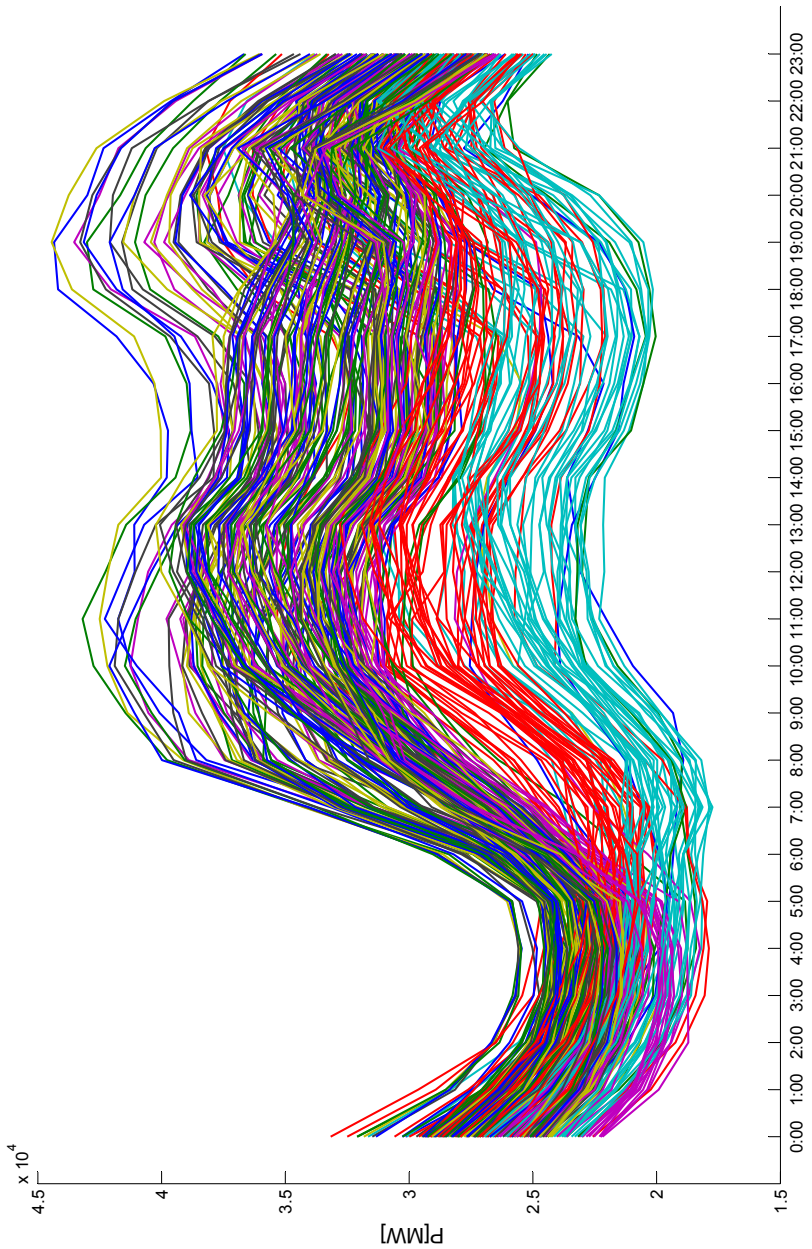

Figure 5.1: Daily load curves of Spain from January to September of 2009

The data corresponding to the months with a high variation of temperature (March, June and September) has not been considered because of the distortion caused in the model. The autumn months (October, November and December) have not been considered in the pattern definition because the results obtained in this season can be extended to the Spring's results [131]. Therefore, three patterns are established:

- Winter (January, February)
- Spring (April, May)
- Summer (July, August)

If the consumption profiles are grouped according to the previous classification, it is possible to get a probability distribution for each hour which follows a normal distribution [131]. As an example, Figure 5.2 shows a winter weekdays histogram for 24 hours of the power demand for Spain (Figure 5.2(a)) and its standard deviation (Figure 5.2(b)), both in MW.

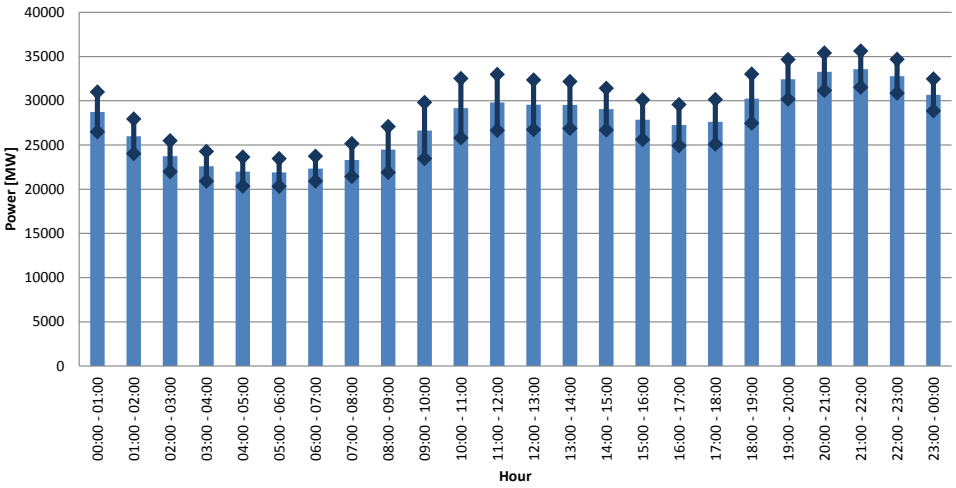

(a) Mean, maximum and minimum value of the power demand

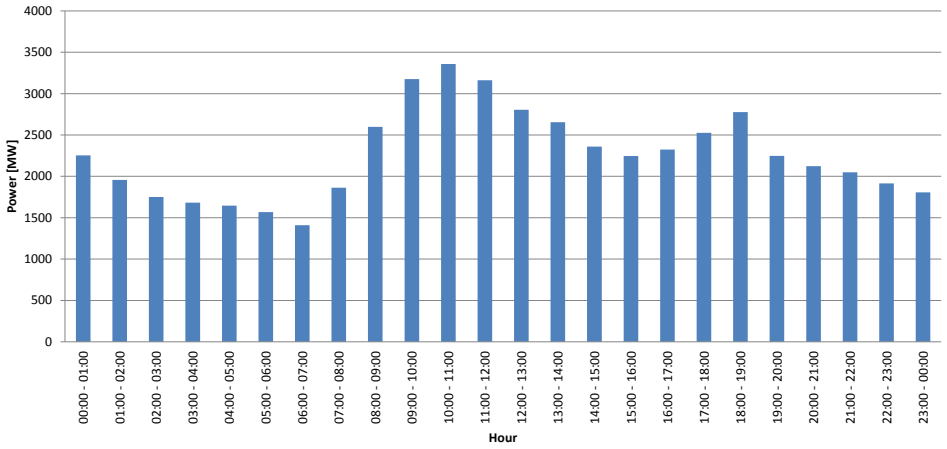

(b) Standard deviation of the power demand

Figure 5.2: Variation of the overall demand on a labour winter day of Spain

5.2 Adapting national demand to a standard distribution grid

Because the studied grid is a distribution grid for a specific region, it is necessary to adapt the load patterns extracted for the entire country. Therefore, the national load curve has been adapted to the study grid. The hypothesis that the placed transformers will be able to supply energy to all the types of loads (household, commercial and industrial) without exceeding the allowed loading levels when no EVs are connected to the grid is supported.

The process begins with the national load curve reduced to a unitary curve, and then a base change is performed in order to adapt the power to the capacity of each transformer station. In order to generate active and reactive power, the hypothesis of a constant power factor of 0,9 was made in order to comply with the worst case considered in the Spanish legislation [134].

Chapter 6

Generation of the probabilistic model for EV demand

The objective of this section is to model the consumption generated by the EV recharge in the distribution grid in order to evaluate its impact together with the household demand. The EV consumption is difficult to model in a deterministic way because it depends on factors such as urban mobility, the EVs' technical features and the number of EVs. Therefore, it appears to be necessary to create a methodology able to take into account all these factors and also able to generate a valid statistical variable for the EVs' consumption.

The main difficulty when creating the EV statistical variable is the lack of available data. Because of this, the statistical variable which represents the EV consumption cannot be obtained from historical data, but will have to be generated from a determined number of random variables following this process:

1. Determination of a study area.
2. Determination of the total number of vehicles through the total number of trips in our area during the whole day.
3. Distribution of the previously determined travels during the day hours.
4. Distribution of the EVs along the nodes of the grid in order to recharge.
5. Determination of the energy to be recharged for each vehicle (depends on SOC and on the penetration of EVs).
6. Association of each recharge to an EV battery type.

In general terms, the previously defined steps can be summarized in a two main stages methodology (Figure 6.1):

1. Generation of the EVs' number of connections for each hour, node and iteration.
2. Transformation of the number of connections to its corresponding consumed power aggregated per node.

Accordingly, the EVs' consumption will be obtained (following the defined methodology) through Monte Carlo method using the following random variables:

- Distribution of the EV along the grid nodes
- Connection time of the EV
- Load curve of the battery of the EV
- Energy consumed by the EV before its connection

Finally, in order to accomplish the objective of this chapter some assumption have been made during the process:

- One trip is equivalent to one vehicle.
- The 80% of the grid power is intended for domestic use.
- An EV must have its battery partially or completely discharged in order to start a recharge.
- An EV will always be able to recharge its battery because there will always be available outlets.
- It is assumed that EV drivers show a cautious attitude towards the possibility of ending up with a depleted battery and will therefore arrive at their destination before the battery is depleted.

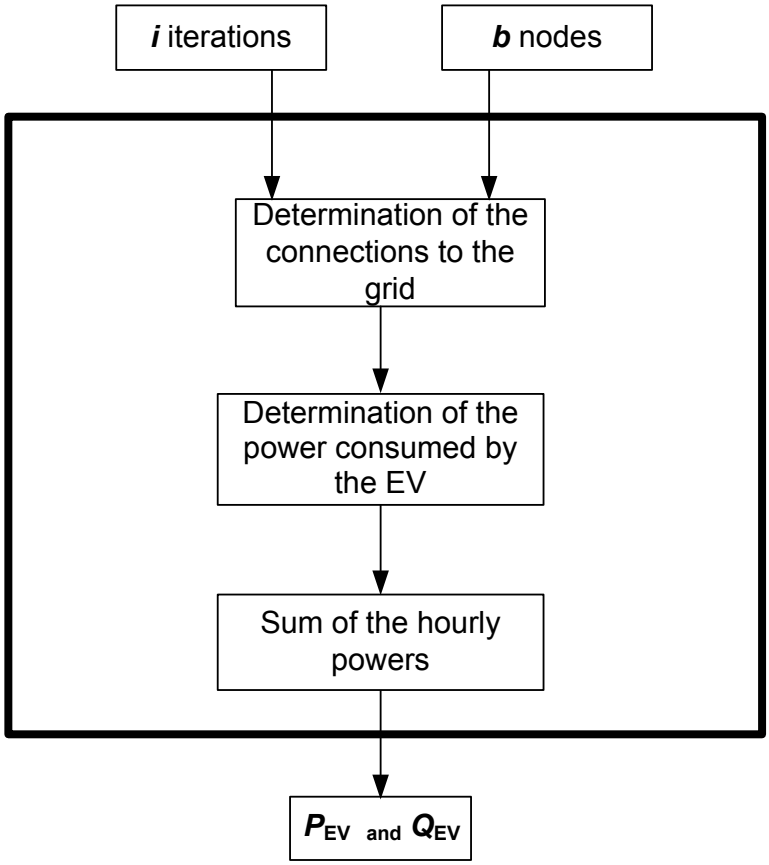

Figure 6.1: Flow diagram of the process *"Sample generation for EV active and reactive power (P_{EV} and Q_{EV})"*

6.1 Determination of the number of vehicles per hour in our scenario

In order to set how the EVs are distributed along the nodes of the grid to recharge their batteries, the following variables will be taken into account:

- Number of EVs in the scenario to study
- Distribution of the connection along the nodes of the grid
- Connection time of the EV

6.1.1 Number of EV in the studied scenario

Since each EV can travel several times a day, the number of EVs available does not represent the number of EVs that will recharge. Thus, the decisive variable is the number of trips per node, hour and iteration (Figure 6.2). Because the EVs' penetration depends on the chosen scenario, the first step is to estimate the number of trips for both combustion engine vehicles and for EVs, then establish a fraction of these as electrical. For the simulations in this paper, the values for the EVs' penetration are 20% and 40% of the full number of vehicles.

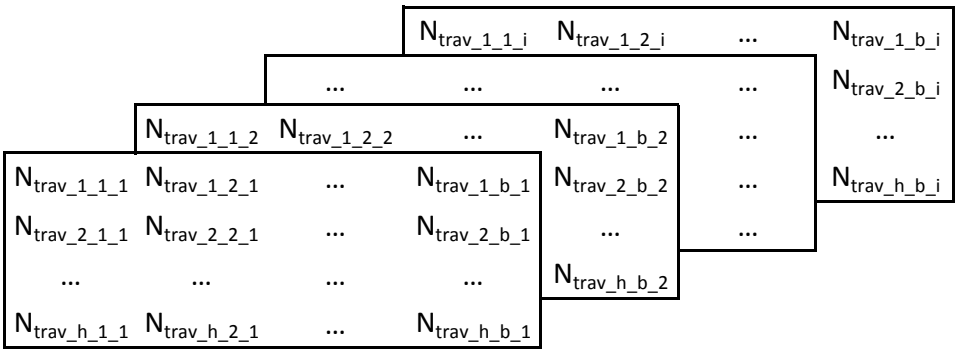

Figure 6.2: Matrix N_{trips}

In order to determine the number of EVs, it is necessary to set [131]:

- Number of houses (n_{houses})
- Number of vehicles per house($n_{veh/houses}$)
- Mean number of trips made for each vehicle in one day ($n_{trips/day}$)

- Ratio of how many of these trips are made through the private vehicle (F_{trips})

With these values it is possible to determine the trips in a day n_{trips_day} through equation 6.1. The number of houses is calculated by [131]

$$n_{trips\_day} = n_{houses} \cdot n_{veh/houses} \cdot n_{trips/day} \cdot F_{trips} \tag{6.1}$$

Because the studied grid is an urban distribution grid, the hypothesis that 80% of the grid power is for household use is made. It is also important to consider that the contracted power in urban areas is five times the grid's capacity [131]. Finally, we assume that the contracted power for each house is 4,4 kW [131].

$$n_{houses} = \frac{P_{Grid} \cdot 5 \cdot 0,8}{4,4} \tag{6.2}$$

6.1.2 Connection time of the EVs

The massive recharge of EVs during a specific time period could lead to an excessive demand of power that the system cannot deal with and to too low voltages that will break the current standards. Therefore, a realistic model is required to avoid this non-feasible situation. This model is achieved by implementing two scenarios:

1. The EV recharges its batteries after every trip (figure 6.3). For example: right after getting to work, during any stop made moving through the city, arriving home at the end of the day...

2. The EV recharges its batteries at the end of the day when all trips are completed (figure 6.4). For example, at the end of the day back at home when all the trips have been already made.

The connection time of the EVs is obtained from the mobility curve of the private transport in Barcelona [135]. Because the mean trip time is 21,11 minutes on weekdays and 28,34 minutes at weekends, it is assumed that vehicles will start their recharge in the same hour when the trip is started. As a consequence, the hourly recharge curve of the EVs will have the same pattern as the mobility curve for private transport (figure 6.3 and figure 6.4).

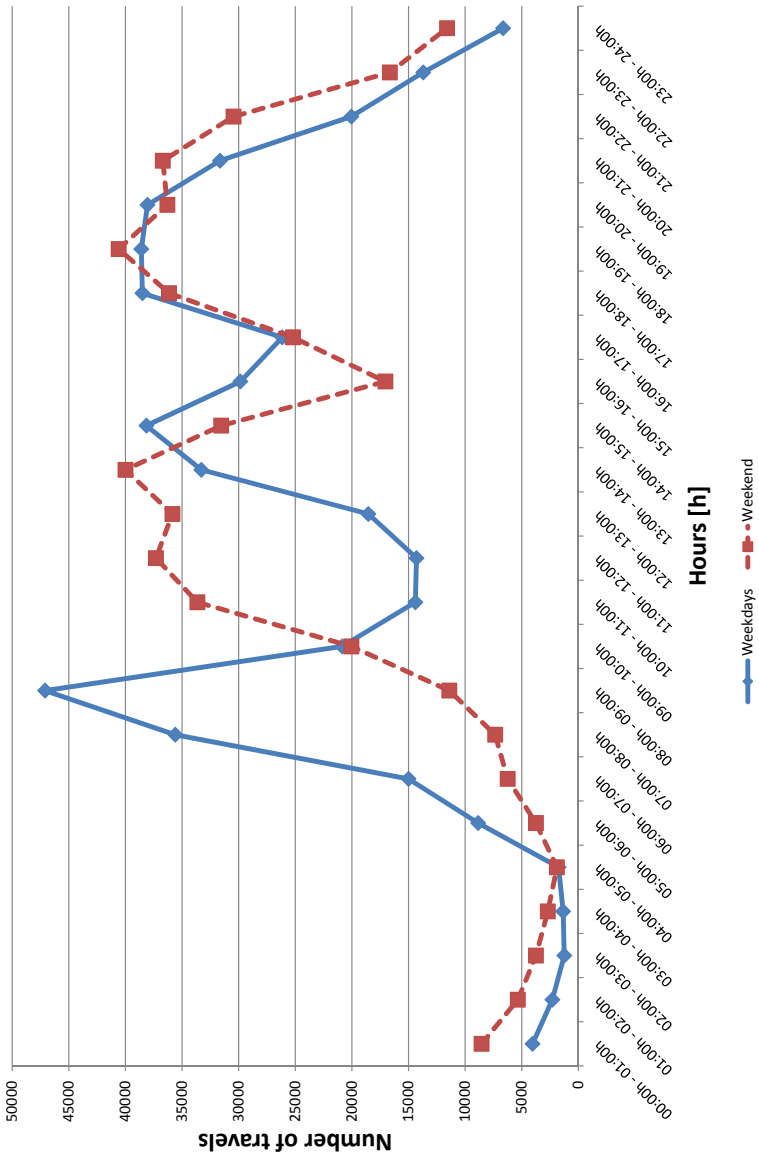

Figure 6.3: Mobility curve of the Metropolitan area of Barcelona of vehicles traveling inside the area

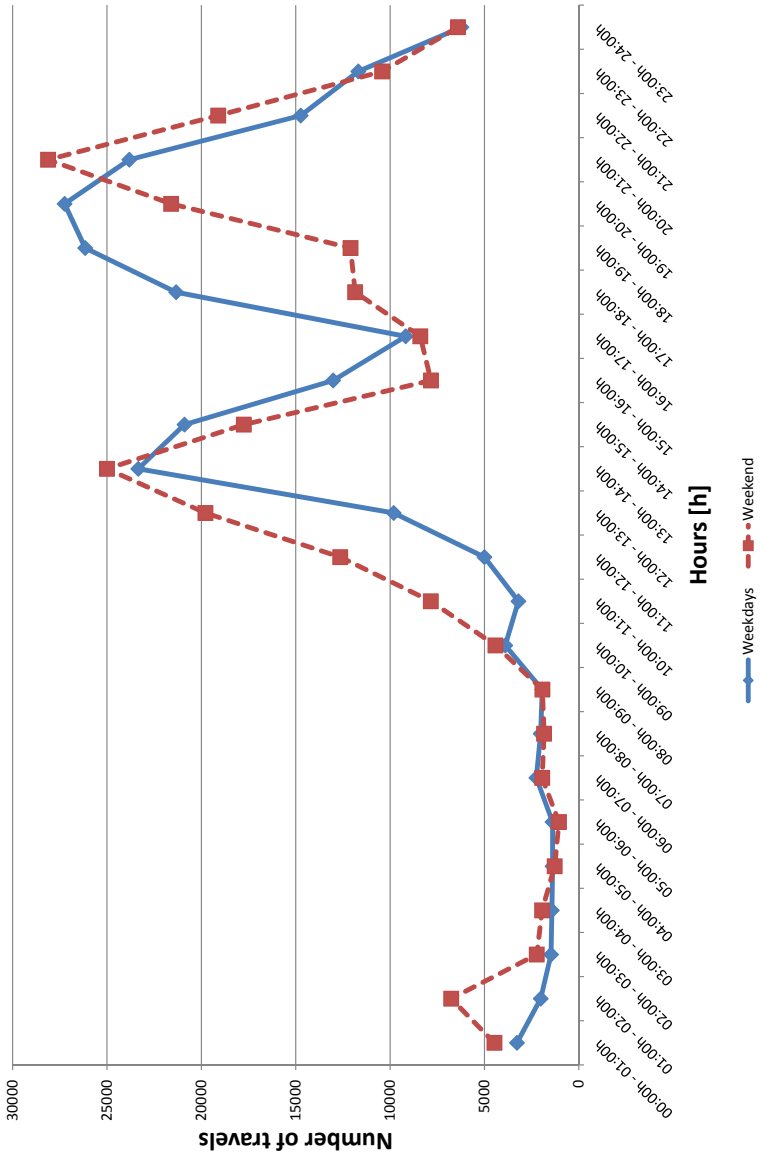

Figure 6.4: Mobility curve of the Metropolitan area of Barcelona of vehicles traveling outside the area

Although the mobility patterns in the entire Metropolitan area of Barcelona are known, it is necessary to adapt these to our area of study. Equation 6.3 shows how to adapt the number of travels to the proposed study grid with a specific power (N_{trips_hour}), where $n_{trips'\_day}$ are all trips in the metropolitan area of Barcelona during the day, n_{trips_day} are all trips in our area (with a specific power) during the day and $N_{trips'\_hour}$ are trips in Barcelona for the hour h.

$$N_{trips\_hour} = \frac{n_{trips\_day}}{n_{trips'\_day}} \cdot N_{trips'\_hour} = \begin{bmatrix} n_{trips\_1} \\ n_{trips\_2} \\ ... \\ n_{trips\_h} \end{bmatrix}, \tag{6.3}$$

In order to model the number of vehicles recharging at a specific time of the day as a non-deterministic variable, it can be assumed that the arrivals will follow a Poisson distribution [136]. The Poisson distribution establishes the probability that a number k of events could happen in a determined period of time if they occur with a known frequency and are independent of the time of the last event. In some situations, in which the expected value is bigger than 5, it is possible to transform the Poisson distribution into a normal function [137] (equation 6.4), where $N_{\mu\_trips\_h}$ stands for the vector with average values and $N_{\sigma\_trips\_h}$ stands for the vector with the standard deviations for each hour. Then, the values can be determined for each hour, node and iteration (figure 6.2).

$$N_{\mu\_trips\_h} = \begin{bmatrix} n_{trips\_1} \\ n_{trips\_2} \\ ... \\ n_{trips\_h} \end{bmatrix} \quad and \quad N_{\sigma\_trips\_h} = \begin{bmatrix} \sqrt{n_{trips\_1}} \\ \sqrt{n_{trips\_2}} \\ ... \\ \sqrt{n_{trips\_h}} \end{bmatrix} \tag{6.4}$$

6.2 Distribution of the EVs along the nodes of the grid

The assumption made for the distribution of the EVs along the nodes of the grid are as follows:

1. Each node has the same probability of recharging an EV.
2. The number of trips in the studied area remains constant. It is assumed that the number of trips going outside the studied area is the same as the number of trips going inside the studied area.

6.3 Consumed power associated with EV consumption

Once the number of trips has been determined, it is possible to associate each travel with an EV's recharge. In order to define each recharge, it is necessary to have previously defined the duration of the recharge, the amount of energy to be recharged and the battery's load curve. In summary, the analogy of the matrix active power of the EV's recharge for each hour, node and iteration will be obtained from the matrix number of trips.

6.3.1 Consumed power by EV recharge, $P_{EV\_h\_b\_i}$

Figure 6.5 describes the process of creating the vector for the consumed power associated with the EV's consumption. As can be seen from the figure, the needed inputs are: the *Number of trips* matrix ($n_{trips\_h\_b\_i}$), the probability distribution of the consumed energy and the probability distribution of the battery's capacity.

The *Number of trips* matrix ($n_{trips\_h\_b\_i}$) establishes the number of vehicles recharging for each hour, node and iteration (its obtainment process is described in Section 6.1).

It is important to highlight that even if two vehicles have travelled the same distance using the same battery, the process of recharging the battery does not necessarily have to be the same, since it directly depends on its SOC. Therefore, a statistical model for the total energy to be recharged has been generated from a list of batteries (Table 6.1). The total energy to be recharged is defined by equation 6.5, where C_e is the specific consumption. In this case it is 0,158 kWh/km, obtained as the mean from Table 6.1, and D is the travelled distance which follows a log normal distribution with a shape value of 1.929 and a scale factor of 1,508 [135, 131].

$$E_{cons\_EV} = C_e \cdot D \tag{6.5}$$

The type of battery which defines the load curve was also generated from (Table 6.1). A log normal function was created from the capacities to be generated for random batteries; and depending on the value, a known load curve from an existent model was assigned, as Figure 6.6 shows. Additionally, Figure 6.6 depicts in its label the location parameter (Loc), scale parameter ($Scale$) and sample size (N) of the log normal function obtained.

Once the number of the EV's trips is known, the EV's consumed energy per trip as well as the type of battery per trip are then determined. With these two variables, the power consumed during the EV recharge ($P_{EV\_h\_b\_i}$) is calculated. Additionally, this algorithm also considers the fact that the

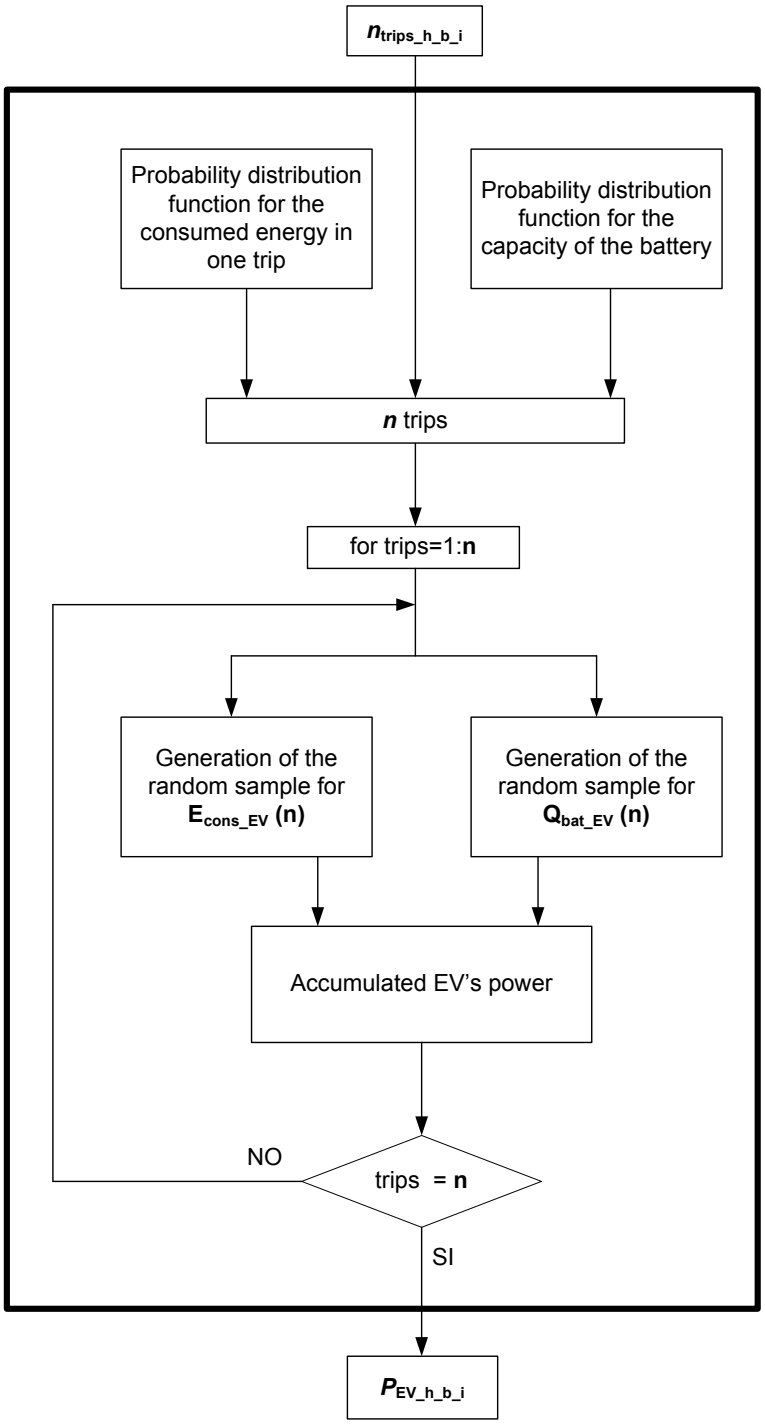

Figure 6.5: Flow diagram of the consumed power by the EV's recharge

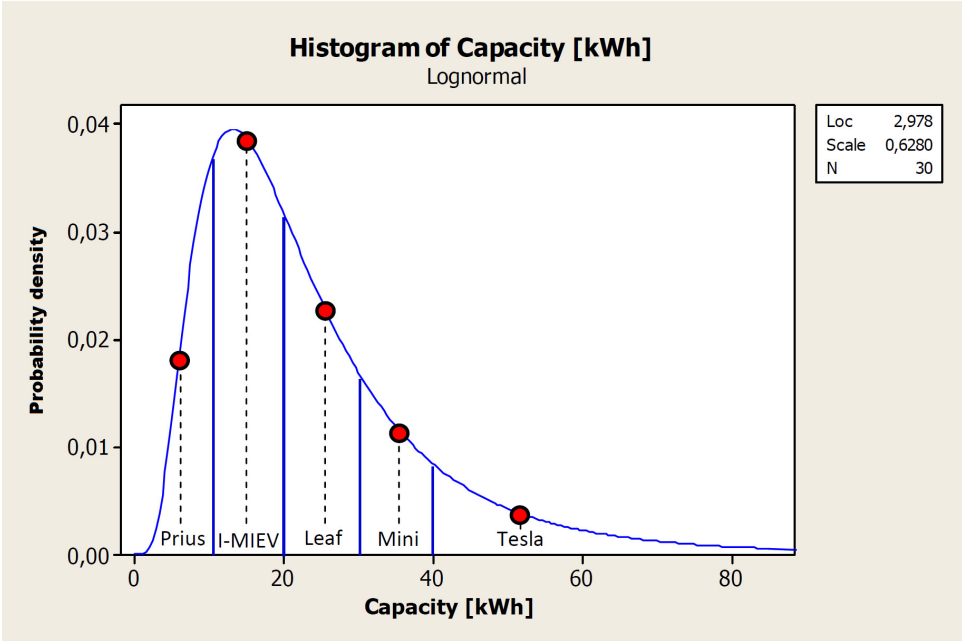

Figure 6.6: Distribution function of the batteries capacity

EV's recharge could last for more than one hour in the *Accumulated EV's power* block. As a result, the EV's power that would be in each node would be the power of the EVs that have arrived at the node b and the power of those which are still recharging because they had arrived during the previous hours.

Following this algorithm, the EV's power to recharge in each hour, node and iteration ($P_{EV\_h\_b\_i}$) can be obtained. It is important to note that this algorithm takes into account the random characteristics of the number of EV's that would recharge in each node, the consumed energy for each EV during its trip and the type of battery that the EV would have.

Finally, it can be drawn from that the connection time for each EV depends directly on the travelled distance D (which follows a log normal distribution) and the specific consumption C_e which depends on the type of battery (which also is chosen by following a log normal function).

Table 6.1: EV and Plug-in Hybrid EV Models, Battery Type and Capacity, and Consumption

Electric Vehicle (EV)	Capacity [kWh]	Consumption [kWh/km]	Technology
BYD F3DM	16,5	0,160	Li-Ion
BYD e6 (75kW)	59,4	0,160	Li-Ion
BYD e6 (200kW)	59,4	0,175	Li-Ion
CHANA BENNI	9,0	-	AGM
Micro-Vett Fiat 500	22,0	-	Li-Ion
Mitsubishi i MiEV	16,5	0,100	Li-Ion
Smart electric drive Coupe	14,5	0,122	Li-Ion
Subaru Estella	9,0	-	Li-Ion
Tata Indica Vista EV	26,5	0,133	Li-Ion
SEAT Leon Twin Drive Ecomotive	12,0	0,240	Li-Ion
Zytel Gorila	10,8	0,150	Lead-Acid
Opel Ampera	16,5	0,133	Li-Ion
REVA NXR	13,5	0,090	Li-Ion
Micro-Vett Fiorino M1-Fi(LC-EG)-Li	13,5	-	Li-Ion
Micro-Vett Fiorino M1-Fi(HC-Eg)-Li(S)	21,0	0,240	Li-Ion
Micro-Vett Fiorino M1-Qu(HC-Eg)-Li(S)	21,0	0,240	Li-Ion
Micro-Vett Fiorino M1-Qu(HC-Eg)-Li(L)	32,0	0,240	Li-Ion
Smart electric drive Cabrio	14,5	0,122	Li-Ion
Think City 2010	83,0	0,144	NiNa
Peugeot ION	16,5	0,125	Li-Ion
Tesla Roadster	51,5	0,231	Li-Ion
TOYOTA Prius Plug-In Hybrid	5,0	0,062	Li-Ion
Citroen C-Zero	16,5	-	Li-Ion
Mini-E	35,0	0,130	Li-Ion
Volkswagen Golf	26,5	-	Li-Ion
Nissan Leaf	24,0	-	Li-Ion
Chevrolet Volt	16,5	-	Li-Ion
Brusa Spyder	16,0	-	Li-Ion
Phoenix SUT	35,0	-	Li-Ion
Lumeneo Smera	10,0	-	Li-Ion

Part III

Study Case

Chapter 7

Study Case

In order to evaluate the impact caused by the EV on the grid, it is important to choose the scenario for the simulations, which basically consists of choosing a grid to be used. The type of grid chosen will define the accuracy of the results; thus, the more realistic the grid is, the more reliable the results will be.

When choosing the grid for the impact study, four aspects are important, namely: the real grid, the testing grid, medium voltage and low voltage. A real grid has the main advantage of its practically-oriented results, although it has the disadvantage of obtaining the data. On the other hand, a testing grid - not even being a real grid - has the advantage of the availability of the data and the certainty of working properly. Regarding the grid voltage level, the following assumption has been made: the extra high voltage grid (transmission grid) has been dismissed because this grid type is intended to deal with high amounts of energy and therefore the impact of the recharge of EVs will not have a clear effect. However, an MV (Medium Voltage) or LV (Low Voltage) distribution grid with a radial topology will allow a better interpretation of the results. Even though these grids do not have massive generation units, it is possible to find distributed generation units. Table 7.1 shows the advantages and disadvantages of the different types of grids.

Taking into account the specific aim of the study to be performed and the benefits and drawbacks analyzed in Table 7.1, the grid to be used will be a urban medium voltage grid. Due to the fact that it is no possible to use real data from an existing grid and neither its exact layout configuration and approximation has to be made. This approach consists in using a IEEE standard to deal with the issue of the layout configuration and to deal with the issue of the parameters and transformers the Spanish's *Distribute Generator Standards* will be used.

Table 7.1: Benefits and drawbacks of performing the study with different types of grids

Voltage	**Topology**	**Benefits**	**Drawbacks**
High	Meshed	Introduces the possibility of assessing the impact of large generation units. Lower error in the demand's modeling.	Due to the high short-circuit grid's power and its topology, a reduced impact on the grid is expected.
Medium	Radial	Brings the opportunity of introducing distributed generation units and assessing its impact. Lower error in the demand's modeling.	Due to the high short-circuit grid power, a reduced impact on the grid is expected.
Low	Radial	Due to its low short-circuit power, a high impact on the grid is expected.	It is not feasible to include all small generation units. Higher error in demand modeling.

7.1 Proposed grid

In order to perform the study, the test system chosen is the IEEE 37 bus test system because its length [138] (5.5 km) and its topology are makes this type of grid the closest test system to a typical distribution underground grid in Barcelona. Even through the IEEE 37 node test grid has features in common with the desired distribution grid, aspects like voltages and impedances have been adapted. Other grids were also studied, such as the IEEE 13 node and the IEEE 123 node, but were discarded because of their length.

In regard to the previous discussion, it has been concluded that the study will be based on an IEEE 37 node standard test feeder (Figure 7.1), but adapting it to 25 kV and with all the necessary adaptations for its elements (Table 7.2, Table 7.3 and Table 7.4). These parameters come from Endesa's technical standards published in their web page [139, 140, 141, 142, 143] or from their manufacturers or providers [144, 145].

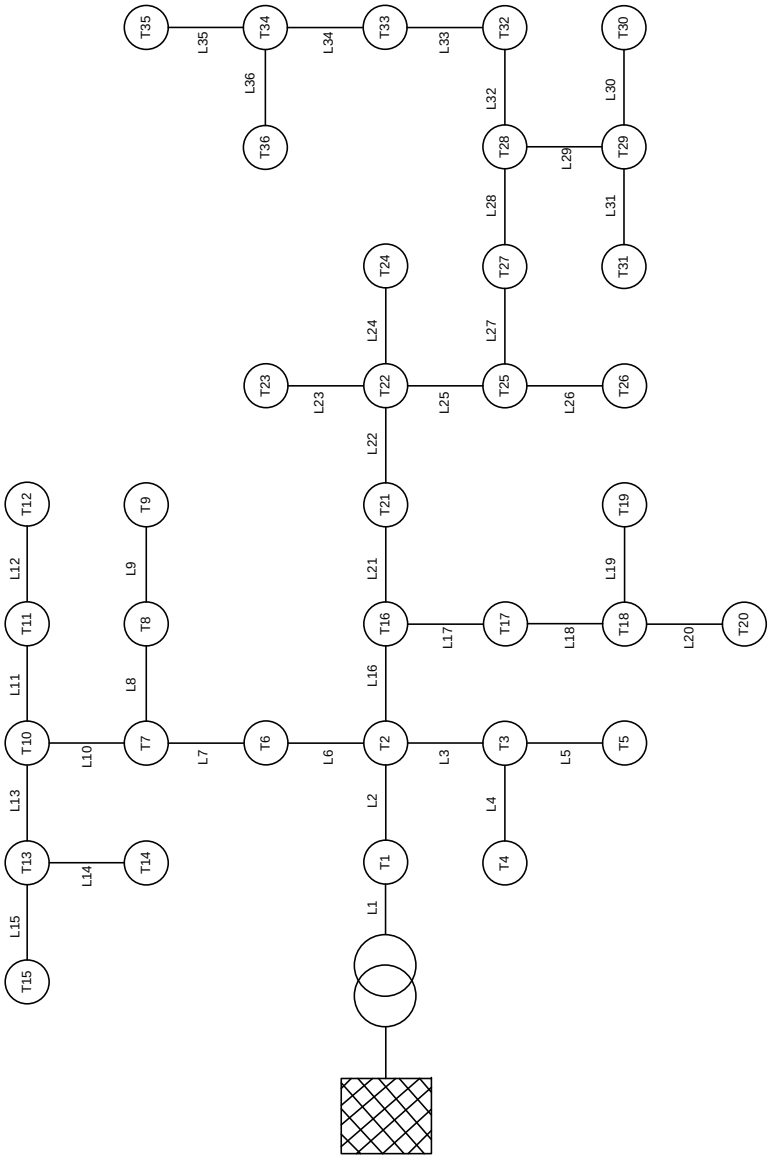

Figure 7.1: Studied distribution grid layout.

Table 7.2: Features of the proposed lines for the studied grid: subterranean RHZ cables 18-30 kV of Al

$A\ [mm^2]$	$R\ [Ohm/km]$	$X_L\ [Ohm/km]$	$I_{max}\ [A]$
240	0,125	0,116	415
400	0,0778	0,105	530

Table 7.3: Features of the transformers used in the studied grid

Feature	**Assigned Value**
Power	160-250-400-630 kVA
Connection type: 250-400-630 kVA	Dyn11
Voltage of the HV coupling	25 kV
No-load voltage of the LV coupling	420 V
Transformer's tap positions	-5 -2,5 0 +2,5 +5 +10
Capacity of resisting short-circuit events in the LV side	22,2 I_{nom}

Table 7.4: Features of the elements used in the studied grid

Transf. st,	**Num. transf.**	**Pnom [kVA]**	**Line**	**L [km]**	**S [mm2]**
T0	1	25000	-	-	-
T1	1	160	L1	0,3	400
T2	3	250+250+400	L2	0,2	400
T3	1	400	L3	0,4	240
T4	2	160+250	L4	0,4	240
T5	1	160	L5	0,3	240
T6	1	400	L6	0,2	240
T7	1	250	L7	0,3	240
T8	2	250+250	L8	0,2	240
T9	1	400	L9	0,3	240
T10	1	160	L10	0,2	240
T11	2	250	L11	0,3	240
T12	1	250	L12	0,3	240
T13	2	250+250	L13	0,3	240
T14	1	160	L14	0,3	240
T15	2	250+630	L15	0,2	240
T16	2	630+250	L16	0,4	240
T17	2	400+160	L17	0,4	240
T18	1	250	L18	0,2	240
T19	1	160	L19	0,5	240
T20	2	250+160	L20	0,1	240
T21	1	250	L21	0,4	240
T22	2	160+250	L22	0,2	240
T23	2	160+250	L23	0,3	240
T24	1	630	L24	0,2	240
T25	2	250+400	L25	0,5	240
T26	2	400+250	L26	0,2	240
T27	1	160	L27	0,3	240
T28	1	400	L28	0,2	240
T29	1	160	L29	0,2	240
T30	2	250+250	L30	0,3	240
T31	1	250	L31	0,2	240
T32	2	160+250	L32	0,7	240
T33	1	400	L33	0,3	240
T34	2	160+250	L34	0,5	240
T35	2	400+250	L35	0,3	240
T36	1	400	L36	0,4	240

7.2 Proposed scenario

This section describes the chosen conditions for the scenario of the study case. The conditions of the regular electrical grid demand are:

- **Type of demand:** electrical household demand.
- **Season:** winter.
- **Type of day:** weekday.

In order to generate the EV's demand following the methodology proposed in section 6, it is necessary to know the total number of trips of per day (equation 6.1) and number of houses in our study case day (equation 6.2). Therefore the first variable needed is P_{GRID}. After adapting the reference curve to our study grid, the obtained value is:

$$P_{GRID} = 14540kW$$

The number of vehicles per houses is a direct value extracted from IDESCAT:

$$n_{veh/houses} = 1,5$$

In order to get number of trips per day, the table B.1 from the appendix B is needed. The chosen value is the average of this table:

$$n_{trips/day} = 3,64$$

The ratio of trips made through the private vehicle (F_{trips}) comes from [135]:

$$F_{trips} = 0,358$$

Finally, using the calculated values, the total number of trips per day is:

$$n_{trips\_day} = 25837$$

Chapter 8

Results without the electrical demand: recharge curve of the EV

Several authors [78, 79, 80, 81, 83, 85] performed the grid impact analysis, using a constant recharge load model. The novelty of this study is the use of a detailed recharge curve for the impact analysis. Thus, the objective of this chapter is to compare the impact of the different models of batteries for the recharge of EVs, regardless of the situation of the grid. Therefore, only the demand created by the EV's recharge is considered in these simulations, which will provide a better idea of the EV's recharge effect. The different models for the EV's battery recharge are:

- **Constant Power:** The recharge is performed at constant power (Figure 8.1(b)).
- **Variable Power:** The recharge is performed based on the battery's recharge model (Figure 8.1(a)).
- **Variable power model with average values for the power to recharge:** The recharge is performed based on the battery's recharge model but the chosen value for the power is the average for the established periods (Figure 8.1(c)).

Three softwares have been considered to perform the simulations: Matlab, PSSE and *DIgSILENT Power Factory*. Comparing *DIgSILENT Power Factory* with Matlab, *DIgSILENT Power Factory* has been chosen because it already incorporates the load-flow algorithm and the electric system components are already modelled in the program. PSSE is presented as a strong option because, like *DIgSILENT Power Factory* does, it also offers load flow algorithm and electrical system models. However, *DIgSILENT Power Factory* offers the DPL programming language which allows automating the performance of time-consuming simulations, process the results or even apply further sequential changes to the network, subroutines or to the main

script itself. Therefore, *DIgSILENT Power Factory* was chosen among the other programs because best fits the requirements of simulations needed for this thesis.

In order to evaluate the above mention battery models, simulations are performed on the chosen grid (Figure 7.1), with 1000 EVs during a regular weekday with 50 iterations per hour, using the above mention software *DIgSILENT Power Factory*.

Both the recharge at the end of each trip and at the end at all day trips have been considered.

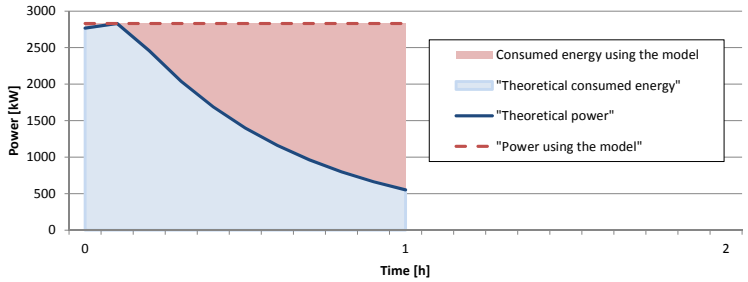

(a) Recharge curve of a Toyota Prius's battery

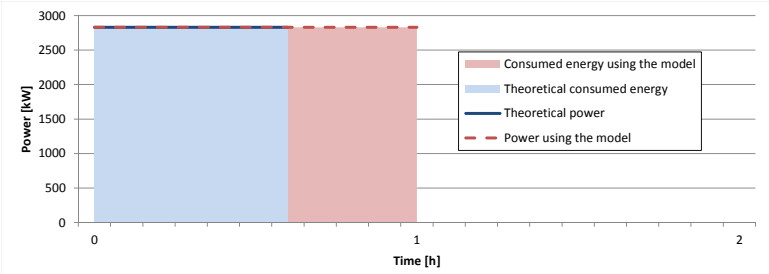

(b) Recharge curve of a battery at constant power

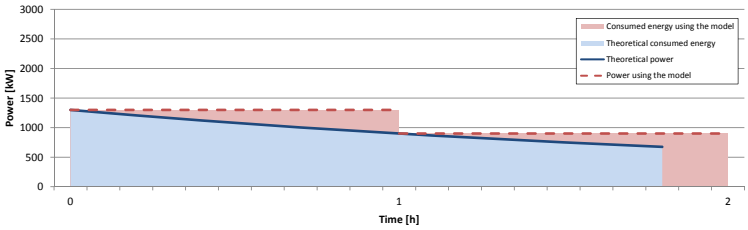

(c) Recharge curve of a Nissan Leaf's battery

Figure 8.1: Recharge profile of the recharging process of three different types of batteries

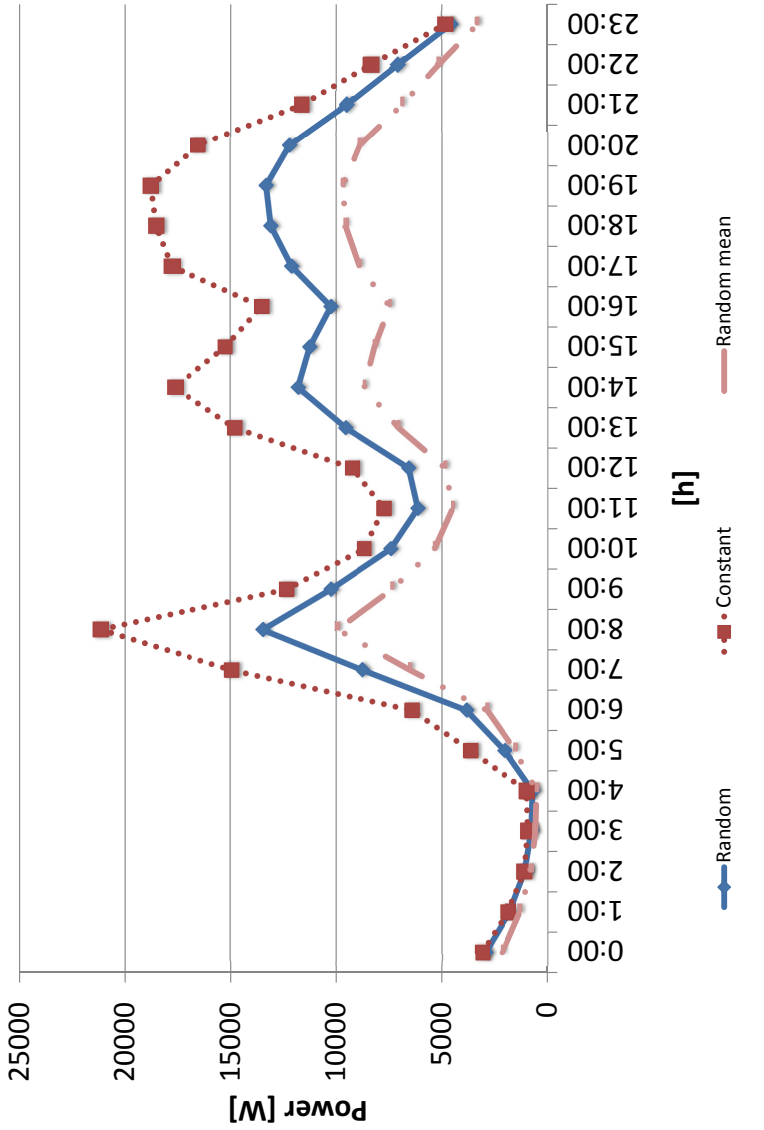

Figure 8.2: EV's recharge after each trip using the following batteries recharge model: constant model, the variable power model and the variable model with average values

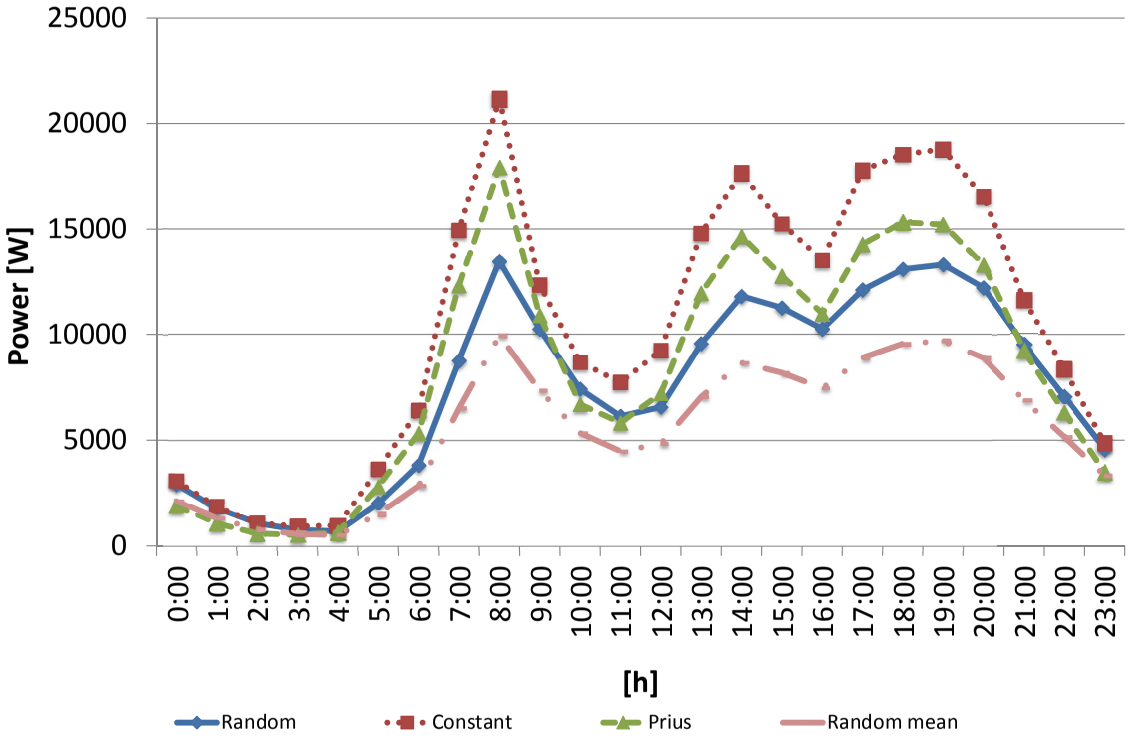

Figure 8.3: Comparison between PRIUS model (recharging after each trip) and the constant model, the variable power model and the variable model with average values

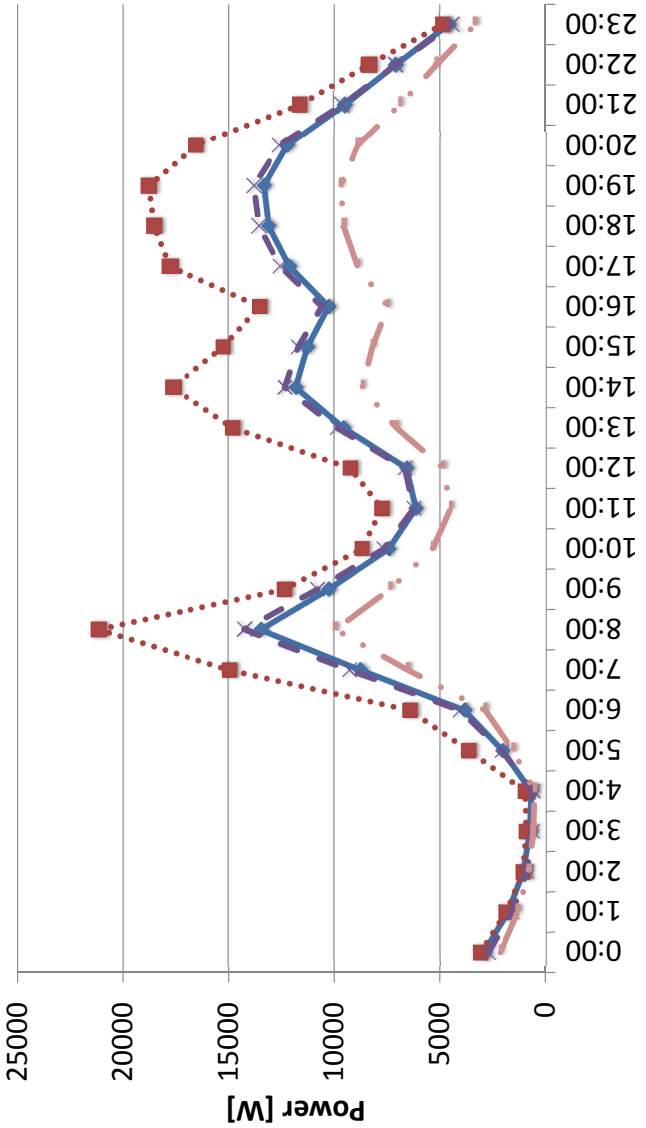

Figure 8.4: Comparison between IMIEV model (recharging after each trip) and the constant model, the variable power model and the variable model with average values

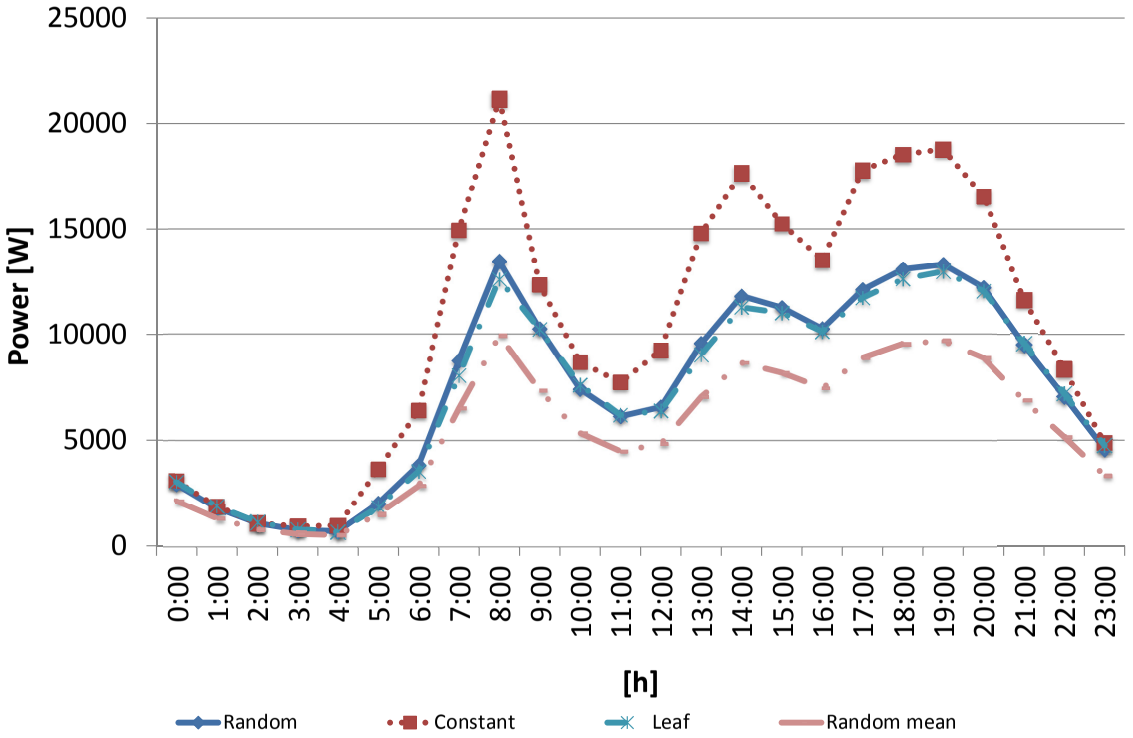

Figure 8.5: Comparison between LEAF model (recharging after each trip) and the constant model, the variable power model and the variable model with average values

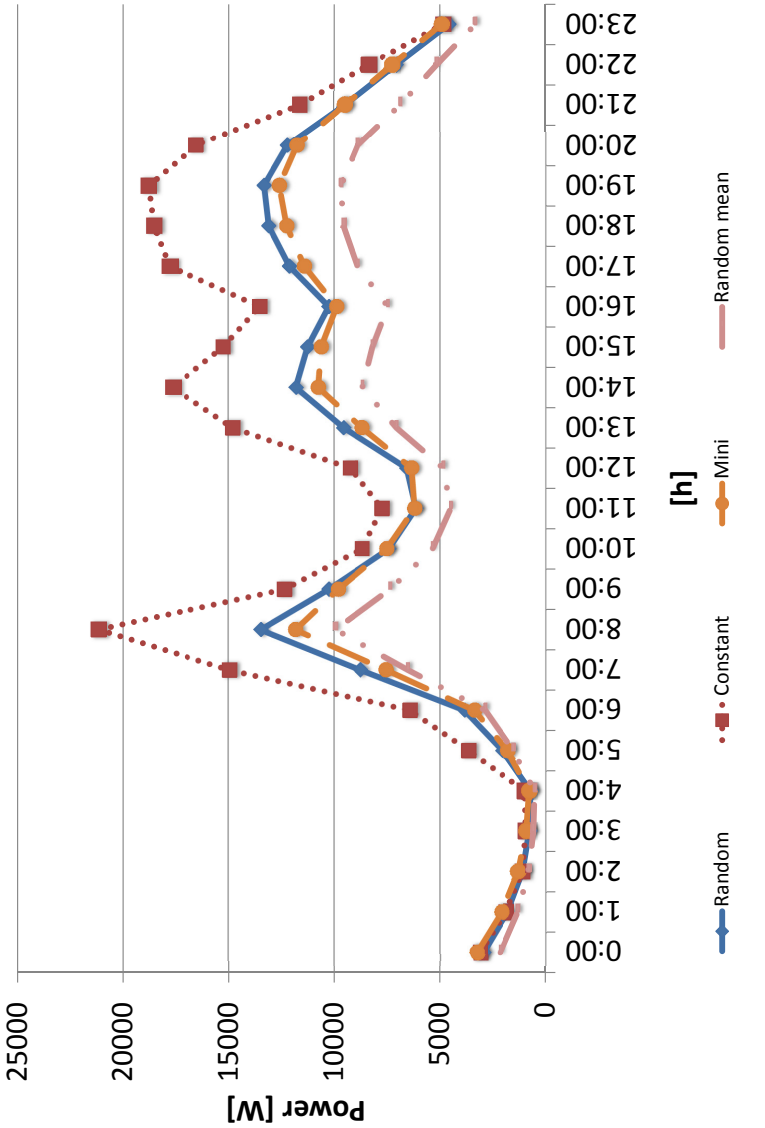

Figure 8.6: Comparison between MINI model (recharging after each trip) and the constant model, the variable power model and the variable model with average values

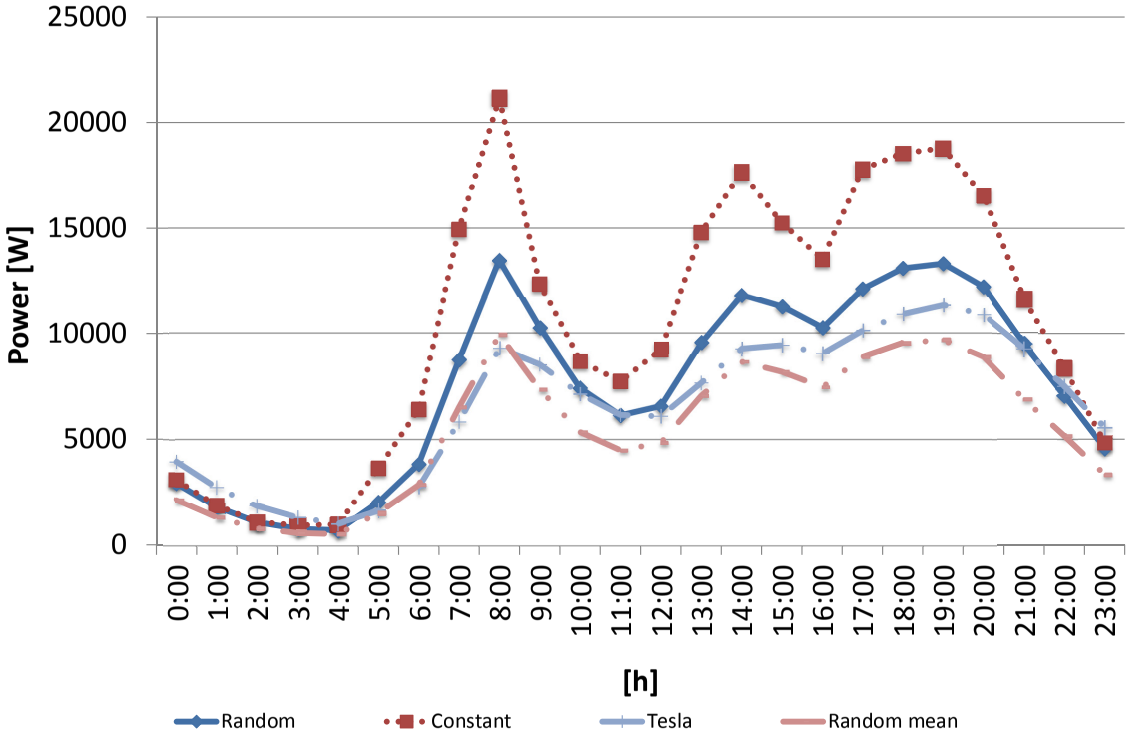

Figure 8.7: Comparison between TESLA model (recharging after each trip) and the constant model, the variable power model and the variable model with average values

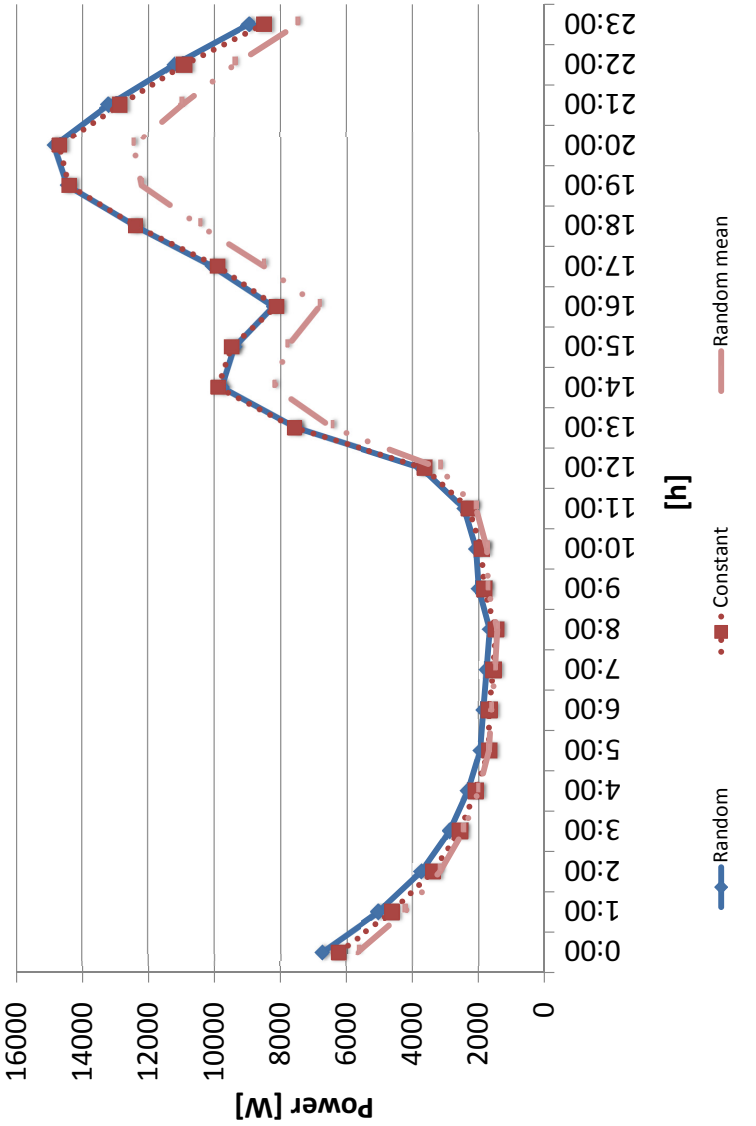

Figure 8.8: EV's recharge at the end of all day trips using the following batteries recharge model: constant model, the variable power model and the variable model with average values

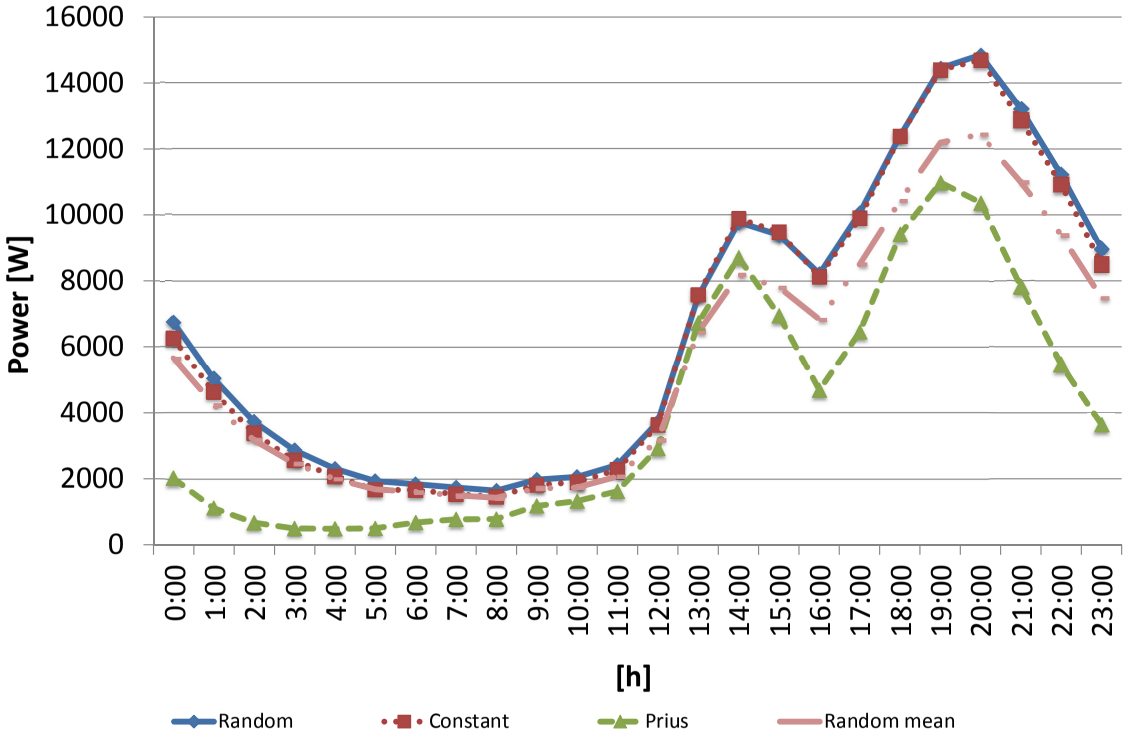

Figure 8.9: Comparison between PRIUS model (at the end of all day trips) and the constant model, the variable power model and the variable model with average values

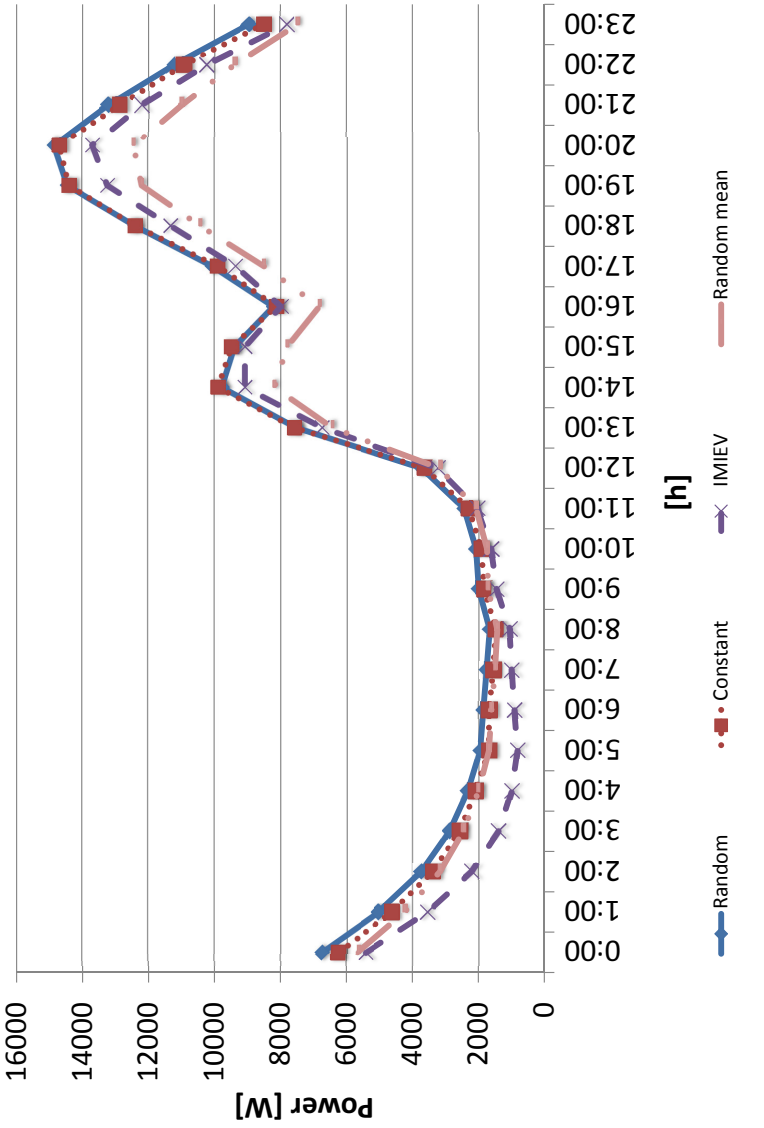

Figure 8.10: Comparison between IMIEV model (at the end of all day trips) and the constant model, the variable power model and the variable model with average values

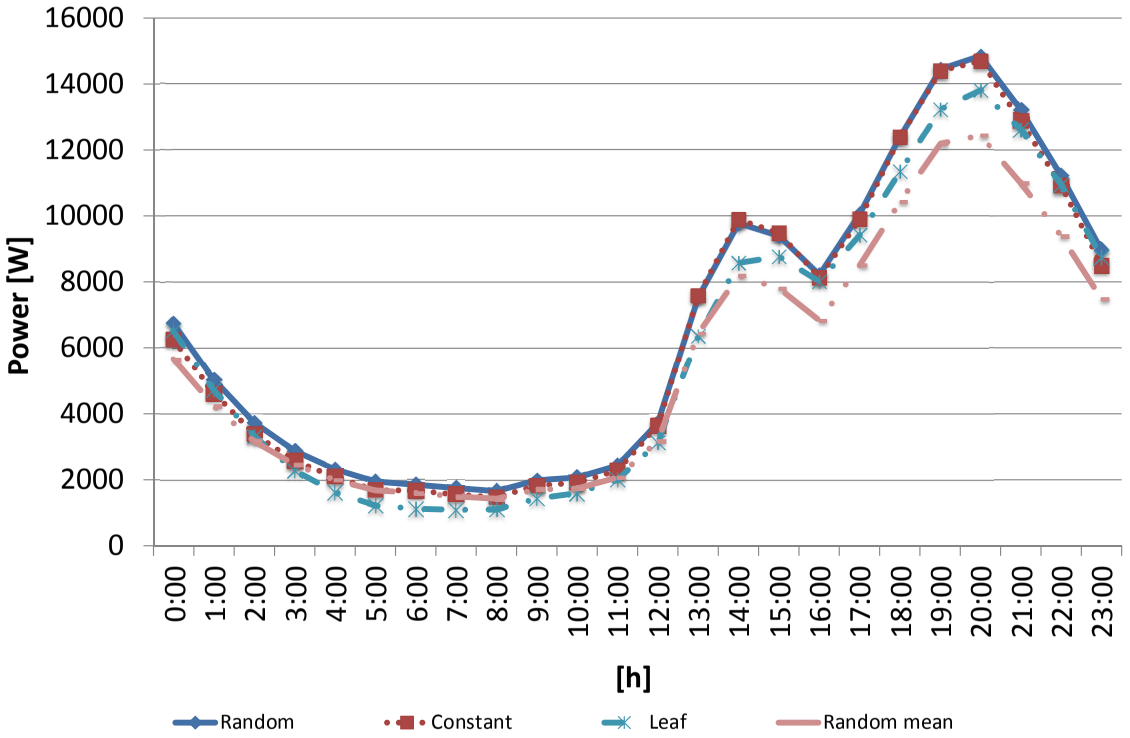

Figure 8.11: Comparison between LEAF model (at the end of all day trips) and the constant model, the variable power model and the variable model with average values

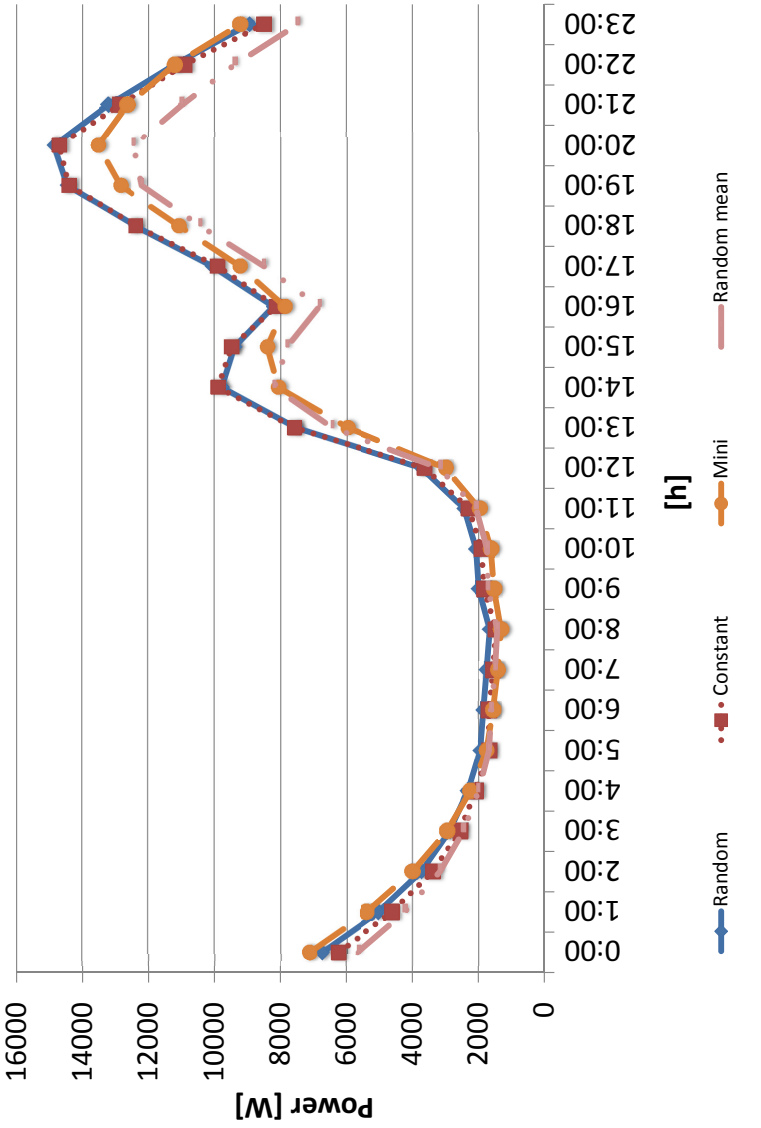

Figure 8.12: Comparison between MINI model (at the end of all day trips) and the constant model, the variable power model and the variable model with average values

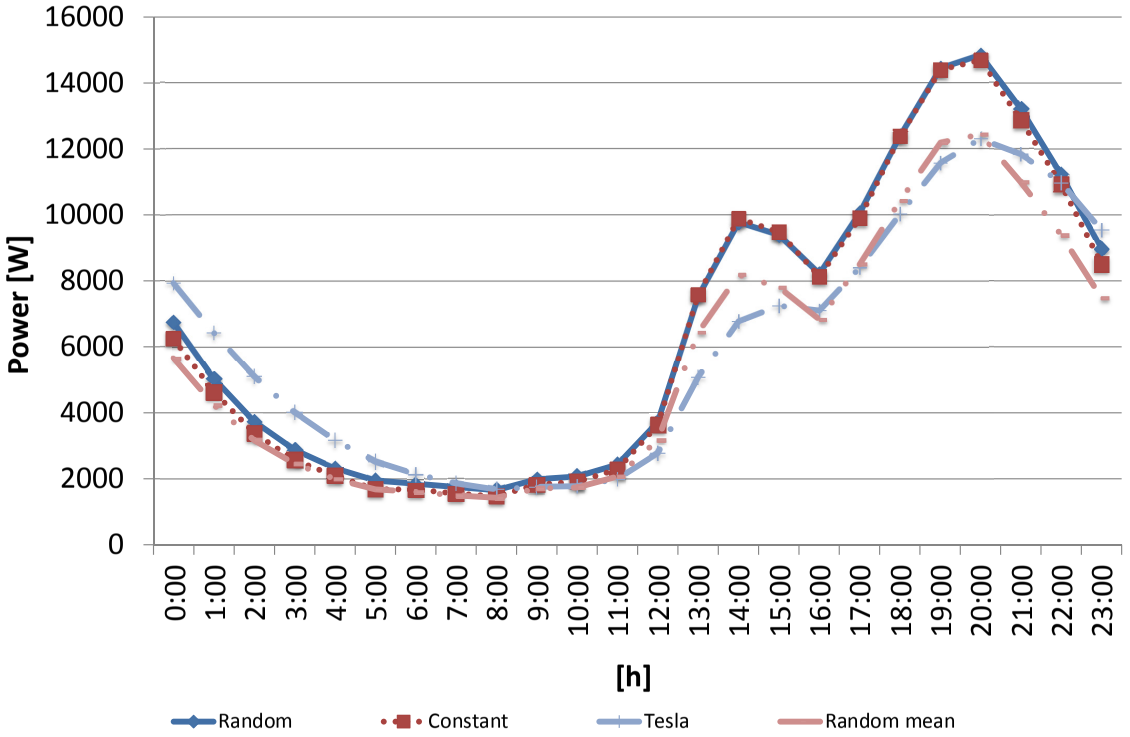

Figure 8.13: Comparison between TESLA model (at the end of all day trips) and the constant model, the variable power model and the variable model with average values

Figures 8.2 to 8.13 show the results of these simulations. It is important to note the difference between the recharge power in each simulation. In the case of the recharge after each trip (Figures 8.2 to 8.7), it can be seen that the recharge power directly depends on the used battery model type. This difference is based on the consideration that in the same hour all vehicles will be connected to the grid, recharging at the maximum battery power. Figure 8.1 shows the three model types for the battery recharge of 1650 kWh The blue colour stands for the real energy required and red stands for the additional energy assumed in this simulation. Several studies from [135, 131] demonstrate that the majority of the population consume less than 4 kWh during each trip. Accordingly, battery recharges would take place in the exponential part of the curve. Therefore, in order to achieve a more precise model and not include this unrealistic extra energy, it would be necessary to measure in periods smaller than one hour when the recharge takes place in the exponential part of the model's curve.

For the case of the recharge at the end of all day trips (Figures 8.8 to 8.13), the error is much smaller, since recharges are deeper and take place in the bulk part of the curve of the recharge model where the error is minimized due to the exponential part of the curve.

As it can be observed in the figures (from figure 8.2 to 8.13), the worst case scenarios corresponds to the case when the *Constant power recharge battery model* is used. The explanation to this result is described by the fact that this model performs the recharge at the battery's maximum recharge power. Therefore, this case represents the worst case scenario.

Chapter 9

Results with electrical demand: impact into the distribution grid

The EV's impact on the study grid (Figure 7.1) is studied in this section. Prior to the simulations, it had been studied which results can provide a better understanding of the impact of EVs. Because of the topology of the grid and the household load profiles, it has been observed [131] that the greatest impact is in Line 1 (L1), and because the difference is not significant in the transformers' loadings, the value will be the mean of them all (equation 9.1).

$$L_{transf} = \frac{\sum_{i=1}^{N_{transf}} L_{transf\_i}}{N_{transf}} \tag{9.1}$$

9.1 Comparison of the constant power battery's recharge model and variable model with mean values for the power to recharge

The results of the Monte Carlo simulation are depicted below with 0%, 20% and 40% of EV penetration for the most unsuitable scenario (the one with the highest household consumption, which in this case is the *"winter weekday"* case), using the constant power model (Figure 8.1(a)) and the variable model with mean values (Figure 8.1(c)).

As Figure 9.1(a) shows, the maximum load increase occurs in Line 1 (L1) for a penetration of 40% with the constant power model. This maximum load increase takes place when household demand reaches its maximum (20:00h), taking the loading level from 60 % (with no EV) to 74%. In the case of the mean value model, the loading level in the same hour is 66%, which corresponds with the expected accuracy of this model (Section 8). It is important to point out that with a 40% EV penetration, the grid has already experienced a violation of the admissible level of 60% at 8:00h; with the constant power model and it reaches 68% and with the mean value model it reaches 63%.

Taking into account the conclusions extracted from Section 8 (discussion of the figures), it can be seen that for the recharge at the end of all day trips, the differences between the batteries' recharge models are not as significant as in the previous scenario (Figure 8.9); the maximum difference between the models is 1%.

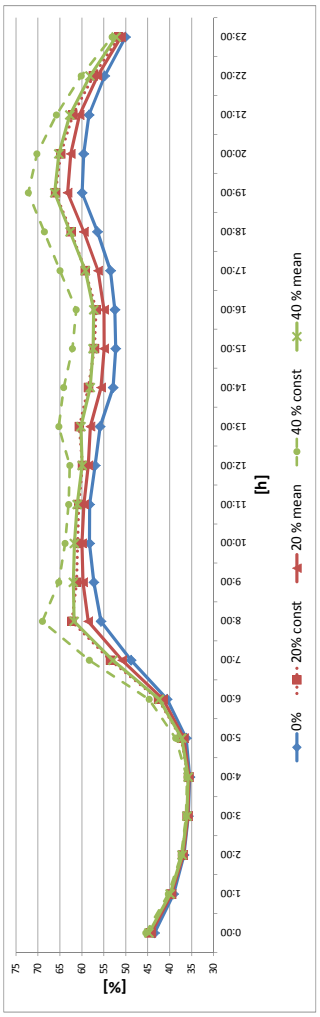

(a) Recharge of the battery at the end of each travel

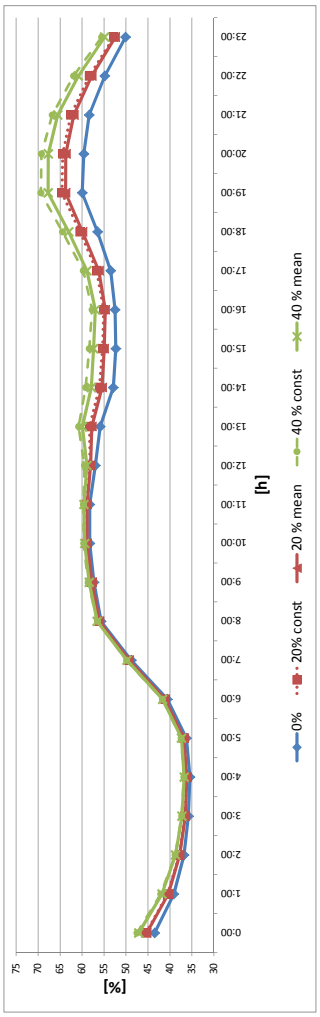

(b) Recharge of the battery at the end of all day travels

Figure 9.1: Loading profile of the Line 1 (L1) through a winter weekday [%]

Figure 9.2 shows the loading level for the transformers. Comparing the loading levels of the transformers with the line loading levels, it can be observed that the load pattern remains the same although the transformer case reaches higher loading levels.

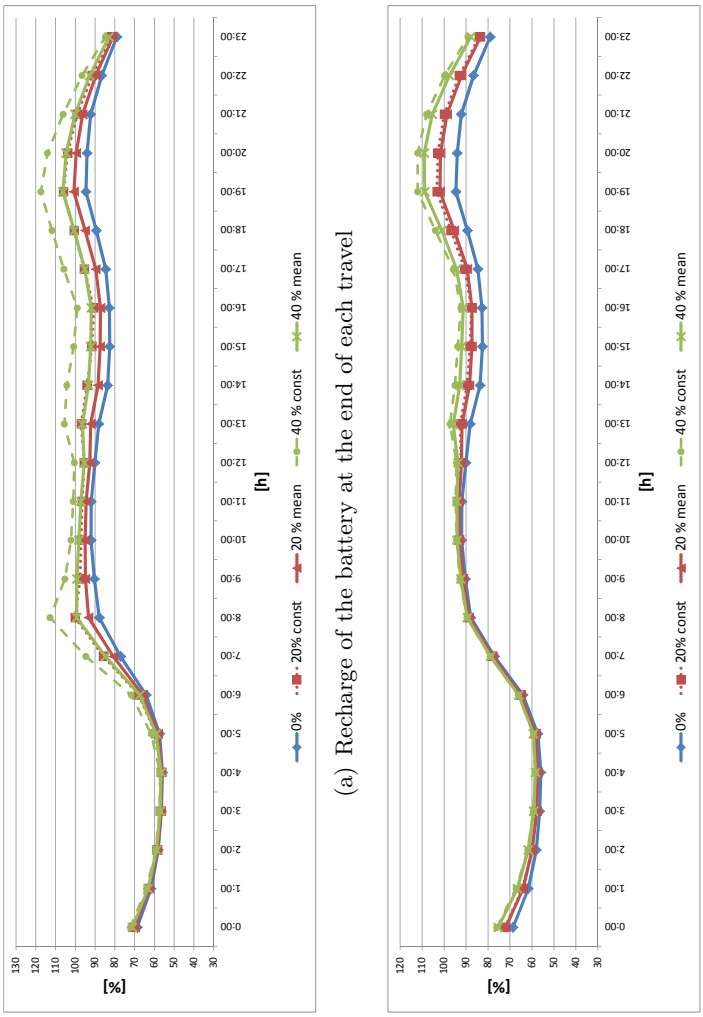

(a) Recharge of the battery at the end of each travel

(b) Recharge of the battery at the end of all day travels

Figure 9.2: Loading profile of the transformers through a winter weekday [%]

9.2 Extreme scenario: EV penetration of 100%

The purpose of this section is to study the effect of a 100% EV penetration in the grid. Two situations will be considered: recharging after every trip and recharging at the end of the day. Results will be compared with the 0% EV penetration case.

Figure 9.3 depicts the loading profile of L1 and the transformer when the recharge is performed after every trip. As it can be seen in the Figure 9.3(a), lines do not overload their maximum value. Nevertheless, depending on the country's legislation, these values can be considered not suitable under normal operating conditions. Regarding the transformer's loading level (Figure 9.3(b)), it can be seen that overloading is produced all day long except during the off-peak time period.

The EV's recharging after all the trips of the days is shown in Figure 9.4. For the case of the line's loading (Figure 9.4(a)), as in the previous case, it does not exceed 100% of its capacity but it reaches higher values (the hour when this maximum value is achieved is the same for both scenarios). The transformer's loading level (Figure 9.4(b)) presents a decrease of its loading until 17:00h. At the time of the maximum loading level (20:00h) the loading is approximately 10% above of the "*Recharging after every trip case*" transformer's loading level.

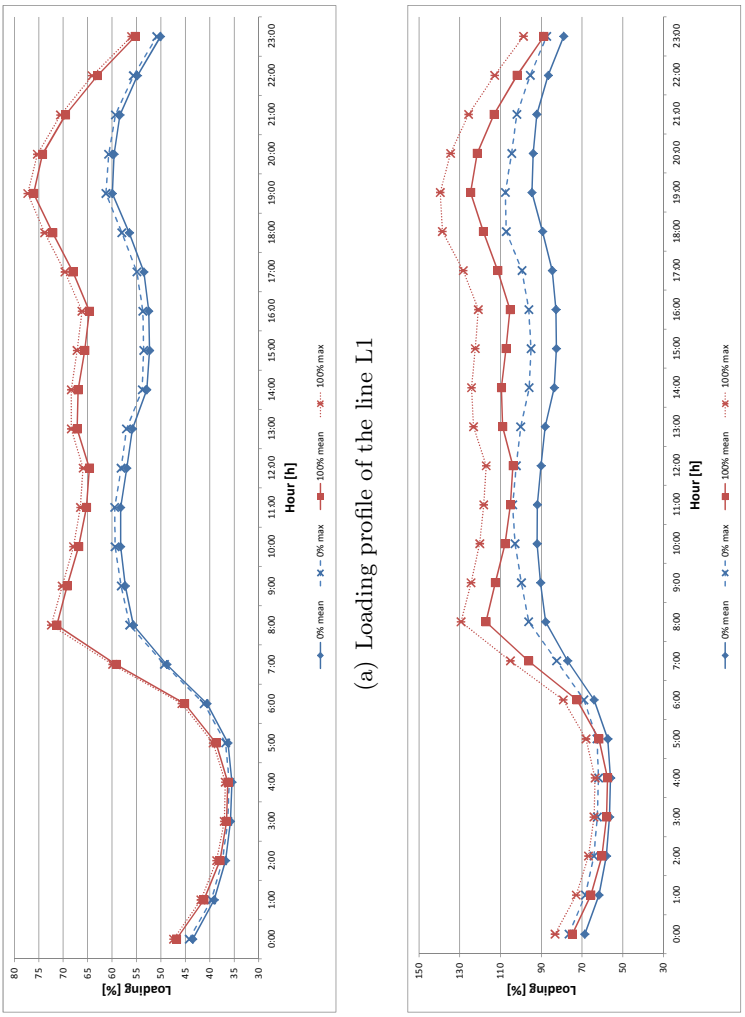

(a) Loading profile of the line L1

(b) Loading profile of the transformers

Figure 9.3: Grid's loading profile with an EV's penetration of 100% recharging at the end of each travel [%]

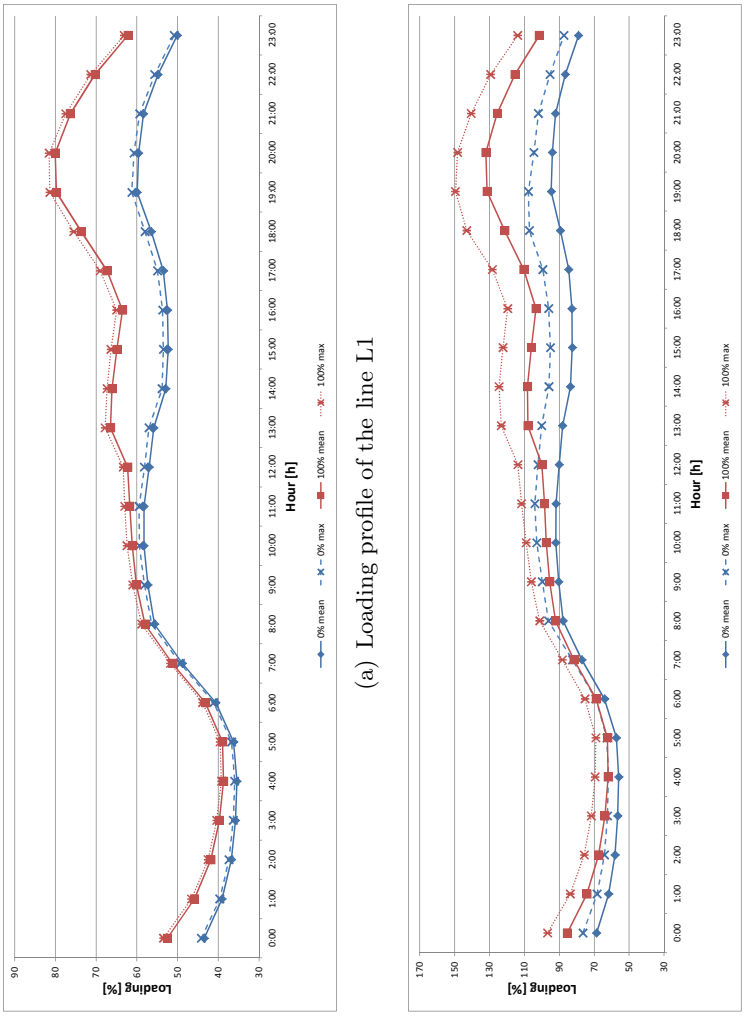

(a) Loading profile of the line L1

(b) Loading profile of the transformers

Figure 9.4: Grid's loading profile with an EV's penetration of 100% recharging at the end of all day travels [%]

Part IV

Conclusions

Chapter 10

Conclusions

The objective of this PhD thesis is to analyse the impact of the recharge of a fleet of EVs in a standard IEEE test system adopted to an underground distribution grid in Barcelona (Spain), implementing an improved model for the recharge of the batteries. In order to achieve this objective, the following tasks have been performed:

- Obtainment of the probabilistic model for electrical demand. It consists of creating a statistical model able to generate random values according to the available data of the Spanish hourly load profile (rescaled to the study grid). The seasonal patterns of the consumption were obtained in order to generate a normal distribution for each hour of each pattern. Using these normal distributions, the random values for the hourly power due to the electrical demand can be generated. The pattern chosen for the simulation is the winter pattern because the highest consumptions are experienced, which results in the most critical case.

- Battery model creation. The load curves of the different types of batteries have been implemented in order to include their behaviour in the simulations and maintain accuracy.

- Obtainment of the probabilistic model for the electrical demand due to the EV consumption. In order to get the EV consumption, several steps had to be taken:

    1. Study of the mobility patterns of Barcelona and adaptation to the studied area in order to get the number of EVs that would be recharging in the area. The distribution of the number of EVs along the nodes has been done considering that each node has the same probability of recharging vehicles.

    2. Determination of the consumed power of the EVs for each recharge. The consumed energy per travel is based on the specific consump-

tion of the battery and the distance travelled. In this study the travelled distance follows a log normal distribution with a shape value of 1.929 and a scale factor of 1.508.

3. Obtainment of the type of battery of each EV. The type of battery determines the specific consumption of the previous step. In the study, a log normal function was created from the capacities to be generated for random batteries, and depending on the value, a known load curve from an existent model was assigned (Figure 6.6).

- One of the main interests of this study is to obtain the impact of EVs recharging in a real distribution grid situation. Thus, an IEEE test system has been adapted to an underground cable system used, like in Barcelona. The main advantage of this new test system is that it also contains mobility-related data that can be used in future studies.

- Simulation using the Monte Carlo method of the possible scenarios using the power system simulator *DIgSILENT*. Once all the consumptions per node, hour and iteration have been determined (EV's consumption and conventional demand), deterministic load flows with these values can be performed in order to get the confidence interval for the result variables.

The results show that the impact of non-constant recharge battery models on the grid is smaller than the impact of the constant one (Figures 8.2 to 8.13). This is caused by the significant inaccuracy of the energy consumed during the recharge of the constant power model, due to the following two factors:

1. The constant battery model does not take into account that during the last stage of the recharge, consumption decreases in an exponential way (constant voltage stage). This inaccuracy gets accentuated when the recharge is performed during this stage (recharge after each trip).

2. The simulation using time periods with one hour resolution results in an imprecision when the recharge lasts less than one hour. This situation results in the recharge of more energy during the simulation than required.

Despite the simulations using a non-constant battery model in order to procure the results where the impact is not the highest, during the days

of the year with the highest household consumption, transformer stations could experience an overload of 11% due to the combination of the household electrical consumption and the EV recharge consumption (Figure 9.2). The lines will not have such severe problems (Figure 9.1), even though it is possible that some lines cannot remain under 60% of admissible loading power established by the utility. The same results can be observed for the critical case of the 100% of EVs penetration (Figure 9.3 and Figure 9.4).

Finally, it is essential to highlight that the variables regarding mobility aspects are some of the key factors for these kinds of studies.

10.1 Future work

The present work have arisen a number of interesting topics for further research:

- Implement EV fast charge in order to assess its impact in these type of scenarios.
- Combine both EV fast charge and EV standard charge with different levels of penetrations and proportions to foresee possible situations.
- Implement control strategies of the charge process which consider in real-time basis the status of the grid and allow or not the recharge of the EV.
- Consider the EV as an energy source able to inject power on the grid in order to improve grid's performance and stability.

Bibliography

[1] S. F. Tie and C. W. Tan, "A review of power and energy management strategies in electric vehicles," in *Intelligent and Advanced Systems (ICIAS), 2012 4th International Conference on*, vol. 1, 2012, pp. 412–417. xv, 2, 3, 4, 5, 6, 8, 10, 11, 12, 13, 14, 15, 16

[2] M. Yilmaz and P. Krein, "Review of battery charger topologies, charging power levels, and infrastructure for plug-in electric and hybrid vehicles," *Power Electronics, IEEE Transactions on*, vol. 28, no. 5, pp. 2151–2169, 2013. xix, 17, 18, 19, 20, 21

[3] *SAE Electric Vehicle and Plug-in Hybrid Electric Vehicle Conductive Charge Coupler*, SAE Standard J1772 Std. xix, 17, 19, 22

[4] N. Y. ISO, "Alternate route: Electrifying the transportation sector," NY: New York ISO, Tech. Rep., 2009. [Online]. Available: http://www.nyiso.com/public/webdocs/newsroom/press_releases/2009/Alternate_Route_NYISO_PHEV_Paper_062909.pdf 1

[5] P. Denholm and W. Short, "An evaluation of utility system impacts and benefits of optimally dispatched plug-in hybrid electric vehicles," National Renewable Energy Laboratory, Tech. Rep., 2006. [Online]. Available: http://www.nrel.gov/docs/fy06osti/40293a.pdf 1

[6] Q. Gong, S. Midlam-Mohler, V. Marano, and G. Rizzoni, "Study of pev charging on residential distribution transformer life," *IEEE Transactions on Smart Grid*, vol. 3, no. 1, pp. 404–412, 2012. 1

[7] L. Dickerman and J. Harrison, "A new car, a new grid," *Power and Energy Magazine, IEEE*, vol. 8, no. 2, pp. 55 –61, 2010. 1

[8] C. Gonzalez, R. Villafafila, R. Ramirez, A. Sudria, A. Sumper, and M. Chindris, "Assess the impact of photovoltaic generation systems on low-voltage network: software analysis tool development," in *Proc. 9th Int. Conf. Electrical Power Quality and Utilisation EPQU 2007*, 2007, pp. 1–6. 1

[9] S. Hadley, "Impact of plug-in hybrid vehicles on the electric grid," Oak Ridge National Laboratory, Tech. Rep., 2006. [Online]. Available: http://www.ornl.info/info/ornlreview/v40_2_07/2007_plug-in_paper.pdf 1

[10] S. Lukic, J. Cao, R. Bansal, F. Rodriguez, and A. Emadi, "Energy storage systems for automotive applications," *Industrial Electronics, IEEE Transactions on*, vol. 55, no. 6, pp. 2258–2267, 2008. 2

[11] S. Lukic and A. Emadi, "Effects of drivetrain hybridization on fuel economy and dynamic performance of parallel hybrid electric vehicles," *Vehicular Technology, IEEE Transactions on*, vol. 53, no. 2, pp. 385–389, 2004. 2

[12] S. F. Tie and C. W. Tan, "A review of energy sources and energy management system in electric vehicles," *Renewable and Sustainable Energy Reviews*, vol. 20, no. 0, pp. 82 – 102, 2013. [Online]. Available: http://www.sciencedirect.com/science/article/pii/S1364032112006910 2, 3, 5

[13] J. M. Ahmad Pesaran, "Ultracapacitor applications and evaluation for hybrid electric vehicles," in *7th annual advance capacitor world summit conference, National Renewable Energy Laboratory (NREL): Hotel Torrey Pines La Jolla, CA*, 2009. 3

[14] S. W. L. Xin, "Assessment of effiency improvement techniques for future power electronics intensive hybrid electric vehicle drive trains," in *Electrical Power Conference, EPC. IEEE*, 2007. 3

[15] A. Emadi, Y.-J. Lee, and K. Rajashekara, "Power electronics and motor drives in electric, hybrid electric, and plug-in hybrid electric vehicles," *Industrial Electronics, IEEE Transactions on*, vol. 55, no. 6, pp. 2237–2245, 2008. 3

[16] S. Wirasingha and A. Emadi, "Classification and review of control strategies for plug-in hybrid electric vehicles," *Vehicular Technology, IEEE Transactions on*, vol. 60, no. 1, pp. 111–122, 2011. 7

[17] L. Sun, R. Lian, and Q. Wang, "The control strategy and system preferences of plug-in hev," in *IEEE Vehicle Power Propulsion Conference, Harbin, China*, Sep. 2008, pp. 1-5. 7

[18] D. Karbowski, A. Rousseau, S. Pagerit, and P. Sharer, "Plug-in vehicle control strategy: from global optimization to real-time application" in proc. 22nd int. battery, hybrid fuel cell electr. vehicle symp. exhib., yokohama, japan, oct. 2006." 7

[19] M. Westbrook, "The electric and hybrid electric car." in *London: The institution of Electrical Engineers*, 2001. 8, 9, 10

[20] K. Mikkelsen, "Design and evaluation of hybrid energy storage systems for electric powertrains." in *Waterloo, Ont: University of Waterloo*, 2010. 8, 9, 11

[21] e. a. Tony Markel, "Energy storage system requirements for hybrid fuel cell vehicles," in *Advance automotive battery conference. National Renewable Energy Laboratory Nice, France*, 2003. 8

[22] C.-H. Dustmann, "Advances in zebra batteries," *Journal of Power Sources*, vol. 127(1-2), pp. 85–92, 2004. 9, 14

[23] J. Sudworth, "The sodium/nickel chloride (zebra) battery," *Power Sources*, vol. 100(1-2), pp. 149–63, 2001. 9, 14

[24] J. Kopera, *Inside the nickel metal hydride battery*, COBASYS, Ed. COBASYS, 2004. 11

[25] G. Bromaghim, P. Serfass, and E. Wagner, "Hydrogen and fuel cells: the u.s. market report," 2010. 14

[26] P. Giuseppe, "Vehicle featuring an auxiliary solar cell elecrical system, particularly for powering the air conditioning system of a stationary vehicle," in *FIAT AUTO S.P.A*, 1994. 15

[27] I. Garner, "Vehicle auxiliary power applications for solar cells," in *Eighth international conference on automotive electronics*, 1991. 15

[28] J. Connors, "On the subject of solar vehicles and the benefits of the technology," in *ICCEP 07. International Conference on Clean Electrical Power*, 2007. 15

[29] W. Young, "Photovoltaics and the automobile," in *Southcon, Conference Record*, 1994. 15

[30] D. Rekioua and E. Matagne, "Photovoltaic applications overview optimization of photovoltaic power systems," in *London: Springer*, 2012. 15

[31] G. Conibeer, "Thir-generation photovoltaics," 2007. 15

[32] S. Temple, *Future PV technologies review*, D. A. J.-W. B.R. Bernhard Dimler, Ed. Energy Focus, 2010. 15

[33] D. Carlson, "The status and the future of the photovoltais industry," BP solar, 2012. 15

[34] L. E. Chaar, L. Lamont, and N. E. Zein, "Review of photovoltaic technologies," *Renewable and Sustainable Energy Reviews*, vol. 15(2), pp. 2165–75, 2011. 15

[35] R. Miles, K. Hynes, and I. Forbes, "Photovoltaic solar cells: and overview of the state-of-the-art cell development and environmental issues," *Progress in Crystal Growth and Characterization of Materials*, vol. 51(1-3), pp. 1–42, 2005. 15

[36] V. Bosetti, G. Fiorese, and E. Verdolini, "Solar pv and csp technologies," *Policy recommendations from the ICARUS survey on current state and future developments*, vol. 1, p. 57, 2011. 15

[37] B. Parida, S. Iniyan, and R. Goic, "A review of solar photovoltaic technologies," *Renewable and Sustainable Energy Reviews*, vol. 15(3), pp. 1625–36, 2011. 15

[38] L. Reichertz, Y. Iulian, K. K. Man, M. Walukiecwicz, and W. J. Ager Wladek III, "Demonstration of a iii-nitride-silicon tandem solar cell," *Applied Physics Express*, vol. 2(12), pp. 122 202–122 202–3, 2009. 15

[39] Q. Wang, L. Sun, and R. Lian, "Dynamic reconfiguration of photovoltaic energy harvesting system in hybrid electric vehicles," *Proceedings of the ACM/IEEE international symposium on low power electronics and design, ACM: redondo Beach CA*, vol. -, pp. 109–114, 2012. 15

[40] C. Schuss, B. Eichberger, and T. Rahkonen, "A monitoring system for the use of solar energy in electric and hybrid vehicles," in *Instrumentation and measurement technology conference (I2MTC), IEEE International*, 2012. 15

[41] M. Nikolic and H. Zimmermann, "Photovoltaic energy harvesting for hybrid/electric vehicles: topology comparison and optimization of a discrete power stage for european efficiency," in *9th International multi-conference on systems, signals and devices (SSD)*, 2012. 15

[42] F. Stabler, "Automotive thermoelectric generator design issues. in doe thermoelectric applications workshop, future tech llc," 2009. 15

[43] J.-P. Fleurial, "Design and discovery of highly efficient thermoelectric materials. national aeronautics and space administration," 1993. 15

[44] D. Crane, "Progress towards maximizing the performance of a thermoelectric power generator," in *Proceeding of the 25th International Conference on Thermoelectrics, Viena, Austria: BSST LLC*, 2006. 15

[45] A. Bandivadekar, L. Cheah, C. Evans, T. Groode, J. Heywood, E. Kasseris, E. Kromer, and M. Weiss, "On the road in 2035: reducing transportation's pertroleum consumption and ghg emissions, massachusets institute of technology," 2008. 16

[46] M. Baglione, "Development of system analysis methodologies and tools for modeling and optimizing vehicle system efficiency," in *Mechanical engineering. Michigan: University of Michigan*, 2007 p.207. 16

[47] J. Hong, P. W. Guang, and N. Sui, "Simulation of a regenerative braking system producing controlled braking force," *Advance material research. Manufacturing Science and Technology*, vol. -, pp. 5729–37, 2011. 16

[48] C. Chan and K. Chau, "An overview of power electronics in electric vehicles," *Industrial Electronics, IEEE Transactions on*, vol. 44(1), pp. 3–13, 1997. 16

[49] D. Mackay, "Sustainable energy - without the hot air. cambridge: Uit combridge; 2009 p. 125-126." 16

[50] "Energy use in cars 4: Renegerative braking systems. 2010; available from: $http://c21.phas.ubc.ca/article/energy-use-cars-4-regenerative-braking-systems$." 16

[51] S. Valente and H. Ferreira, "Braking energy regeneration using hydraulic systems. portugal: Polytechnic institute of porto (ipp); 2008 p.8." 16

[52] J. Beretta, "Automotive electricity," New York: Wiley, 2010. 17

[53] C. Chan and K. Chau, "An overview of power electronics in electric vehicles," *Industrial Electronics, IEEE Transactions on*, vol. 44, no. 1, pp. 3–13, 1997. 17

[54] L. De Sousa, B. Silvestre, and B. Bouchez, "A combined multiphase electric drive and fast battery charger for electric vehicles," in *Vehicle Power and Propulsion Conference (VPPC), 2010 IEEE*, 2010, pp. 1–6. 17

[55] K. Morrowa, D. Karnerb, and J. Francfort, "Plug-in hybrid electric vehicle charging infrastructure review," *U.S. Dep. Energy Veh. Technol. Program, Final Rep. 58517*, vol. -, pp. –, Nov. 2008. 17, 18

[56] D. Tuttle and R. Baldick, "The evolution of plug-in electric vehicle-grid interactions," *Smart Grid, IEEE Transactions on*, vol. 3, no. 1, pp. 500–505, 2012. 18

[57] T. Motors, "Tesla roaster spec sheet. [online]. available: *http* : $//teslamotors.com/display_data/teslaroadster_specsheet.pdf$." 18

[58] M. Thomason, "Plug-in recharge (2011). [online]. available: *http* : $//www1.eere.energy.gov$." 18

[59] "Electrification of the transportation system, mit energy inititative, cambridge, ma, apr. 2010." 18

[60] T. Brown, J. Mikulin, N. Rhazi, J. Steel, and M. Zimring, "Bay area electrified vehicle charging infrastructure: options for accelerating consume." Renewable and Appropiate Energy Laboratory (RAEL), University of California, Berkeley, June 2010. 18

[61] B. Singh, B. Singh, A. Chandra, K. Al-Haddad, A. Pandey, and D. Kothari, "A review of three-phase improved power quality ac-dc converters," *Industrial Electronics, IEEE Transactions on*, vol. 51, no. 3, pp. 641–660, 2004. 20

[62] Y. Du, S. Lukic, B. Jacobson, and A. Huang, "Review of high power isolated bi-directional dc-dc converters for phev/ev dc charging infrastructure," in *Energy Conversion Congress and Exposition (ECCE), 2011 IEEE*, 2011, pp. 553–560. 20

[63] E. Sortomme and M. El-Sharkawi, "Optimal charging strategies for unidirectional vehicle-to-grid," *Smart Grid, IEEE Transactions on*, vol. 2, no. 1, pp. 131–138, 2011. 20

[64] G.-Y. Choe, J.-S. Kim, B. kuk Lee, C.-Y. Won, and T.-W. Lee, "A bi-directional battery charger for electric vehicles using photovoltaic

pcs systems," in *Vehicle Power and Propulsion Conference (VPPC), 2010 IEEE*, 2010, pp. 1–6. 20

[65] J. Gallardo-Lozano, M. Milanes-Montero, M. Guerrero-Martinez, and E. Romero-Cadaval, "Three-phase bidirectional battery charger for smart electric vehicles," in *Compatibility and Power Electronics (CPE), 2011 7th International Conference-Workshop*, 2011, pp. 371–376. 20

[66] H. Chen, X. Wang, and A. Khaligh, "A single stage integrated bidirectional ac/dc and dc/dc converter for plug-in hybrid electric vehicles," in *Vehicle Power and Propulsion Conference (VPPC), 2011 IEEE*, 2011, pp. 1–6. 20

[67] N. Tan, T. Abe, and H. Akagi, *Power Electronics, IEEE Transactions on*, no. 3, pp. 1237–1248. 20

[68] X. Zhou, S. Lukic, S. Bhattacharya, and A. Huang, "Design and control of grid-connected converter in bi-directional battery charger for plug-in hybrid electric vehicle application," in *Vehicle Power and Propulsion Conference, 2009. VPPC '09. IEEE*, 2009, pp. 1716–1721. 20

[69] B. Singh, B. Singh, A. Chandra, K. Al-Haddad, A. Pandey, and D. Kothari, "A review of single-phase improved power quality ac-dc converters," *Industrial Electronics, IEEE Transactions on*, vol. 50, no. 5, pp. 962–981, 2003. 20

[70] X. Zhou, G. Wang, S. Lukic, S. Bhattacharya, and A. Huang, "Multi-function bi-directional battery charger for plug-in hybrid electric vehicle application," in *Energy Conversion Congress and Exposition, 2009. ECCE 2009. IEEE*, 2009, pp. 3930–3936. 21

[71] S. Haghbin, K. Khan, S. Lundmark, M. Alakula, O. Carlson, M. Leksell, and O. Wallmark, "Integrated chargers for ev's and phev's: examples and new solutions," in *Electrical Machines (ICEM), 2010 XIX International Conference on*, 2010, pp. 1–6. 21

[72] M. Grenier, M. Hosseini Aghdam, and T. Thiringer, "Design of on-board charger for plug-in hybrid electric vehicle," in *Power Electronics, Machines and Drives (PEMD 2010), 5th IET International Conference on*, 2010, pp. 1–6. 21

[73] S. Lacroix, E. Laboure, and M. Hilairet, "An integrated fast battery charger for electric vehicle," in *Vehicle Power and Propulsion Conference (VPPC), 2010 IEEE*, 2010, pp. 1–6. 21

[74] O. Stielau and G. A. Govic, "Design of loosely coupled inductive power transfer system," in Proc. POWERCON, 2000 pp. 85-90. 22

[75] J. B. M. Budhia, G. Covic, "A new ipt magnetic coupler for electric vehicle charging system," in Proc. Ind. Electron. Conf., 2010, pp. 2487-2492. 22

[76] J. Huh, S. Lee, W. Lee, G. Cho, and C. Rim, "Narrow-width inductive power transfer system for online electrical vehicles," *Power Electronics, IEEE Transactions on*, vol. 26, no. 12, pp. 3666–3679, 2011. 22

[77] H. L. L. Li, A. Hu, and G. Covic, *Power Electronics, IEEE Transactions on*, no. 2, pp. 661–668. 22

[78] S. Shao, M. Pipattanasomporn, and S. Rahman, "Challenges of phev penetration to the residential distribution network," in *Power Energy Society General Meeting, 2009. PES '09. IEEE*, 2009, pp. 1 –8. 23, 24, 25, 85

[79] K. Clement-Nyns, E. Haesen, and J. Driesen, "The impact of charging plug-in hybrid electric vehicles on a residential distribution grid," *Power Systems, IEEE Transactions on*, vol. 25, no. 1, pp. 371 –380, 2010. 23, 24, 25, 85

[80] S. Acha, T. C. Green, and N. Shah, "Effects of optimised plug-in hybrid vehicle charging strategies on electric distribution network losses," pp. 1 –6, 2010. 23, 24, 25, 85

[81] A. Karnama, "Analysis of integration of plug-in hybrid electric vehicles in the distribution grid," Master's thesis, Royal Institute of Technology (KTH), Stockholm, Sweden, 2009. 23, 24, 25, 85

[82] VREG, "De verbruiksprofielen van huishoudelijke en niethuishoudelijke elektriciteitsverbruikers voor het jaar 2007," Online, 2007, `http://www.vreg.be`. 23

[83] J. Taylor, A. Maitra, M. Alexander, D. Brooks, and M. Duvall, "Evaluation of the impact of plug-in electric vehicle loading on distribution system operations," in *Power Energy Society General Meeting, 2009. PES '09. IEEE*, 2009, pp. 1 –6. 23, 24, 25, 85

[84] S. O. of Research and S. 2009, "Ab, stockholms stads utrednings och statistikkontor. statistisk Årsbok för stockholm 2009." 2009. 23

[85] S. Judd and T. Overbye, "An evaluation of phev contributions to power system disturbances and economics," in *Power Symposium, 2008. NAPS '08. 40th North American*, 2008, pp. 1 –8. 24, 25, 85

[86] J. Axsen and K. S. Kurani, "Anticipating plug-in hybrid vehicle energy impacts in california: Constructing consumer-informed recharge profiles," *Transportation Research Part D: Transport and Environment*, vol. 15, no. 4, pp. 212 – 219, 2010. 25

[87] K. Clement, E. Haesen, and J. Driesen, "Coordinated charging of multiple plug-in hybrid electric vehicles in residential distribution grids," in *Proc. IEEE/PES Power Systems Conf. and Exposition PSCE '09*, 2009, pp. 1–7. 25

[88] G. J. Anders, *Probability concepts in electric power systems.* Wiley-Interscience, 1990. 30, 35

[89] A. Papoulis and S. U. Pillai, *Probability, Random Variables and Stochastic Processes.* McGraw-Hill, 2002. 30

[90] A. Seppaelae, "Load research and load estimation in electricity distribution," Ph.D. dissertation, Technical Research Centre of Finland, 1996. 30

[91] V. Neimane, "On development planning of electricity distrbution networks," Ph.D. dissertation, Royal Institute of Technology (KTH), 2001. 30

[92] L. Pedersen, "Load modelling of buildings in mixed energy distribution systems," Ph.D. dissertation, Norwegian University of Science and Technology Faculty of Engineering Science and Technology Department of Energy and Process Engineering, 2007. 30

[93] J. H. Chow, F. F. Wu, and J. A. Momoh, *Applied Mathematics for restructurated Electric Power Systems*, M. Pai and A. Stankovic, Eds. Springer Science+Business Media Inc., 2005. 30

[94] G. K. Tso and K. K. Yau, "Predicting electricity energy consumption: A comparison of regression analysis, decision tree and neural networks," *Energy*, vol. 32, no. 9, pp. 1761–1768, 2007. 30

[95] J. Paatero and P. D. Lund, "A model for generating household electricity load profiles," *International Journal of Energy Research*, vol. 30, no. 5, pp. 283–290, July 2006. 31

[96] M. Caramanis, R. Tabors, K. Nochur, and F. Schweppe, "The introduction of nondiispatchable technologies a decision variables in long-term generation expansion models," *Power Apparatus and Systems, IEEE Transactions on*, vol. PAS-101, no. 8, pp. 2658–2667, Aug. 1982. 31

[97] B. Bak-Jensen, J. Bech, C. Bjerregaard, and P. Jensen, "Models for probabilistic power transmission system reliability calculation," *Power Systems, IEEE Transactions on*, vol. 14, no. 3, pp. 1166–1171, Aug 1999. 31

[98] G. Papaefthymiou, P. H. Schavemaker, L. van der Sluis, W. L. Kling, D. Kurowicka, and R. M. Cooke, "Integration of stochastic generation in power systems," in *15th Power Systems Computation Conference PSCC2005*, August 2005. 31, 35

[99] REE, "Atlas de la demanda electrica espanola. proyecto indel," 1998. [Online]. Available: http://www.ree.es/sistema_electrico/pdf/indel/Atlas_INDEL_REE.pdf 31

[100] A. Suwannarat, B. Bak-Jensen, Z. Chen, H. Nielsen, J. Hjerrild, P. Sorensen, and A. D. Hansen, "Power system operation with large scale wind power integration," *Power Tech, 2007 IEEE Lausanne*, pp. 671–676, July 2007. 31

[101] P. Pinson, "Estimation of the uncertainty in wind power forecasting," Ph.D. dissertation, ENSMP - CEP, March 2006. 31

[102] G. Sideratos and N. Hatziargyriou, "An advanced statistical method for wind power forecasting," *Power Systems, IEEE Transactions on*, vol. 22, no. 1, pp. 258 – 265, February 2007. 31

[103] M. Lei, L. Shiyan, J. Chuanwen, L. Hongling, and Z. Yan, "A review on the forecasting of wind speed and generated power," *Renewable and Sustainable Energy Reviews*, vol. 13, no. 4, pp. 915 – 920, 2009. 31

[104] G. Papaefthymiou, A. Tsanakas, M. Reza, P. H. Schavemaker, and L. van der Sluis, "Stochastic modelling and analysis of horizontally-operated power systems with a high wind energy penetration," in *2005 St. Peters-burg PowerTech Conference*, June 2005. 33

[105] G. Papaefthymiou, A. Tsanakas, D. Kurowicka, P. H. Schavemaker, and L. van der Sluis, "Probabilistic power flow methodology for the modelling of horizontally-operated power systems," in *International Conference on Future Power Systems (FPS2005)*, November 2005. 33

[106] J. L. Myers and A. D. Well, *Research Design And Statistical Analysis*, 2nd ed. Lawrence Erlbaum, November 2002. 34

[107] G. Papaefthymiou, "Integration of stochastic generation in power system," Ph.D. dissertation, Delft University of Technology, 2006. 34

[108] P. Rodrigues, R. Castro, R. Villafafila-Robles, and A. Sumper, "Modeling the stochastic dependencies in a probabilistic load flow including wind generation," in *Sustainable Alternative Energy (SAE), 2009 IEEE PES/IAS Conference on*, 2009, pp. 1 –7. 34

[109] G. Papaefthymiou and D. Kurowicka, "Using copulas for modeling stochastic dependence in power system uncertainty analysis," *Power Systems, IEEE Transactions on*, vol. 24, no. 1, pp. 40–49, Feb. 2009. 34

[110] M. Schilling, A. Leite da Silva, R. Billinton, and M. El-Kady, "Bibliography on power system probabilistic analysis (1962-88)," *Power Systems, IEEE Transactions on*, vol. 5, no. 1, pp. 1–11, Feb. 1990. 35

[111] P. Chen, Z. Chen, and B. Bak-Jensen, "Probabilistic load flow: A review," *Electric Utility Deregulation and Restructuring and Power Technologies, 2008. DRPT 2008. Third International Conference on*, pp. 1586–1591, April 2008. 35

[112] B. Borkowska, "Probabilistic load flow," *power apparatus and systems, ieee transactions on*, vol. PAS-93, no. 3, pp. 752–759, May 1974. 35

[113] N. Hatziargyriou, T. Karakatsanis, and M. Papadopoulos, "Probabilistic load flow in distribution systems containing dispersed wind power generation," *Power Systems, IEEE Transactions on*, vol. 8, no. 1, pp. 159–165, Feb 1993. 35

[114] J. Usaola, "Probabilistic load flow with wind production uncertainty using cumulants and cornishi fisher expansion," *International Journal of Electrical Power & Energy Systems*, 2009. 35

[115] R. Allan and A. Leite da Silva, "Probabilistic load flow using multilinearisations," *Generation, Transmission and Distribution, IEE Proceedings C*, vol. 128, no. 5, pp. 280–287, September 1981. 35

[116] A. Leite da Silva and V. Arienti, "Probabilistic load flow by a multilinear simulation algorithm," *Generation, Transmission and Distribution, IEE Proceedings C*, vol. 137, no. 4, pp. 276–282, Jul 1990. 35

[117] L. Xiaoming, C. Xiaohui, Y. Xianggen, X. Tieyuan, and L. Huagang, "The algorithm of probabilistic load flow retaining nonlinearity," *Power System Technology, 2002. Proceedings. PowerCon 2002. International Conference on*, vol. 4, pp. 2111–2115 vol.4, 2002. 35

[118] M. Sailaja Kumari and M. Sydulu, "A fast and reliable quadratic approach for q-adjustments in fast decoupled load flow model," *Probabilistic Methods Applied to Power Systems, 2006. PMAPS 2006. International Conference on*, pp. 1–5, June 2006. 35

[119] P. Zhang and S. Lee, "Probabilistic load flow computation using the method of combined cumulants and gram-charlier expansion," *Power Systems, IEEE Transactions on*, vol. 19, no. 1, pp. 676–682, Feb 2004. 35

[120] R. N. Allan and M. R. G. Al-Shakarchi, "Linear dependence between nodal powers in probabilistic a.c. load flow," *Proc. Inst. Elect. Eng.*, vol. 124, no. 6, pp. 529–534, 1977. 35

[121] A. M. L. da Silva, V. L. Arienti, and R. N. Allan, "Probabilistic load flow considering dependence between input nodal powers," *IEEE Transactions on Power Apparatus & Systems*, vol. PAS-103, no. 6, pp. 1524–1530, Jun. 1984. 35

[122] J.-U. Lim and J. N. Jiang, "Bibliography review on applications of correlation analysis in power system operation and planning," *European Transactions on Electrical Power*, 2008. [Online]. Available: http://dx.doi.org/10.1002/etep.294 35

[123] P. Jorgensen, J. Christensen, and J. Tande, "Probabilistic load flow calculation using monte carlo techniques for distribution network with wind turbines," in *Harmonics And Quality of Power, 1998. Proceedings. 8th International Conference on*, vol. 2, 1998, pp. 1146 – 1151. 35

[124] P. Caramia, G. Carpinelli, M. Pagano, and P. Varilone, "Probabilistic three-phase load flow for unbalanced electrical distribution systems with wind farms," *Renewable Power Generation, IET*, vol. 1, no. 2, pp. 115 – 122, June 2007. 35

[125] S. Conti and S. Raiti, "Probabilistic load flow using monte carlo techniques for distribution networks with photovoltaic generators," *Solar Energy*, vol. 81, no. 12, pp. 1473–1481, 2007. 35

[126] O. Tremblay, L. Dessaint, and A. Dekkiche, "A generic battery model for the dynamic simulation of hybrid electric vehicles," *Vehicle Power and Propulsion Conference, 2007.*, pp. 284–9, 2007. 38

[127] C. M. Shepherd, "Design of primary and secondary cells - part 2. an equation describing battery discharge," *Journal of Electrochemical Society*, vol. 112, pp. 657–64, 1965. 39

[128] K. Clement-Nyns, E. Haesen, and J. Driesen, "The impact of charging plug-in hybrid electric vehicles on a residential distribution grid," *IEEE Transactions on power systems*, vol. 25(1), pp. 371–80, 2010. 43

[129] http://www.st.com/stonline/books/pdf/docs/5995.pdf. [Online]. Available: http://www.st.com/stonline/books/pdf/docs/5995.pdf 43

[130] http://preview.powerelectronics.com/mag/504pet23.pdf. [Online]. Available: http://preview.powerelectronics.com/mag/504PET23.pdf 43

[131] D. Martinez-Vicente, "El impacto del vehiculo electrico en la red de distribucion," Master's thesis, Universitat Politecnica de Catalunya (UPC), 2011. 53, 58, 64, 65, 70, 100, 101

[132] A. Seppälä, "Load research and load estimation in electricity distribution," Ph.D. dissertation, Helsinki University of Technology, 1996. 55

[133] V. Neimane, "On development planning of electricity distribution networks," Ph.D. dissertation, Royal Institute of Technology, 2001. 55

[134] M. of Science and Technology, *Reglamento Electrotecnico de Baja Tension (Low Voltage Electrical Standard).*, S. Goverment, Ed. Spanish Goverment, 2002. 60

[135] *EMQ 2006 de la Regió Metropolitana de Barcelona.* Generalitat de Catalunya - Departament de Política Territorial i Obres Públiques, 2006. 65, 70, 83, 100

[136] J. Vlachogiannis, "Probabilistic constrained load flow considering integration of wind power generation and electric vehicles," *IEEE Transactions on power systems*, vol. 24(4), pp. 1808–17, 2009. 68

[137] R. E. Walpole, R. H. Myers, S. L. Myers, and K. E. Ye, *Probability and Statistics for Engineers and Scientists*, 9th ed. Prentice Hall, 2011. 68

[138] "Radial distribution test feeders," *Transactions on Power System*, vol. 6(3), pp. 975–85, 1991. 79

[139] *Norma Técnica Particular - Generalidades (NTP-GEN)*, FECSA-ENDESA Std., 2006. 79

[140] *Norma Técnica Particular - Líneas Subterráneas de Media Tensión (NTP-LSMT)*, FECSA-ENDESA Std., 2006. 79

[141] *Norma Técnica Particular - Centros de Transformación en Edificio (NTP-CT)*, FECSA-ENDESA Std., 2006. 79

[142] *Especificación técnica - Distribución media y baja tensión - Cables para redes subterraneas de MT y BT - Ref. 6700023*, FECSA-ENDESA Std., 2006. 79

[143] *Especificación técnica - Distribución media y baja tensión - Cables para redes subterraneas de MT y BT - Ref. 6700024*, FECSA-ENDESA Std., 2006. 79

[144] http://www.nexans.es/. [Online]. Available: http://www.nexans.es/ 79

[145] http://www.generalcable.es/. [Online]. Available: http://www.generalcable.es/ 79

Appendix A

Load flow: Newton-Raphson

This chapter describes the load flow algorithm through which the voltages and the currents have been found when performing the Montecarlo simulation. The chosen method is the Newton-Raphson load flow algorithm.

A.1 Statement of the problem

Electrical grid nodes can be classified into three types:

1. **Power consumption nodes (PQ nodes):** in this type of nodes there is no generation ($P_{Gi} = 0$ and $Q_{Gi} = 0$) and the consumed active power ($P_{Ci} = P_{Ci}^{\text{esp}}$) and the consumed reactive power ($Q_{Ci} = Q_{Ci}^{\text{esp}}$) are known.

2. **Generation nodes (PV nodes):** in this type of nodes the active power consumption ($P_{Ci} = P_{Ci}^{\text{esp}}$), the active power generation ($P_{Gi} = P_{Gi}^{\text{esp}}$) and the voltage module ($V_i = V_i^{\text{esp}}$) are known.

3. **Reference node (also known as *slack* or *swing* node):** there is only one of this type of nodes in the grid when performing the analysis due to the fact that this node is the one where the voltage angle reference ($\theta_n = 0$) is established and therefore known. The active power consumption is also known ($P_{Ci} = P_{Ci}^{\text{esp}}$).

A grid with n nodes, can be arranged as:

$i = 1, 2, ..., n_D$	being n_D the number of PQ nodes
$i = n_D + 1, n_D + 2, ..., n_D + n_G$	being n_G the number of PV nodes
$i = n$	being n the index of the *slack* node
where	
$n = n_D + n_G + 1$	

The admittance matrix of the grid, Y, can be defined as:

$$Y = \begin{bmatrix} \underline{Y}_{11} & \underline{Y}_{12} & \cdots & \underline{Y}_{1n} \\ \underline{Y}_{21} & \underline{Y}_{22} & \ddots & \vdots \\ \vdots & \ddots & \ddots & \underline{Y}_{(n-1)n} \\ \underline{Y}_{n1} & \cdots & \underline{Y}_{n(n-1)} & \underline{Y}_{nn} \end{bmatrix} \tag{A.1}$$

where

$\underline{Y}_{ii} = \sum$ admittances of the circuits connected to i
(elements of the diagonal of the matrix Y)
$\underline{Y}_{ij} = -\sum$ admittances of the circuits between i i j
(elements outside of the diagonal of the matrix Y)

The Y matrix is a $n \times n$ complex matrix and therefore can be expressed as the sum of a real matrix and a complex matrix:

$$Y = G + jB \tag{A.2}$$

where

$$G = \begin{bmatrix} G_{11} & G_{12} & \cdots & G_{1n} \\ G_{21} & G_{22} & \ddots & \vdots \\ \vdots & \ddots & \ddots & G_{(n-1)n} \\ G_{n1} & \cdots & G_{n(n-1)} & G_{nn} \end{bmatrix} \tag{A.3}$$

$$jB = j \begin{bmatrix} B_{11} & B_{12} & \cdots & B_{1n} \\ B_{21} & B_{22} & \ddots & \vdots \\ \vdots & \ddots & \ddots & B_{(n-1)n} \\ B_{n1} & \cdots & B_{n(n-1)} & B_{nn} \end{bmatrix} \tag{A.4}$$

The load flow problem is a non-linear problem which can be formulated from the known variables of the net injected power in every grid's node:

$$P_i^{\text{esp}} = P_{Gi}^{\text{esp}} - P_{Ci}^{\text{esp}} \qquad i = 1, 2, ..., n_D + n_G$$
$$Q_i^{\text{esp}} = Q_{Gi}^{\text{esp}} - Q_{Ci}^{\text{esp}} \qquad i = 1, 2, ..., n_D$$

Where the load flow equations are:

$$P_i^{\text{esp}} = V_i \sum_{j=1}^{n} V_j \left(G_{ij} \cos\theta_{ij} + B_{ij} \sin\theta_{ij}\right) \qquad i = 1, 2, ..., n_D + n_G \quad \text{(A.5)}$$

$$Q_i^{\text{esp}} = V_i \sum_{j=1}^{n} V_j \left(G_{ij} \sin\theta_{ij} - B_{ij} \cos\theta_{ij}\right) \qquad i = 1, 2, ..., n_D \quad \text{(A.6)}$$

Defining the variables as:

G_{ij} element of the i row and j column of G,

B_{ij} element of the i row and j column of B.

V_i voltage module of the node i,

V_j voltage module of the node j,

P_i^{esp} *active* net power injected in the node i,

Q_i^{esp} *reactive* net power injected in the node i,

Thus, in order to solve $2n_D + n_G$ equations, the following variables need to be solved:

V_i, $i = 1, 2, ..., n_D$ voltage module

θ_i, $i = 1, 2, ..., n_D + n_G$ voltage angle

A.2 The Newton-Raphson method

The Newton-Raphson method is an iterative process through which the variables in the non-linear equations get a value until a maximum allowed error ε is reached or, when this error can not be reached, the system has no solution.

For every node i the difference Δ between the initially specified power and the calculated is defined as follows:

$$\begin{aligned}
\Delta P_i &= P_i^{\text{esp}} - V_i \sum_{j=1}^{n} V_j \left(G_{ij}\cos\theta_{ij} + B_{ij}\sin\theta_{ij}\right) \\
i &= 1, 2, ..., n_D + n_G \\
\Delta Q_i &= Q_i^{\text{esp}} - V_i \sum_{j=1}^{n} V_j \left(G_{ij}\sin\theta_{ij} - B_{ij}\cos\theta_{ij}\right) \\
i &= 1, 2, ..., n_D
\end{aligned}$$

It can also be expressed in the matrix form as:

$$\begin{bmatrix} H & N \\ M & L \end{bmatrix}^k \begin{bmatrix} \Delta\theta \\ \Delta V/V \end{bmatrix}^k = \begin{bmatrix} \Delta P \\ \Delta Q \end{bmatrix}^k \tag{A.7}$$

The problem solving process starts through the assignation of the initial values to the voltage module and angle variables:

$$\left[\left[\theta\,|V\right]^T\right]^0 = \left[\left[\theta_1, \theta_2, ..., \theta_{n_D+n_G}\,|V_1, V_2, ..., V_{n_D}\right]^T\right]^0 \tag{A.8}$$

For every iteration k corrections are introduced in the system:

$$\left[\left[\Delta\theta\,|\Delta V/V\right]^T\right]^k \tag{A.9}$$

and new values $\left[\left[\theta\,|V\right]^T\right]^{k+1}$ of:

$$\begin{bmatrix} \theta \\ V \end{bmatrix}^{k+1} = \begin{bmatrix} \theta \\ V \end{bmatrix}^k + \begin{bmatrix} \Delta\theta \\ \Delta V \end{bmatrix}^k \tag{A.10}$$

being H, N, M and L sub-matrix where its terms can be calculated as:

$$\left.\begin{aligned} H_{ij} = L_{ij} &= V_i V_j \left(G_{ij}\sin\theta_{ij} - B_{ij}\cos\theta_{ij}\right) \\ N_{ij} = -M_{ij} &= V_i V_j \left(G_{ij}\cos\theta_{ij} + B_{ij}\sin\theta_{ij}\right) \end{aligned}\right\} \text{terms outside the matrix diagonal}$$

$$\left.\begin{array}{l} H_{ii} = -Q_i - B_{ii}V_i^2 \\ L_{ii} = Q_i - B_{ii}V_i^2 \\ N_{ii} = P_i + G_{ii}V_i^2 \\ M_{ii} = P_i - G_{ii}V_i^2 \end{array}\right\} \text{terms of the matrix diagonal}$$

When the error ε reaches its acceptable maximum value, the process stops and the system is considered solved:

$$\max\left(\left|\Delta P_1^k\right|, ..., \left|\Delta P_{n-1}^k\right|, \left|\Delta Q_1^k\right|, ..., \left|\Delta Q_{n_D}^k\right|\right) \leq \varepsilon$$

Appendix B

Mobility data of the metropolitan area of Barcelona

The following tables have been extracted from the mobility data of the Barcelona's city council mobility web (year 2006). The table B.1 stands for number of trips that a single driver does in a day. The tables B.2 and B.3 show the distance of the daily trips.

Table B.1: Number of daily trips.

Number of trips	**Frequency**	**Percentage**
1	768	0,7
2	38.202	36,0
3	4.814	4,5
4	31.439	29,6
5	5.497	5,2
6	8.884	8,4
7	2.058	1,9
8	2.043	1,9
9	735	0,7
10	552	0,5
11	260	0,2
12	281	0,3
13	75	0,1
14	5	0,0
15	5	0,0
16	1	0,0
17	2	0,0
18	1	0,0
Total	**106.091**	**100,0**

Table B.2: Distance per trip (from 1 km to 25 km).

Distance [km]	**SUV**	**Motorbike**	**Total**
0	238.083	30.059	268.143
1	602.950	88.765	691.715
2	290.177	79.876	370.053
3	324.435	78.808	403.243
4	208.109	54.428	262.537
5	201.670	50.056	251.726
6	124.534	29.065	153.599
7	162.700	26.749	189.448
8	120.299	13.085	133.384
9	134.415	13.391	147.806
10	126.709	17.245	143.954
11	94.242	9.767	104.009
12	99.693	7.922	107.615
13	76.374	5.609	81.982
14	84.391	5.887	90.278
15	76.074	6.403	82.477
16	54.130	4.988	59.117
17	49.746	5.317	55.064
18	50.680	3.451	54.131
19	47.240	1.460	48.700
20	45.921	2.355	48.276
21	43.880	3.842	47.722
22	42.915	2.164	45.079
23	32.629	811	33.440
24	33.904	2.026	35.931
25	35.958	3.474	39.432

Table B.3: Distance per trip (from 26 km to 50 km).

Distance [km]	**SUV**	**Motorbike**	**Total**
26	32.240	1.744	33.984
27	23.444	1.109	24.553
28	27.236	1.012	28.249
29	22.792	436	23.229
30	18.264	674	18.938
31	20.960	721	21.681
32	18.662	545	19.207
33	19.220	375	19.594
34	15.579	237	15.816
35	17.791	624	18.415
36	17.009	643	17.652
37	12.411	520	12.931
38	11.685	505	12.190
39	10.189	426	10.615
40	9.969	.	9.969
41	11.078	.	11.078
42	5.338	380	5.717
43	8.306	.	8.306
44	8.919	277	9.195
45	6.302	.	6.302
46	6.026	152	6.178
47	5.913	.	5.913
48	5.625	154	5.779
49	5.065	.	5.065
50	6.731	.	6.731

Appendix C

Publications

This chapter presents the publications related to the specific topics of this thesis the author has contributed to.

Journal papers

Published

2012

Eduardo Valsera-Naranjo, Andreas Sumper, Roberto Villafafila-Robles, David Martínez-Vicente, "Probabilistic Method to Assess the Impact of Charging of Electric Vehicles on Distribution Grids", 2012. *Energies*, 2012, 5(5), 1503-1531; DOI:10.3390/en5051503.

Conference papers

Presented

2011

Eduardo Valsera-Naranjo, David Martínez-Vicente, Andreas Sumper, Roberto Villafafila-Robles, Antoni Sudria-Andreu, "Deterministic and probabilistic assessment of the impact of the electrical vehicles on the power grid", 2011. Conference Location : San Diego, CA. ISSN: 1944-9925. E-ISBN: 978-1-4577-1001-8. Print ISBN: 978-1-4577-1000-1.

Roberto Villafafila-Robles, Andreas Sumper, B. Bak-Jensen,Eduardo Valsera-Naranjo, "Probabilistic analysis in normal operation of distribution system with distributed generation", 2011. Conference Location : San Diego, CA. ISSN: 1944-9925. E-ISBN: 978-1-4577-1001-8. Print ISBN: 978-1-4577-1000-1.

2009

Eduardo Valsera-Naranjo, Andreas Sumper, Pau Lloret-Gallego, Roberto Villafafila-Robles, Antoni Sudria-Andreu, "Electrical vehicles: State of art and issues for their connection to the network". *Electrical Power Quality and Utilisation, 2009. EPQU 2009.* 10th International Conference on Electrical Power Quality and Utilisation. Conference Location : Lodz. ISSN: 2150-6655. E-ISBN: 978-1-4244-5172-2. Print ISBN: 978-1-4244-5171-5.